DEVELOPMENT AND ASSESSMENT OF NEW SENSOR SYSTEMS IN FOOD PACKAGING APPLICATIONS

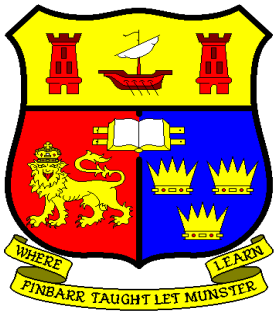

A thesis submitted to the National University of Ireland, Cork in fulfilment of the requirements for the degree of Doctor of Philosophy by

Nicolas Borchert, M.Sc.

School of Food and Nutritional Sciences
University College Cork
November 2012

Head of School: Prof. Kevin Cashman
Supervisors: Dr. Joseph Kerry
Prof. Dmitri Papkovsky

Declaration

This thesis has not been submitted in whole or part to this or any other university for any degree, and is, unless stated, the original work of the author.

_____ _____

Nicolas Borchert April 2013

Acknowledgements

The writing of this dissertation has been the most significant academic challenge I have ever had. Without the endorsement, patience and guidance of the following people, this study would not have been completed. It is to them that I owe my deepest gratitude.

- Dr Joe Kerry and Prof Dmitri Papkovsky who acted as my supervisors despite their many other academic and professional commitments. Their wisdom, knowledge and commitment to the highest standards encouraged and motivated me.
- Dr Malco Cruz-Romero who was a grand project coordinator and a caring ally during my work.
- Dr Michael Cronin and Mr Eddie Beatty who helped me with lab equipment and assisted me whenever I faced trouble.
- My friends and colleagues of the Biochemistry Department and School of Food and Nutritional Sciences.
- Finally, and most importantly, I would like to thank my wife Diana for her support, inspiration and quiet patience.

This dissertation is dedicated to Diana and Charlotte, and to all my family.

Table of Contents

Abstract

The use of optical sensor technology for non-invasive determination of key quality pack parameters improved package/product quality. This technology can be used for optimization of packaging processes, improvement of product shelf-life and maintenance of quality. In recent years, there has been a major focus on O_2 and CO_2 sensor development as these are key gases used in modified atmosphere packaging (MAP) of food. The first and second experimental chapters (chapter 2 and 3) describe the development of O_2, pH and CO_2 solid state sensors and its (potential) use for food packaging applications. A dual-analyte sensor for dissolved O_2 and pH with one bi-functional reporter dye (meso-substituted Pd- or Pt-porphyrin) embedded in plasticized PVC membrane was developed in chapter 2. The developed CO_2 sensor in chapter 3 was comprised of a phosphorescent reporter dye Pt(II)- tetrakis(pentafluorophenyl) porphyrin (PtTFPP) and a colourimetric pH indicator α-naphtholphthalein (NP) incorporated in a plastic matrix together with a phase transfer agent tetraoctyl- or cetyltrimethylammonium hydroxide (TOA-OH or CTA-OH). The third experimental chapter, chapter 4, described the development of liquid O_2 sensors for rapid microbiological determination which are important for improvement and assurance of food safety systems. This automated screening assay produced characteristic profiles with a sharp increase in fluorescence above the baseline level at a certain threshold time (TT) which can be correlated with their initial microbial load and was applied to various raw fish and horticultural samples. Chapter 5, the fourth experimental chapter, reported upon the successful application of developed O_2 and CO_2 sensors for quality assessment of MAP mushrooms during storage for 7 days at 4°C.

List of Abbreviations

ALS:	automated liquid sampler
AOAC:	American Organization of Analytical Chemists
AP:	active packaging
BHA:	butylated hydroxianisole
BHT:	butylated hydroxitoluene
BI:	browning index
CA:	controlled atmosphere
CFU:	colony forming unit
CTA-OH:	cetyltrimethylammonium hydroxide
DEFT:	direct epifluorescent filter technique
DLR:	dual luminophore reference
DOS:	bis(2-ethylhexyl) sebacate
DT:	doubling time
EC:	ethyl cellulose
Eu(III)-complexes:	Europium(III) complex
EVOH:	ethylene vinyl alcohol copolymer
F:	filter
FD:	frequency domain
FDA:	US food and drug administration
FITC:	fluorescein isothiocyanate
FRET:	Förster resonance energy transfer
FT-IR:	Fourier transformed-infrared
GC:	gas chromatography
(r)HDPE:	(recycled) high density polyethylene
HPLC:	high pressure liquid chromatography
HPTS:	1-hydroxypyrene-3, 6, 8-trisulfonate
IBM:	isobutyl methacrylate
IP:	intelligent packaging
IR:	infrared
LD50:	lethal dose, 50%

LED:	light emission diode
LOD:	limit of detection
LT:	lifetime
MA:	modified atmosphere
MAP:	modified atmosphere packaging
MDI:	microwave doneness indicator
MgTFPP:	Mg- tetrakis(pentafluorophenyl) porphyrin
MPN:	most probably number
MS:	mass spectroscopy
NP:	alpha-naphtholphthalein
ORMOSIL:	organically modified silica
P(IBM):	poly(isobutyl methacrylate)
P(TMSP):	poly(1-(trimethylsilyl)-1-propyne)
PAA:	polyacrylic acid
PAN:	polyacrylonitrile
PBW:	peptone buffered water
PD:	photodiode
PdCP:	Pd-coproporphyrin-I tetraester
PDMS:	Polydimethylsiloxane
PE:	polyethylene
PEG:	poly(ethyleneglycol)
PET:	polyethylene terephthalate
PMMA:	polymethyl methacrylate
PP:	polypropylene
PPO:	polyphenol oxidase
PS:	polystyrene
PTA:	phase transfer reagent
PtOEP:	Pt(II) octaetylporphyrin
PtOEPK:	Pt(II)- octaethylporphyrinketone
PtTBP:	Pt(II)-tetrabenzoporphyrin
PtTFPP:	Pt(II)- tetrakis(pentafluorophenyl) porphyrin
PVA:	poly (vinyl alcohol)

PVC:	polyvinyl chloride
PVCD:	polyvinylidene chloride
PVP:	polyvinylpyrroline
QC:	quality control
QD:	quantum dot
R:	reflectance
RFID:	radio frequency identification
RH:	relative humidity
RT:	room temperature
Ru(dpp):	ruthenium(II)-tris(diphenyl-phenanthroline)
Ru(II)-complexes:	ruthenium(II) complex
SB:	Schiff-base group
SD:	standard deviation
SML:	specific migration limit
SV:	Stern-Volmer
TBA-OH:	tetrabutylammonium hydroxide
TBHQ:	tert-butyldroquinone
TBP:	tributyl phosphate
TBPB:	potassium tetrakis (4-tert-butylphenyl)borate
TCPB:	potassium tetrakis(4-chlorophenyl)borate
TD:	time domain
TFA:	trifluoroacetic acid
THF:	tetrahydrofuran
TOA-OH:	tetraoctylammonium hydroxide
TPP:	tetraphenylporphyrin
TT:	threshold time
TTB:	sodium tetra(p-tolyl)borate
TTI:	time temperature indicator
TVC:	total viable count
UV:	ultra violet
VIS:	visible
WI:	whiteness index

Chapter 1: Literature Review

1.1 Smart Packaging Developments

1.1.1 Food Packaging Functions

Food packaging science is a discipline which applies principles from four different scientific areas, namely: a) material science, b) food science, c) information science and d) socioeconomics. The relationship between these areas results in a technology push and a market pull, which means that new products are created through advances in material, food and information science and are pushed forward to seek market acceptance and those market needs are created by the dynamics of socioeconomics which are to be satisfied by technology, respectively (Lee *et al.*, 2008).

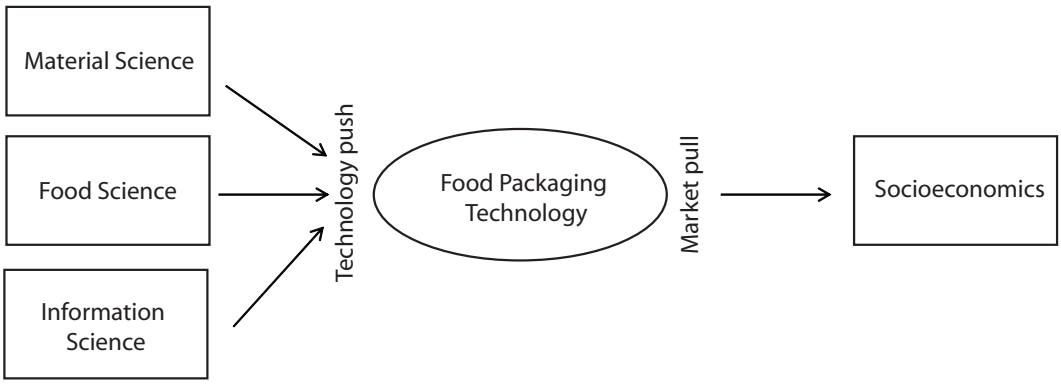

Figure 1.1: Dynamics of packaging science and technology (adapted from Lee *et al.*, 2008).

The fundamental aspects of all packaging materials is that in an economical manner, they must contain, protect, preserve, inform (throughout the entire distribution process from point of manufacture to point of consumer usage) and provide convenience (at many different levels) while acknowledging the constraints placed upon their usage from both legal and environmental perspectives. As these fundamental principles apply to all forms of packaging materials and systems, it follows that irrespective of the

specific level at which the packaging is industrially applied, all must conform to these same principles (Cruz-Romero and Kerry, 2008).

1.1.2 Active and Intelligent Packaging

As the world of consumer packaged goods becomes mature and the market becomes saturated, food packaging is expected to transform and adapt new packaging developments, beyond their original task of preventing external influences such as mechanical stress, microorganisms, oxygen, moisture, off-odours and light (Dainelli *et al.*, 2008; Yam *et al.*, 2005). Quality and safety of perishable goods need to be improved while enhancing and stabilising food composition and nutrition, leading to extended shelf-life, information and consumer convenience. Advanced packaging must provide a more compelling value position to the consumer, by leaving its passive role and entering a role which is considered active, as it starts to interact with food and its environment in a positive way (Dainelli *et al.*, 2008). Therefore various terms were created to describe these new technologies, such as 'active', 'interactive', 'clever', 'smart', 'intelligent', 'diagnostic', 'functional', 'enhanced', etc. (Dainelli *et al.*, 2008; Kerry and Butler, 2008). Two main groups of technology that have been established in the literature and incorporated in new Framework Regulations on Food Contact Materials, are called 'active packaging' (AP) and 'intelligent packaging' (IP). They are designed to extend shelf-life or achieve some characteristics that cannot be obtained otherwise and to sense and inform about the history of the package and quality of the food (Kerry and Butler, 2008; Yam *et al.*, 2005). In other words AP is the component which is taking some action while IP is the component for sensing and sharing the information (Yam *et al.*, 2005). Yam *et al.* (2005) created a model where AP was mantled around the protective area of food packaging and IP around the area of communication. This basically means that AP enhances the protection function and the uniqueness of IP lies in its ability to communicate (Fig. 1.2) (Yam *et al.*, 2005). However, the term 'smart packaging' can be considered an overall term encompassing both active and intelligent packaging and

packaging systems and some technologies such as modified atmosphere packaging (MAP) which cannot be allocated to one or the other (Han, 2005; Robertson, 2006).

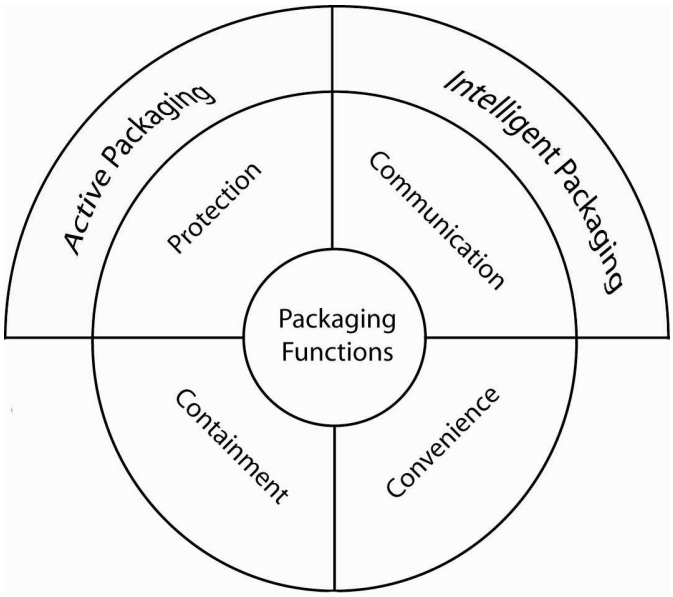

Figure 1.2: Model of packaging functions (adapted from Yam *et al.*, 2005).

There are many published definitions for active and intelligent packaging which differ from each other slightly. The following definitions are given by the Framework Regulation EC (1935/2004) on Food Contact Materials which sets standards for food contact materials based on scientific fundamentals to support EU policies on food safety.

A) 'Active food contact materials and articles' mean materials and articles that are intended to extend the shelf-life or to maintain or improve the condition of packaged food. They are designed to deliberately incorporate components that would release or absorb substances into or from the packaged food or the environment surrounding the food.

B) 'Intelligent food contact materials and articles' mean materials and articles which monitor the condition of packaged food or the environment surrounding the food.

First introduced in mid 70s in Japan, active and intelligent packaging gained significant attention only in the mid 90s in Europe and the USA. In this period many patents were filed and market tests carried out with the outlook of strong growth of this field in the future, especially for such promising technologies as oxygen scavengers and moisture absorbers (Dainelli *et al.*, 2008).

Active Packaging

Active packaging refers to the incorporation of certain additives into packaging with the objective of increasing food preservation and hence the shelf-life (Kirwan *et al.*, 2003). This includes components capable of scavenging oxygen; absorbing carbon dioxide, moisture, ethylene, flavours and light; releasing carbon dioxide, ethanol, preservatives such as antioxidants and antimicrobial substances; controlling and compensating the temperature; anti fogging agents; gas permeating films and microwave susceptors (Kerry and Butler, 2008).

As active food packaging is used with many food products, its main beneficial applications and their possible mechanisms are listed in Table 1.1. However, before applying this technique one must understand the different ways in which food deterioration occurs, including; extrinsic (storage temp, relative humidity, gas composition) and intrinsic factors (pH, water activity, nutrient content, antimicrobial compounds, redox potential, respiration rate, biological structure). These factors influence directly the chemical, biochemical, physical and microbial spoilage mechanisms and product shelf-life (Kirwan *et al.*, 2003).

Table 1.1: Active packaging devices (adapted from Kerry and Butler, 2008 and Restuccia *et al.*, 2010).

Type of Application	**Principle or Mechanisms**	**Foods**
Oxygen scavengers	Enzyme based (glucose oxidase, alcohol oxidase); chemical based (powdered iron oxide, catechol, ferrous carbonate, iron-sulphur, sulfite salt-copper sulfate, photosensitive dye oxidation, ascorbic acid oxidation, catalytic conversion of oxygen by platinum catalyst)	Ground coffee, bread, cakes, snack foods, dried foods, beverages, pizza, cured meats and fish
Carbon dioxide absorbers/emitters	Iron powder-calcium hydroxide, ferrous carbonate-metal halide	Coffee, fresh meats and fish
Moisture absorbers	Silica gel, propylene glycol, polyvinyl alcohol, PVA blanket, activated clays and minerals	Dry and dehydrated products, fish, meats, poultry, snack foods, cereals
Ethylene absorbers	Activated charcoal, potassium permanganat, Kieselguhr, bentonite, Fuller's earth, silicon dioxide powder, zeolite, ozone	Fruit and vegetables
Ethanol emitters	Encapsulated ethanol	Bread, cakes, fish
Antimicrobial releaser	Sorbates, benzoates, propionates, ethanol, ozone, peroxide, sulphur dioxide, antibiotics, silver-zeolite, quaternary ammonium salts, spice and herb extracts	Dried apricots
Antioxidant releaser	BHA, BHT, TBHQ, ascorbic acid, tocopherol, baking soda, active charcoal	Cereals
Flavour absorbers	Baking soda, active charcoal/ clays/ zeolites, citric acid, cellulose triacetate, Ferrous salt	Fruit juices, fried snack foods, fish, poultry
Anti-fogging	Biaxially orientated vinylon, compression rolled orientated HDPE	Fresh fruit and vegetable packages
Light absorbers	UV blocking agents, hydrobenzophenone	Pizza, milk
Temperature control	Non-woven plastic, double-walled containers, hydrofluorocarbon gas, ammonium nitrate/ water, calcium chloride/ water, super corroding alloys/ salt water, potassium permanganat/ glycerine	Ready meals, meats, fish, poultry, beverages
Temperature compensating films	Side chain crystallisable polymers	Fruit, vegetables
Gas permeable/ breathable	Surface treated, perforated or microporous films	Ready-to-eat salads
Microwave susceptors	Metallized thermoplastics	Ready-to-eat meals

Intelligent Packaging

As a result of the growing usage of active components in food packaging, the need for monitoring certain packaging conditions increases. Changes inside the pack, including gas composition, humidity, microorganisms, ethylene, temperature, which are associated with active packaging devices, need to be monitored, especially in the process of development of these packaging devices. Traditional monitoring systems, such as Dansensor, gas chromatography (GC), microbial determination following the ISO:4833:2003 standard method or sensory evaluation are destructive, time consuming and/or expensive in general.

A new technology, which can overcome these limitations, is based on indicators and sensors that can be incorporated inside the packages to provide fast, non-destructive and reliable determination of important packaging conditions. Indicators are devices that indicate the presence, absence or concentration of a substance or physical parameter through direct visual colour change. The majority of indicators were initially developed to test package integrity focused on visual detection of O_2. Indicators for freshness, ripeness and time-temperature control are also gaining increasing attention.

In contrast, sensors comprise receptor and transducer components which allow them to respond reversibly and quantitatively to the analyte of interest. While the physical or chemical information is measured by the receptor, the transducer is a device that is capable of transforming their signal into useful analytical information. Gas sensors, chemical sensors and biosensors have been developed rapidly in recent years, with optical O_2 sensors as the most developed technology. A number of instruments and solid state materials for optical O_2 sensing have been described in recent years (Papkovsky and Ponomarev, 1995; Trettnak *et al*., 1995). Progress has been observed with some other sensors which are coming close to industrial viability.

Intelligent packaging contains components that sense internal compositions or transmit general information and informs researchers, manufacturers, retailers and consumers. It provides aspects of the history of the pack, provides information about the

function and properties of packaged food, assures pack integrity, provides tamper evidence, and assures product safety and quality (see Table 1.2 for overview).

The following main types of intelligent systems can be defined (Robertson, 2006):

a) Product quality and value improving systems, such as time temperature indicators (TTIs), quality indicators, chemical and gas sensors.

b) Conveniences enhancing systems, such as microwave doneness indicators, thermochromic inks and radio frequency identification (RFID) tags.

c) Tamper proof, anti-counterfeiting and anti-theft technologies.

Category a: Quality indicators which determine temperature at certain time intervals are a well evaluated technology and commercially available. These TTI devices accumulate the effect of exposure to temperature over time and produce a change of colour or other physical characteristic. There are two categories which can be defined as 'partial history indicators' which do not respond unless the predetermined threshold temperature is exceeded, and 'full history indicators' which respond continuously to all temperatures. One example of a full history indicator is the TTI CheckPoint^{TM} (VITSAB A.B., Malmö, Sweden). This enzymatic system is based on colour change from bright yellow to orange red upon enzymatic hydrolysis of a lipid substrate causing a pH change (Hogan and Kerry, 2008; Robertson, 2006; Taoukis, 2008). Other commercial systems are the full history indicator Fresh-Check^{TM} TTI (Lifelines Technology, Morris Plains, New Jersey, USA) based on a 1,4-addition polymerization reaction of diacetylene crystals to a coloured polymer and the 3M MonitorMark^{TM} TTI (3M Co., St Paul, Minnesota, USA) which is based on diffusion of a coloured fatty acid ester along porous wick (Robertson, 2006; Taoukis, 2008).

Another group of indicators provides information about the quality of a product; for example, freshness or ripeness via microbial growth or chemical changes. The number of practical concepts is limited, but there is a potential for freshness indicators based on quality indicating metabolites, such as O_2, CO_2, diacetyl, ammonia, organic acids, ethanol, biogenic amines, hydrogen sulfide, food pathogens. One example is the

Ageless-EyeTH oxygen indicator (Mitsubishi Gas Chemical Co., Japan) which changes in colour from pink (no oxygen, 0.1% or less) to blue (0.5% or more) in about 5 minutes after contact with oxygen (Hogan and Kerry, 2008), but this system is expensive which makes it unattractive for industrial use. Other examples include CO_2 indicators based on colorimetric films changing subsequently from violet (0% CO_2) to yellow (100% CO_2) (Mills and Skinner, 2010) and fizziness indicators for carbonated beverages which, depending on the headspace pressure of CO_2 change their colour (Mills and Skinner, 2011). These indicators can also be used for integrity checks of MAP and controlled atmospheres (CAs) packages providing non-destructive leak detection. One indicator for ammonia detection uses pH indicator bromocresol basic green incorporated in a cellulose acetate matrix. A visual colour change is reported within approximately 5 min when exposed to an ammonia step from 0 to 14.29 ppm and a shelf-life of up to four months when kept in dark and dry conditions. The sensor indicates the spoilage of the product through visual colour change for convenient use in food packages (Pacquit *et al.*, 2006).

The ripeness indicator RipeSense^{TM} works by detecting aroma components released by the fruit as it ripens. Originally developed for pears (Sharrock and Henzell, 2009) to quantify the changes in ethylene via colour changes, this allows the consumer to choose fruit that best appeals to their taste (Pocas *et al.*, 2008; Robertson, 2006).

In addition to the indicators, different gases, chemicals and microorganisms can be detected and quantified by sensors. O_2 gas sensors are the most developed and already commercialized by PreSense, OxySense, Mocon and Luxcel Biosciences (Cork, Ireland). These sensors are based on luminescent quenching of phosphorescent platinum(II)-porphyrin complexes incorporated in polystyrene matrix giving signals in the microsecond range and optimized for O_2 sensing in the range 0-21% O_2. They have already been tested in many different food matrices, including meat (Smiddy *et al.*, 2002a), fresh produce (Borchert *et al.*, 2012), cheese (Hempel *et al.*, 2012b), beer (Hempel *et al.*, 2012a). Other approaches being used successfully include resonance energy transfer and phase fluorimetric detection (Neurauter *et al.*, 1999).

Several CO_2 sensors are described in the literature as being feasible for food packaging. One common strategy is to use 1-hydroxypyrene-3, 6, 8-trisulfonate (HPTS) and Ru-(dpp) in a sol-gel matrix applying the Dual Luminophore Reference (DLR) scheme (Bültzingslöwen *et al.*, 2002). This approach is compatible with established phase domain instrumentation for lifetime-based detection (described in chapter 1.2.1.3).

Furthermore, sensors for the detection of chemical compounds, such as ammonia and humidity are available as well. One approach for ammonia makes use of fluorescence energy transfer applying donor-acceptor complexes immobilized in PVC and a sol gel. This system comprises the use of rhodamine B which has a fluorescence intensity which is proportional to the concentration of the analyte and when exposed to ammonia it gets converted into a colourless, non-fluorescent lacton (Preininger and Mohr, 1997). An optical and inexpensive relative humidity (RH) optode was fabricated using the water-sensitive luminescent dye $[Ru(phen)_2(dppz)]^{2+}$ immobilized in poly(tetrafluoroethylene). This sensor was applied to a_w measurements in foods; its operational range is reported from 4-100% RH and response and recovery times are shorter than 1.4 and 1.2 minutes, respectively. The sensor is validated in the temperature range 10-30°C; its stability is 2.5 years in discontinuous measurements (Bedoya *et al.*, 2006).

Biosensors provide information about biological species and reactions. They consist of bioreceptors, such as enzymes, antigens, microbes, hormones or nucleic acids specific to target analyte, capable of detecting food pathogens, such as Staphylococcal enterotoxin A and B, Salmonella typhimurium, Salmonella group B, D and E, E.coli 0157:H7, Campylobacter sp. and Listeria monocytogenes (Kuswandi *et al.*, 2011). One commercially available product for pathogen detection is ToxinGuard™ (Toxin Alert, Ontario, Canada) based on the visual diagnostic system of incorporated antibodies printed on polyethylene-based plastic (Bodenhammer, 2002). Furthermore, a time-temperature biosensor has been developed based on a chipless radio frequency circuit that can be read with a hand-held scanner. This can be integrated with the barcode and

simultaneously read with one scanner to keep track during refrigerated transports (http://www.aditus).

Category b: Convenience represents a lifestyle that customers are willing to pay additionally. One example of this is thermochromic inks. They are printed on labels or containers and if heated or cooled they give colour indication on the optimal consumption temperature. Microwave doneness indicators (MDI) work on the same principle, indicating when the product is heated enough to be served. As the field distribution in microwave ovens is complicated optimal effects are not always provided. The observation as to whether or not the colour of the indicator has changed is also not easy to observe, especially when the microwave is still closed.

Traceability and supply chain management has been strongly improved by the introduction of RFID. Small tags are incorporated in food packaging containing information about the history of the product and other useful details about storage and handling after manufacturing. Because RFID tags are still expensive, they are mainly used in secondary and tertiary packaging (Robertson, 2006).

Category c: Theft and counterfeiting devices include holograms, special inks and dyes, laser label and electronic tags (Jotcham, 2005) so far have had limited use in food packaging because of cost reasons, but are actively developing. Tamper-evident technologies have been developed based on permanently colour changes or words such as ‘open’ becoming visible on labels or seals.

Table 1.2: Intelligent packaging devices. The indicators/sensors are ranked in order of appearance based on their commercialization and usage (adapted from Kerry and Butler, 2008).

Cat.	Indicators/ Sensors	Determination of	Principle	Packaging types (Products)	Status	Ref.
a)	TTI (external)	Temperature	Mechanical, chemical, enzymatic	Chilled and frozen products (meats, poultry)	Commerc.	(Vaikousi *et al.*, 2009)
a)	Freshness indicators	Microbial growth, chemical changes (diacetyl, ammonia, organic acids, ethanol, biogenic amines, CO_2, hydrogen sulfide)	Biochemical	Perishable foods (fish, meats)	Commerc.	(Barat *et al.*, 2008)
b)	Thermochromic inks	Temperature	Visual	Containers (heated or cooled)	Commerc.	(Vagina *et al.*, 2009)
a)	O_2, CO_2 indicators	Packages integrity, CO_2 and O_2	Optochemical	MAP (meats, cheese)	Commerc.	(Mills, 2005)
b)	Microwave doneness	Temperature	Visual	Microwave food	Commerc.	(O'Farrell *et al.*, 2007)
b)	RFID tags	Identification, tracking	Electronic	All packaging (meats)	Commerc.	(Michael and McCathie, 2005)
a)	Ripeness indicators	Volatile metabolites (diacetyl, ammonia, ethanol, amines, CO_2, hydrogen sulfide	Biochemical	Perishable foods (pears, kiwis, apples)	Commerc. for pears	(Lang and Hübert, Sharrock and Henzell, 2009)
a)	O_2 gas sensors	Packages integrity, permeability, O_2	Electrical, optical, chemical	MAP, CA (meats, cheese, salad)	Commerc. for research	(Papkovsky *et al.*, 2002b)
a)	Biosensors	E.coli, Salmonella sp., Campylobacter sp., Listeria sp., temperature	Biological reactions	MAP, CA (meats, chilled and frozen products)	Some establ. for research	(Terry *et al.*, 2005)
a)	Chemical sensors	Humidity, ammonia, etc.	Optochemical	MAP, CA (fish)	Some establ. for research	(Preininger and Mohr, 1997, Somani *et al.*, 2001)
a)	Other gas sensors (except O_2)	Packages integrity, permeability, CO_2, etc.	Electrical, optical, chemical	MAP and CA	In develop.	(Bültzingslöwen *et al.*, 2002)

1.2 Optochemical Sensors for Food Packaging

An optical sensor is a device that produces optical response to the analyte of interest which can be read by an instrument or by visually detection. These sensors usually comprise an indicator dye in solution or in a suitable polymer matrix for improved sensitivity and selectivity. Of practical use for intelligent packaging are solid-state sensors which can be easily incorporated on the inside of the package and read through the material.

An ideal sensor for food packaging should fulfil a number of requirements. For example it should be inexpensive (i.e. ca. < 1.6 cents per cm^2); it should not require an expensive piece of analytical instrumentation or specially trained persons for the measurement; it should be non-toxic and have non-water soluble components that have food contact approval; it should have a sufficiently long shelf-life under typical conditions of use and it should be easily incorporated in food packages (Mills, 2005).

Very important is the monitoring of the main components of headspace gas, especially O_2 and CO_2, in MAP systems to optimize packaging conditions and improve shelf-life or relate their changes to food quality inside the pack. Other quality parameters signify food deterioration, particularly of microbial growth and enzymatic degradation, and these include RH, pH and ammonia.

For example, the latter is a breakdown product of fish muscle proteins and hence a potential indicator for fish spoilage. The concentration of ammonia in fresh marine fish increases over time, depending on fish species, temperature and other storage conditions (atmosphere, water activity (a_w), microbial cross-contamination, etc.). Increased water activity in packaged products promotes mould, yeast or bacteria growth and is hence unwanted. Sensors for RH detection find application in the research area (such as beef jerky) in order to optimize desiccant usage as an active packaging tool (ammonia and RH sensors are described in chapter 1.1.2).

1.2.1 O_2 Sensors

A number of detection methods for oxygen have been developed and used, such as the Winkler method (Broenkow, 1969; Winkler, 1888), manometric methods (Martin, 1932), oxygen electrodes (Clark, 1956), GC (Mu *et al.*, 2009) and mass spectroscopy (MS) (Boumsellek and Ferran, 2001). Their inherent limitations include intensive labour and cost, long measurement time, no real time analysis and impractical sample handling.

Optical O_2 sensors possess certain advantages over traditional methods and are able to overcome some of their limitations. Quenched luminescence oxygen sensing exploits the ability of molecular oxygen to quench luminescence of certain dyes, and this can be used for O_2 quantification by applying a non-interfering and non-destructive technique. Samples can be measured in kinetic mode, where changing properties of luminophore due to oxygen variations can be monitored or simply end-point measurements can be carried out with no delay between measurement and results. In the 1980s, the first quantitative method based on this principle was described, using either solid state sensors (Lübbers and Opitz, 1983) or (mostly for biological applications) soluble probes (Vanderkooi *et al.*, 1987).

1.2.1.1 Quenched Luminescence O_2 Detection

Luminescence is the emission of light by a substance and occurs from electronically excited states (Lakowicz, 2006). Depending on the nature of the excited state, one can distinguish fluorescence and phosphorescence. The former is the emission of photons from the singlet and the latter from the triplet excited state. When a photon is absorbed by a molecule it is excited from the ground state (S_0) to vibrational levels of excited singlet states (S_1, S_2…S_n). This occurs in approximately 10^{-15} seconds, if the energy of the photon matches the energy difference between the two states. Subsequent internal conversion passes the molecule to the lowest vibrational level of the first excited singlet state (S_1) in ~10^{-12} seconds. Fluorescence is the emission of light due to transition from S_1 to S_0 (approximately in 10^{-9} seconds). Alternatively, molecules in the S1 state can undergo an intersystem crossing to the first triplet state T_1. The emission from T_1 to S_0 is

termed phosphorescence. It typically occurs in millisecond time scale and shifts to longer wavelength (lower energy) relative to fluorescence. Due to the internal conversion of the emitted light, both fluorescence and phosphorescence, is of lower energy than the absorbed one, which is in literature described as ‘Stokes shift’ (Parker, 1968). The entire process is described by a Jablonski diagram (Fig. 1.3).

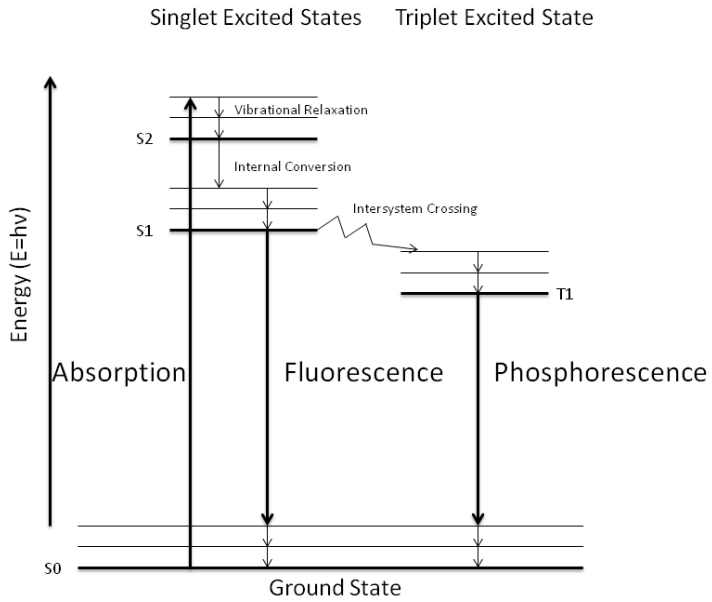

Figure 1.3: Jablonski diagram of energy transitions within molecules

In addition to luminescence emission, excited state molecules can undergo dynamic (collisional) quenching by O_2 and it is therefore diffusion limited. At a constant concentration of fluorophore and excitation intensity the molecule returns radiationlessly to the ground state resulting in a reduction of the luminescence intensity and lifetime (LT) according to the Stern-Volmer (SV) equation:

$$I_0/I = \tau_0/\tau = 1+K_{SV}*[O_2] = 1+k_q*\tau_0*[O_2] \qquad \text{Eqn. 1.1}$$

Where I_0 and I are the intensities and τ_0 and τ are the lifetimes in the absence and presence of quencher, K_{SV} is the SV quenching constant and k_q is the bimolecular

quenching constant. O_2 can be quantified by using the predetermined calibration function for luminescence intensity or LT:

$$[O_2] = (I_0\text{-}I) / (I*k_q*\tau_0) = (\tau_0\text{-}\tau) / (\tau*\tau_0*k_q) \qquad \text{Eqn. 1.2}$$

Besides the collisional quenching by O_2, a number of other quenching processes are known including photobleaching, inner filter effect, energy transfer and molecular rearrangement.

For an ideal situation of homogeneous population of luminophore molecules, a linear SV plots reflect a single quenching process. However, many solid-state sensor systems display heterogeneity of their luminescence and quenching properties resulting in a non-linear behaviour (Fig. 1.4). Due to a number of quenching processes, these sensors require more complex mathematical models to describe.

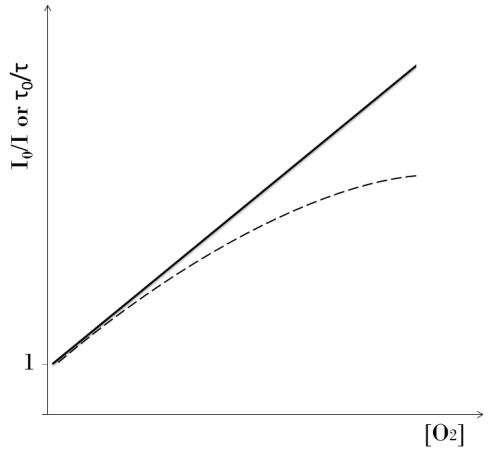

Figure 1.4: Linear (solid line) and non-linear (dashed line) SV plots.

1.2.1.2 O_2-Sensitive Materials

Porphyrin dyes

When choosing optimal dye for O_2 sensing application several aspects should be considered, such as absorbance and emission spectra, quenchability, photostability, brightness, physical-chemical properties, availability and cost. The sensitivity of the dye

is determined by the non-quenched luminescence lifetime and the SV constant. The SV equation shows that a dye with a longer lifetime in the excited state has a greater possibility of being quenched by O_2. Absorbance and emission spectra in the visible and red/near-infrared range allow one to use simple optoelectronic systems, whereas excitation in the UV range is more damaging and prone to optical interferences. High intensity illumination, exposure to ambient light and long term monitoring are key factors for their photostability.

Phosphorescent metallo-porphyrins require less expensive instrumentation and have attractive photophysical properties for practical use in sensor systems (common O_2-sensitive dyes and their properties are shown in Table 1.3). Their chromophoric moiety consists of an aromatic tetrapyrolic macrocycle which can accommodate central ligands (metal ions, protons) and peripheral substituents in pyrrole and meso-positions. Modifications can involve the macrocycle itself giving rise to chlorins, porphyrin-ketones, benzoporphyrins, aza-benzoporphyrins, etc. which have distinct (longwave-shifted) spectral and lifetime characteristics (Dolphin, 1978; Kadish *et al.*, 2010). These features provide flexibility in tuning the optical (absorption, emission) and physical-chemical (functionality, hydrophilicity, linkers) properties of porphyrin dyes and in designing new reporter molecules for sensor applications (Borisov *et al.*, 2010b; Briñas *et al.*, 2005; Khalil *et al.*, 2010).

Pt(II) and Pd(II) based porphyrins have been actively exploited in phosphorescence lifetime based O_2 sensing, providing simple, robust and versatile systems (McDonagh *et al.*, 2008; Papkovsky and O'Riordan, 2005; Stich *et al.*, 2010; Tian *et al.*, 2010; Wolfbeis, 2008). They produce longer lifetime values than ruthenium based dyes (1-5 μs), leading to a better sensitivity to oxygen quenching. Platinum based porphyrins possess lifetimes in the range of 40-100 μs, while it is increased by ~10 times for Palladium based porphyrins (400-1,000 μs).

Table 1.3: Different porphyrins -PtTFPP, PtOEPK, PtTBP- and some of their properties.

Name	Platinum(II)-tetrakis(pentafluorophenyl) porphyrin (in PS)	Platinum(II)-octaethylporphyrinketone (in PS)	Platinum(II)-tetrabenzoporphyrin (in PS)
Abbreviation	PtTFPP	PtOEPK	PtTBP
Structure	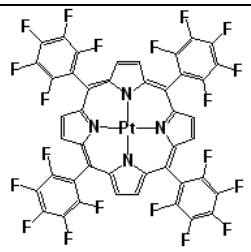	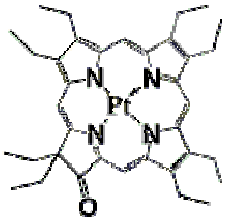	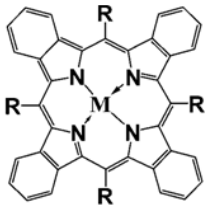
Exc./Em. (nm)	395, 508, 541 / 650	397, 590 / 760	431, 566, 617 / 777
Decay time (τ_0, μs)	~46	~61	~53
Reference	(Amao *et al.*, 2000)	(Papkovsky and Ponomarev, 1995)	(Borisov *et al.*, 2008)

Soluble O_2 probes

Soluble oxygen probes usually consist of a hydrophilic oxygen-sensitive luminescent dye in solution (small molecule probes) or linked to hydrophilic macromolecular carriers such as proteins or PEGs. In recent years micro- and nanoparticle based probes have been under active development, since this approach provides greater flexibility with indicator dyes, higher photostability and brightness. Compared to thin film solid state sensors these probes are directly exposed to the sample, they are more susceptible to interference by sample components, they contaminate the sample and they cannot be reused. On the other hand this type of probes

allows flexibility, high throughput and automation with large number of samples analysed at the same time (on a 96-well plate). These probes have been successfully used in a number of biological applications: such as, microbial growth determination (O'Mahony and Papkovsky, 2006), enzyme and cell-based screening and respirometry (Hynes *et al.*, 2006), and in food quality application such as rapid TVC (total viable count) determination in meat (O'Mahony *et al.*, 2009), fish (Hempel *et al.*, 2011) and green produce (Borchert *et al.*, 2012a).

Solid state sensors

Solid-state O_2 sensors consist of an oxygen-sensitive luminescent dye embedded in polymer material (usually hydrophobic which provides the desired sensitivity, selectivity and other operational requirements. They are usually fabricated by dissolving the components in organic solvent and applying such sensor 'cocktail' on a suitable support material followed by a drying or curing process. As these sensors need to produce a fast response to the analyte of interest, the polymer matrix needs to be permeable to oxygen. Many of such sensors have been reported and a few of them are produced commercially including the silicone rubber (Mills, 1997), modified sol-gel film (ormosils) (Basu, 2007), modified PVC (Papkovsky *et al.*, 1997), polymethyl methacrylate (PMMA) (Mills and Thomas, 1997), PS (Papkovsky, 1995) and solvent crazed polymer based O_2 sensors (Gillanders *et al.*, 2010). This sensor approach has the advantage of not contaminating the sample, continuous (depending on their shelf-life) and disposable use (as their cost is very low), and high optical signals allowing contactless and non-destructive measurements which are important for food packaging applications.

1.2.1.3 Measurement Formats

The main O_2 measurement formats are luminescence intensity at one wavelength, ratiometric intensity measurements and a more sophisticated luminescence lifetime measurement (Papkovsky, 2004). Luminescence intensity measurements on a single

wavelength are influenced by several factors such as luminophore concentration, scattering, detector performance and sample positioning (Demas *et al.*, 1999). Furthermore, a serious problem is represented by photobleaching of the luminophore which reduces luminescent signals and accuracy of O_2 determination. Compensation approaches include the use of luminophore with adequate photostability or the minimising of light exposure by reducing the intensity or duty cycle of excitation. However, alternative methodologies can be considered which are independent of these factors.

Ratiometric intensity based probes typically contain an oxygen–sensitive indicator and a reference dye incorporated in the same polymer matrix. The two dyes should be excitable at one wavelength and their emission spectra should not overlap much to keep energy transfer between the dyes to a minimum. The ratio of the emission intensities of the indicator dye and the reference dye is used to quantify the O_2 concentration, based on the pre-determined calibration. This improves system performance and stability but still cannot fully compensate for light scattering, reflection and differential sample absorbance influencing the measurement (Cywinski *et al.*, 2009).

Another approach consists of phosphorescence LT based methods for O_2 detection which have been widely used. Luminescence LT (τ) is an average time which the luminophore stays in the excited state before emitting a photon and it can be measured by time domain (TD) or frequency domain (FD) methods (Lakowicz, 2006).

In the time domain method the luminescence decay is excited by a short pulse of light (shorter than luminophore lifetime) and its kinetics is measured, and LT determined from the following equation:

$$I_t = I_0 e^{-kt} = I_0 e^{-t/\tau} \qquad \text{Eqn. 1.3}$$

I_0 and I_t are fluorescence intensities at times zero and t, respectively, k is a radiative rate constant and τ is the LT. As this approach is rather complicated a more simple method called Rapid Lifetime Determination (Fig. 1.5) has been established which enables measurement of emission intensity signals (D_1, D_2) at two delay times (t_1, t_2) and LT calculation:

$$\tau = (t_2-t_1) / \ln(D_1/D_2) \qquad \text{Eqn. 1.4}$$

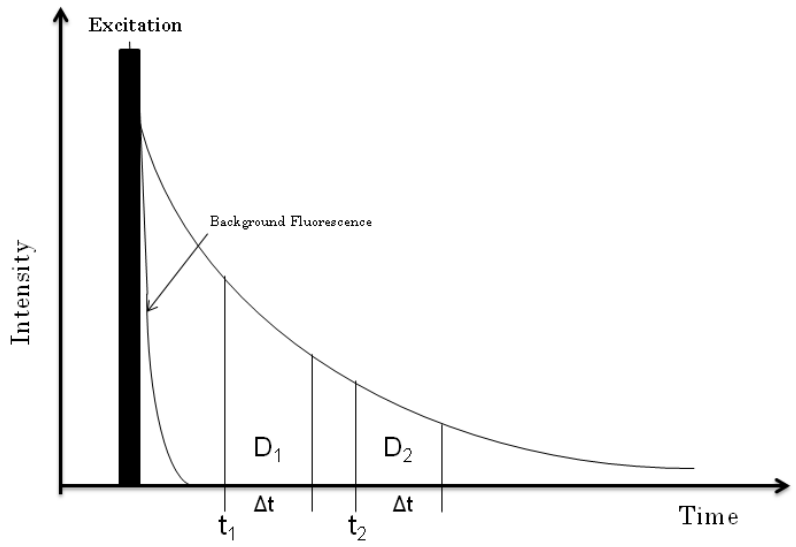

Figure 1.5: Principle of time-resolved fluorometry and Rapid Lifetime Determination method.

FD measurements require luminophore excitation with modulated excitation light (single or square wave). The phase shift (Φ) between the excitation and emission signals is measured and related to the lifetime of the dye as follows (Demas *et al.*, 1999):

$$\Phi = -\arctan(\omega*\tau), \qquad \text{Eqn. 1.5}$$

$$\omega = 2*\pi*f, \qquad \text{Eqn. 1.6}$$

where f is the frequency of excitation in Hz. This method allows simple and more robust measurement of emission lifetime, the principle of which is depicted in Fig. 1.6.

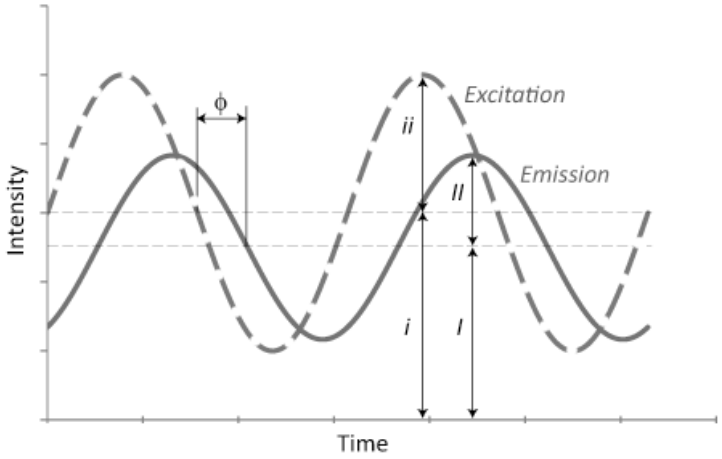

Figure 1.6: Scheme of phase modulation method (Bailey Jr and Rollefson, 1953)

LT based sensing has the advantage of reduced susceptibility to instrumental fluctuations, luminophore degradation, sensor positioning and measurement geometry.

1.2.1.4 O_2 Sensing in Food Packaging

O_2 is the main cause of food spoilage by aerobic microorganisms as they use O_2 for growth. Furthermore, many enzyme-catalyzed reactions, such as browning of fruit and vegetables or degradation of flavours and rancidity of fats are also caused by O_2. Generally, oxygen should be excluded but in certain cases it is beneficial to have elevated O_2 levels in packs, for example to maintain the natural red colour in meats, to maintain respiration (in fruit and vegetables) and to inhibit growth of anaerobic organisms (in some types of fish and in vegetables). The ability of continuous, non-invasive and quantitative measurement of O_2 using optical sensor technology during the shelf-life of a MAP product is therefore precious.A number of different O_2 sensor systems have been developed for food packaging applications.

Another system works with phosphorescent complexes of porphyrin-ketones which were designed for particular use of oxygen probes. By applying PtOEPK in thin film polymer coatings (PS) (Papkovsky, 1995) on a microporus light scattering support (e.g.

filter paper) (Ogurtsov and Papkovsky, 1998) a luminescence LT based O_2 sensor can be fabricated which is suitable for food packaging. This approach was first introduced for food packaging by Papkovsky *et al.* (2000) using FD measuring method and found application in several food products, including vacuum packed raw and cooked meat, smoked fish, MAP sliced ham and bread (Fitzgerald *et al.*, 2001), sliced ham products (Papkovsky *et al.*, 2002a), vacuum packed beef (Smiddy *et al.*, 2002a), MAP and vacuum packed chicken patties (Smiddy *et al.*, 2002b), muscle-based sous vide products (O'Mahony *et al.*, 2004) and cheddar cheese (O'Mahony *et al.*, 2006).

Furthermore, this system was optimized with an altered sensor cocktail (using benzoporphyrins incorporated into PS polymer media (www.luxcel)) and an improved scanning device called Optech™ working in the range of 0-30% with a resolution of 0.001%. Finally commercialized by Luxcel Biosciences™ and Mocon™, this system was used in various food quality studies, such as packaging containment failures in packaged cheese (Hempel *et al.*, 2012b), to monitor residual oxygen in pre- and post-pasteurized bottled beer (Hempel *et al.*, 2012a) and as quality parameter for green produce (Borchert *et al.*, 2012a).

A commercially available system called OxyDot™ and is made of $[Ru(dpp)_3](ClO_4)_2$ in silicone rubber dot (5 mm diameter, 0.2 mm thick) (http://www.oxysense). These sensors withstand pasteurisation and are produced to work in oil, water or air atmosphere. Oxysense system performs measurements in 0.1 seconds with reproducibility better than 1% (0.2% O_2). This system has already found application in oxygen scavenging studies (Li *et al.*, 2008), in MAPed soy bread with and without chemical preservatives (Pascall *et al.*, 2008), during investigations of oxygen indicators (Roberts *et al.*, 2011), etc.

1.2.2 pH Sensors

pH is usually measured in the laboratory for the control of freshness of food during storage (e.g. meat (Young *et al.*, 2004), water (Dybko *et al.*, 1997)) and it is an important parameter in food processing (as in bioreactors (Jeevarajan *et al.*, 2002; Kensy

et al., 2009)). For example, in beer brewing pH determines enzyme activity responsible for protein and saccharide degradation in mash (Briggs *et al.*, 2004).

Optical pH sensors offer the advantages of simplicity, immunity to electromagnetic interferences and they respond by changing their absorbance or fluorescence parameters. Typical absorbance based dyes are phenol red (Wu *et al.*, 2009), bromophenol blue (Ferreira and Girotto, 2009) and cresol red (Truppo and Turner, 2010, Wu *et al.*, 2010); and fluorescent - fluorescein (Jin *et al.*, 2010), pyranine (Wong and Fradin, 2011) and azo dyes (Mohr and Wolfbeis, 1994). Measurement at a single wavelength suffers from dye photobleaching, drifts in optoelectronics and measurement geometry. Ratiometric detection can overcome some of these bottlenecks by measuring at two wavelengths. This has been reported for meso substituted Pt(II) or Pd(II) porphyrin dyes (Papkovsky *et al.*, 1996) and measurement with two different LEDs (400/450 nm) providing pH detection in the range of pH = 2.5 to 7.5 (Borchert *et al.*, 2010) (see also chapter 2). Another approach uses FITC conjugated quantum dots (QD) and fluorescence ratiometric pH determination (515/600 nm). QD possess resistance to photobleaching, high brightness, narrow emission bands and broad excitation spectra (Jin *et al.*, 2010).

Very little is reported on phosphorescent pH indicators and lifetime measurements (Gonçalves *et al.*, 2008, Turel *et al.*, 2008). Luminescence of these dyes is often low and quenchable by oxygen which needs to be accounted for (Borisov *et al.*, 2010a; Niu *et al.*, 2005).

pH-sensitive indicator dyes are incorporated in a suitable polymer matrix which provides proton permeability to produce solid-state sensors. Good attachment to the support material and minimal sensor degradation and leaching of its component(s) are critical. Polyamine and polypyrrole have been found as suitable organic material for pH sensing aqueous solutions. These conducting polymers, which consist of spatially extended T-bonding, eliminate the need of organic dyes (Pringsheim *et al.*, 1997). The pH sensitivity of polyaniline and its derivatives depends on the substituent and the size of the acidic anion dopant in electropolymerization. However, hysteresis observed in UV-VIS measurements with polyaniline membranes restricts their use as optical pH sensors to a narrow pH range of 5 to 8 (Lindfors and Ivaska, 2002). Other applied

polymers are: poly(hydroxyethylmethacrylate) (Ferguson *et al.*, 1997), aminated polystyrene (quaternized) (Shakhsher *et al.*, 1994) or aminoethylcellulose fibres (Posch *et al.*, 1989).

1.2.3 CO_2 Sensors

CO_2 inhibits growth of many aerobic bacteria and moulds. In general, high level of CO_2 extends product shelf-life. Also CO_2 is absorbed by fats and water causing flavour tainting, drip loss or pack collapse. In MAP a balance needs to be struck between the commercially desirable shelf-life of a product and the degree to which its negative effects can be tolerated. Therefore, detection of CO_2 is important for food packaging, shelf-life and freshness studies (Fu *et al.*, 1992). Due to microbial growth the CO_2 concentration in packs can increase during storage, a correlation between CO_2 concentration and growth of microbes has been reported for aseptically packaged soup (Mattila *et al.*, 1990).

The main techniques for CO_2 measurement include Severinghaus type electrode, infrared (IR) spectroscopy, gas chromatography (GC), mass spectroscopy (MS) and optochemical sensors. The Severinghaus CO_2 sensor consists of a glass electrode immersed in bicarbonate buffer and covered with a hydrophobic gas permeable membrane, which detects pH changes (Severinghaus and Bradley, 1958). Its limitations are the use of liquid reagents, indirect detection or ionic form of CO_2, interference by basic or acidic gasses, slow response times and high maintenance costs. IR absorption spectroscopy allows precise and direct CO_2 detection via absorbance at 2.6 and 4.3 μm, however it suffers from strong interference by water vapour and enclosure materials (plastics) and requires rather sophisticated equipment and fixed measurement geometry (Schulz *et al.*, 2004, Thrall *et al.*, 1996). GC and MS techniques are also destructive, slow (~20 minutes), have limited throughput and require sampling and calibration (Sipior *et al.*, 1996).

Optochemical CO_2 sensors have high application potential. Initially such systems relied on the principles of a Severinghaus electrode using a pH-optode instead of the

electrode. They demonstrated simplicity, portability, low cost, fast response and flexibility, but possessed weaknesses similar to the electrodes (Neurauter *et al.*, 1999). This was overcome in 1992 by the approach proposed by A. Mills (Mills *et al.*, 1992, Mills and Chang, 1993, Mills *et al.*, 1997), in which the pH sensitive dye was incorporated in a hydrophobic polymeric membrane together with hydrophobic phase transfer reagent (PTA) such as tetraoctylammonium hydroxide (TOA-OH). The PTA forms ion pairs with the indicator molecules preventing their leaching and also retaining some water necessary for system operation (Burke *et al.*, 2006). To facilitate diffusion of CO_2 and reduce response time, a plasticizer can be added to the polymeric membrane (Schröder and Klimant, 2005).

1.2.3.1 Principle of Optical CO_2 Sensing

The majority of existing optochemical CO_2 sensors are based on pH indicators. When water is present in the sensing system, CO_2 can be detected due to its high solubility in water. Carbonic acid is formed and gets dissociated into hydrogen carbonate and carbonate ions (Mills and Skinner, 2011):

$$CO_2(g) \Leftrightarrow CO_2(aq.) \qquad \text{Eqn. 1.7}$$

$$CO_2(aq.) + H_2O \Leftrightarrow H_2CO_3 \qquad \text{Eqn. 1.8}$$

$$H_2CO_3 \Leftrightarrow H^+ + HCO_3^- \qquad \text{Eqn. 1.9}$$

$$HCO_3^- \Leftrightarrow H^+ + CO_3^{2-} \qquad \text{Eqn. 1.10}$$

As water becomes acidic through this reaction, the pH change is detected and is converted into CO_2 concentration using calibration.

1.2.3.2 Sensing Schemes and Food Packaging

Several CO_2 sensors, based on different sensing schemes, have been developed, characterized and described with the potential for food application.

Intensity based

Absorbance or fluorescence/phosphorescence based measurements usually rely on measurement of changes in absorbance or luminescence intensity. One absorbance based system incorporates m-cresol purple or cresol red in EC plastic film. These sensors are water insoluble, have long shelf-life, response and recovery time of less than 3 seconds (Mills *et al.*, 1992). A pCO_2 sensor for marine sediments is described which uses HPTS and TOA-OH in an EC matrix with a Teflon outer coating to eliminate interferences by ionic species (protons). The sensor shows a fast response in a range of 0.05 -7 hPa pCO_2 with a detection limit of 0.04 hPa (Neurauter *et al.*, 2000).

One recent example of fluorescence based CO_2 sensor uses internal referencing scheme, thus reducing the drawbacks of single wavelength systems (see chapter 1.2.1.3). The sensor comprises of sol-gel incorporation of HPTS and TOA-OH using two LEDs with emission peaks at 405 and 450 nm, quantitative CO_2 determination was achieved in the range of 0 – 30%. Response and recovery times were 39 seconds and 1.8 minutes, respectively, and limit of detection was 35 ppb (Wencel *et al.*, 2010).

Dual Luminophore Referencing (DLR)

A DLR-type CO_2 sensor consists of two luminophores incorporated in one sensing membrane. The indicator dye has typically a short lifetime whereas the reference dye has a long lifetime and ideally is unaffected by CO_2 and O_2. To use one excitation light source, photodetector and filter combination, the luminophores need to have overlapping excitation and emission spectra. Each dye generates its own luminescence signal, which can be represented as two sine waves (shown in Fig. 1.7), resulting in superposed amplitude and phase signals (total signal).

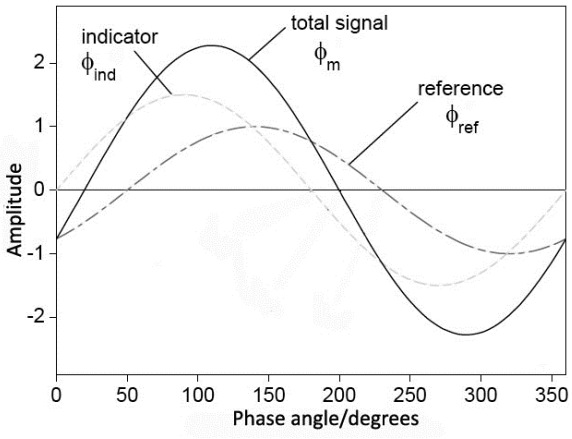

Figure 1.7: Total sine wave signal, generated by superposition of the indicator and reference dye signals (adapted from Bültzingslöwen, 2004).

The phase shift, φ_{ind} for the indicator dye is close to zero due to its very short lifetime, and φ_{ref} for the reference dye is determined by the modulation frequency f and decay time. The resulting phase is a superposition of these two signals and is expressed as total measured signal φ_{total}. If the indicator signal changes its amplitude due to an alteration of the CO_2 concentration, this affects the measured phase shift (Bültzingslöwen *et al.*, 2002). This detection scheme is compatible with the well-established phase-fluorometric oxygen sensor technology and allows robust lifetime-based detection of CO_2 with all the advantages of this method (see 1.2.1.3).

This DLR scheme has been applied to the determination of ions (Huber *et al.*, 2000), pH (Liebsch *et al.*, 2001), amines (Mohr *et al.*, 2001) and CO_2 (Bültzingslöwen *et al.*, 2002). Such CO_2 sensor for the range up to 100% CO_2 uses fluorescent pH indicator 1-hydroxypyrene-3,6,8-trisulfonate (HPTS) and long-decay reference dye $Ru(dpp)_3^{2+}$ immobilized in a hydrophobic organically modified silica (ORMOSIL) matrix. By changing the PTA TOA-OH to CTA-OH it was possible to increase measurable range to 100% CO_2 with a 13.5 degrees change of the phase shift between 0-100% CO_2. This is appropriate for modified atmosphere packaging (Bültzingslöwen *et al.*, 2002), however spectral characteristics of the sensor are not quite optimal.

A commercially available DLR based system developed by PreSens with sensors designed for the monitoring of dissolved CO_2 (beverages) within a concentration of 10-250 hPa. Such sensors spots can be located inside of glass or plastic bottles and measured non-destructively through the vessel applying fibre optic technology (http://www.presens).

Inner Filter Quenching

Absorption of excitation light and/or fluorescence by the sample called inner filter effect was also used in solid-state CO_2 sensors (Leese and Wehry, 1978). When using long-decay indicator dyes, the sensor material needs to be O_2 impermeable to eliminate O_2 quenching (see chapter 1.2.1.1). One such system consists of a phosphorescent platinum octaetylporphyrin (PtOEP) and a pH-sensitive α-naphtholphthalein (NP) dye in poly(vinylidene chloride-co-vinyl chloride-ethyl cellulose) (PVCD-EC) thin films or microparticles having low permeability to oxygen (de Vargas-Sansalvador *et al.*, 2009). These sensors showed fast response times (<9 s), reproducibility and shelf-life of > 4 months. A low-cost handheld optoelectronic device with a paired emitter–detector diode arrangement acts as a colorimetric detector for these sensors (Carvajal *et al.*, 2010, de Vargas-Sansalvador *et al.*, 2011).

Förster Resonance Energy Transfer (FRET)

As the number of luminescent pH indicators with long lifetimes, suitable pKa values for CO_2 detection on low cost instrumentation is limited, FRET scheme can be used to couple colourimetric pH indicators with lifetime based sensors (see chapter 1.2.1.3). In this case, the signal from a colourimetric pH indicator is converted into lifetime information using the reporter dye. In the FRET scheme of CO_2 detection, a pH indicator is interacting with a long decay reference dye which is pH and CO_2 insensitive. To produce efficient energy transfer, the emission band of the reference dye (donor) needs to have high overlap with absorption band of the pH indicator (acceptor) (as shown in Fig. 1.8) and the two dye molecules be in close proximity (usually between

20Å and 60Å) to each other. Then interaction occurs between the electronic excited states of the two dye molecules via dipole-dipole forces resulting in a transfer of energy from the donor to the acceptor molecule without emission of a photon (i.e. radiationless). The acceptor pH-sensitive dye is typically combined with a PTA such as TOA-OH to form ion pairs. Such ion-pairing sensor design usually shows robust optical response to CO_2 and allows tuning of sensitivity by changing the pH-sensitive dye (pKa value), the PTA (Bültzingslöwen *et al.*, 2002), readout modality (absorbance or fluorescence) or spectral characteristics by selecting the pair of pH indicator and reporter dye. The interaction with CO_2 is described as follows:

$$A^-Q^+ xH_2O + CO_2 \Leftrightarrow AH + Q^+HCO_3^- (x-1)\ H_2O \qquad \text{Eqn. 1.11}$$

Where AH is protonated indicator form, A^- - deprotonated form, Q^+ - quaternary ammonium base. Thus, A^- gets stabilized in the matrix by Q^+, whereas CO_2 neutralises Q^+ and forms a lipophilic hydrocarbonate ion pair within the polymer matrix. High CO_2 levels produce more protonated neutral form AH which has low absorption and FRET, while low CO_2 concentrations produce the opposite.

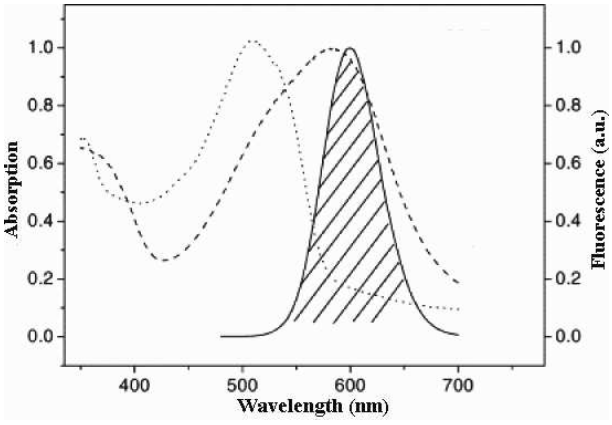

Figure 1.8: Fluorescence emission spectrum of the $Ru(dpp)_3(TSPS)_2$ complex (solid line) and absorption spectra of Sudan III in the absence (dashed line) and presence (dotted line) of carbon dioxide (100%). The hatched area demonstrates the overlap of donor and acceptor spectra (adapted from Bültzingslöwen *et al.*, 2003).

The FRET approach allows the measurement of luminescence intensity or LT (in FD or TD), and exhibits all the advantages of the lifetime based sensing. Thus far, one FRET sensor for measurement dissolved CO_2 was described which uses tetraphenylporphyrin (TPP) and NP in a poly(isobutyl methacrylate) (P(IBM)) matrix and fluorescence intensity measurements (Amao and Nakamura, 2004b). Its response and recovery times were < 6 s, and no hysteresis was observed during the measurement (Amao and Nakamura, 2004a; Amao and Nakamura, 2004b; Amao and Komori, 2005). However, decay time based systems are more suitable for CO_2 sensing and food packaging due to less susceptibility to disturbing factors. Fluorescent dyes, such as sulforhodamine 101 (SR101) (Preininger and Mohr, 1997) or ruthenium complexes (Bültzingslöwen *et al.*, 2003; Kramer *et al.*, 2009) have relatively short lifetimes of only a few nano- or microseconds. Metallo-porphyrins exhibit longer lifetimes (see chapter 1.2.1.2) and promoting the conversion of an absorbance based signal into a phosphorescence decay time signal. Furthermore, a higher sensitivity, selectivity and compatibility with cheap light sources and detectors can be obtained.

1.2.3.3 Materials for CO_2 Sensing

Since optochemical CO_2 sensors have been introduced by applying an ion transfer system using a PTA incorporated into a polymeric membrane for protection (Mills *et al.*, 1992), several systems were developed. In general sensors consist of:

a) dye(s),

b) PTA,

c) polymer(s),

d) plasticizer and

e) support material.

a) Typical indicators used are HPTS (Borisov *et al.*, 2006; Bültzingslöwen *et al.*, 2002; Burke *et al.*, 2006; Cajlakovic *et al.*, 2006; Cajlakovic *et al.*, 2009a; Schroeder *et al.*, 2007; Wencel *et al.*, 2010; Wolfbeis *et al.*, 1988), NP (Amao and Nakamura, 2004a; Amao and Nakamura, 2004b; Amao and Komori, 2005; Amao *et al.*, 2005; Carvajal *et al.*, 2010; de Vargas-Sansalvador *et al.*, 2011), thymol blue (Ali *et al.*, 2011; Borisov *et al.*, 2007; Nakamura and Amao, 2003; Neurauter *et al.*, 1999), bromthymol blue (Borisov *et al.*, 2007), m-cresol purple (Liebsch *et al.*, 2000; Mills *et al.*, 1992; Sipior *et al.*, 1996), phenol red (Cajlakovic *et al.*, 2009b), cresol red (Mills *et al.*, 1992) and recently Sudan III (Bültzingslöwen *et al.*, 2003). Depending on the sensing scheme more than one dye can be used (Cajlakovic *et al.*, 2009a). Two dyes can also be separated in two different polymer films (de Vargas-Sansalvador *et al.*, 2009). For example in the FRET or the DLR scheme the second luminophore is incorporated as reference molecule (section 1.2.3.2 Sensing schemes), in particular TPP (Amao and Nakamura, 2004a; Amao and Nakamura, 2004b; Amao and Komori, 2005; Amao *et al.*, 2005), PtOEP (Carvajal *et al.*, 2010; de Vargas-Sansalvador *et al.*, 2011; de Vargas-Sansalvador *et al.*, 2009), Ru(II)-complexes (Borisov *et al.*, 2007; Bültzingslöwen *et al.*, 2003; Burke *et al.*, 2006; Cajlakovic *et al.*, 2006; Cajlakovic *et al.*, 2009a; Cajlakovic *et al.*, 2009b; Liebsch *et al.*, 2000; Schroeder *et al.*, 2007), Eu (III)-complexes (Nakamura and Amao, 2003), sulforhodamine (SR 101) (Sipior *et al.*, 1996) or nile red (Ali *et al.*, 2011). Ideally, these dyes are insensitive to CO_2 and produce long lived emission for convenient detection. The reasons for separating them may be to protect a dye from ions or gas, or to create a spatial hindrance to avoid close proximity.

b) Phase transfer agents prevent dye leaching and retain water in the system which is necessary for system operation. To build ion pairs with the indicator, most of the developed systems use TOA-OH as PTA. To tune the measurable range of CO_2 concentrations cetyltriammonium hydroxide (CTA-OH) (Bültzingslöwen *et al.*, 2002; Burke *et al.*, 2006) and tetrabutylammonium hydroxide (TBA-OH) (Bültzingslöwen *et al.*, 2002) were used.

c) Ethyl cellulose (EC) is among the most frequently used matrix for CO_2 sensors (Ali *et al.*, 2011; Amao and Nakamura; 2004a, Borisov *et al.*, 2006; Cajlakovic *et al.*,

2009b; Liebsch *et al.*, 2000; Mills *et al.*, 1992; Mills and Chang, 1993; Mills *et al.*, 1998; Nakamura and Amao, 2003; Neurauter *et al.*, 1999; Schroeder *et al.*, 2007; Sipior *et al.*, 1996) as this polymer shows good protection properties and CO_2 permeability. Some other polymeric membranes with similar characteristics were used, for example, PVCD in combination with EC (de Vargas-Sansalvador *et al.*, 2009), sol gel matrices (Bültzingslöwen *et al.*, 2002; Wencel *et al.*, 2010) or their mixtures with EC (Bültzingslöwen *et al.*, 2003), P(IBM), hydrogel (Wolfbeis *et al.*, 1988), Eudragit RL100 (Cajlakovic *et al.*, 2006), PDMS (Burke *et al.*, 2006), P(TMSP) and silicone polymers (Borisov *et al.*, 2007).

d) Plasticizers are additives gelling the polymer, improving processability and flexibility of plastics by decreasing the viscosity, glass transition temperature and elasticity modulus of the final membrane, without alteration of the chemical composition of the polymer (Rahman and Brazel, 2004). Tributyl phosphate (TBP), dimethyl phthalate, diethyl phthalate, dipropyl phthalate, dibutyl phthalate, dioctyl phthalate and diisodecyl phthalate plasticizers were used (Mills *et al.*, 1998). In the latter study, plasticizer/polymer compatibility for EC-based sensing films was assessed including its effects on sensor sensitivity, response and recovery times.

e) A CO_2 sensor support material should facilitate sensor handling and have no influence on the performance. Typical materials are glass (Amao and Nakamura, 2004a; Borisov *et al.*, 2006; Cajlakovic *et al.*, 2006; Mills *et al.*, 1992; Nakamura and Amao, 2003; Sipior *et al.*, 1996), Mylar (Borisov *et al.*, 2007; de Vargas-Sansalvador *et al.*, 2009) and PET (Burke *et al.*, 2006; Ali *et al.*, 2011) films. Not only the working characteristics determine the choice, the intended application needs to be considered as well. For example, an optimal support material of CO_2 sensors for food packaging would be the packaging material itself, with the sensor exposed inside the package headspace.

1.2.4 Multi-Parametric Systems

Multi-parametric-systems combine the measurement of at least two parameters with one sensor system, usually by incorporating several dyes in one polymer encapsulating

media. Since O_2 is omnipresent and plays an important role during chemical, biological or enzymatic reactions, O_2 sensors are often employed in multi-sensors, such as O_2/Temp, O_2/CO_2, O_2/pH, O_2/CO_2/Temp, O_2/pH/Temp.

For determination of different parameters, different detection modalities can be applied or the signals need to be differentiated in spectral or time domains. The use of one sensor for more than one parameter will increase their practicality and cost efficiency. A variety of different systems have been developed but none of them have been used in food packaging so far.

An O_2/Temp sensor can be realized using two metalloporphyrins: PtTFPP-lactone which is highly sensitive to O_2 but also to temperature and MgTFPP which is unaffected by O_2 but responds to temperature (Gouterman *et al.*, 2004).

An approach to O_2/CO_2 sensing makes use of PtTFPP in PS for O_2 detection and HPTS (ion paired with TOA-OH) in EC microparticles incorporated in a PDMS rubber as second layer. Another sensing scheme uses DLR method where the reference molecule is composed of iridium(III) curmarin complex microparticles in a PAN-PAA matrix (Borisov *et al.*, 2006).

Dual sensing of O_2 and pH is from material point of view more difficult as the O_2 sensing requires usually materials that are highly sensitive to O_2 but impermeable to protons and for pH sensing the contrary is the case. This problem was solved in a sensor for natural marine sediments based on time-resolved luminescence pH/pO_2 mapping with a lipophilic fluorescein derivative and PtTFPP immobilized in a hydrogel matrix. As the pH sensitive fluorescein is lipophilic enough not to get washed out from the polymer it is permeable to both O_2 and ions (Schröder *et al.*, 2006). Alternatively, two different sensing modalities can be applied to detect the pH and O_2 individually. An approach has been recently developed based on meso metallo-porphyrins which is described in detail in chapter 2.

1.3 Microbial Sensors

Most natural foods have limited shelf-life and deteriorate quickly. Food spoilage can happen due to moulds, yeast or bacteria or natural degradation and make the product unsuitable for intake as it could cause serious illnesses and death as a result. Enzymes present in food also induce chemical changes and cause loss of flavour, colour and texture, due to breakdown of tissue and other components resulting in oxidation, browning and ripening.

Endogenous microorganisms as well as dangerous pathogens can also be present in food products which can cause their spoilage and serious harm to consumers. Therefore, development on food safety is focused on detection of microbial pathogens *Salmonella*, *Listeria*, *E.coli* and other hazardous microorganisms. TVC determination provides a general estimate of the microbial population. Microbial testing is done by many food microbiology laboratories for the purpose of revealing important information about the status of a food product, whether it can be consumed without causing food poisoning, whether it was handled correctly, and whether it is old or fresh.

1.3.1 Traditional Methods

Conventional microbial tests are based on aerobic plate count methods, which are specified as the standard ISO 4833:2003 method in the food industry (ISO:4833:2003, 2003). Briefly, food homogenate is produced using 10 g of a sample diluted with 90 ml of a non-selective medium (1:10), and a series of ten-fold dilutions are prepared and aliquots and spread on solid agar plates. The plates are incubated for 48-72 hours at 30ºC and colonies formed are counted. This is used to calculate the microbial load (cfu/g) on the basis of the dilution factor used. Instead of using traditional agar plates, direct culture-based methods use rehydrated media contained as sheets or films. These films are covered with a fabric layer or a membrane and subsequently rehydrated by a liquid sample (e.g. food homogenate) and incubated for development of colonies on the surface. Those colonies can also be counted by using a chromogenic medium (with a

redox indicator), such as tetrazolium chloride, which produces red colonies. These methods rely on the formation of visible colonies and include incubations of at least 48 hours and counting. Examples are Compact Dry TC (Kodaka *et al.*, 2005) from Nissui Pharmaceuticals (http://www.nissui-pharm, 2009) and RIDA®COUNT Total made by R-Biopharm (Salo *et al.*, 2006; http://www.r-biopharm).

Several alternative culture-based methods are available. The SimPlate® system from BioControl (Ferrati *et al.*, 2010; http://www.biocontrolsystems) has 84 wells built in to the plate and the medium contains a patented "Binary Detection Technology" which is able to detect certain bacterial enzymes and produce a colour change. The bacteria can be determined by the assessment of the colour change pattern within 24 hours. TEMPO® from bioMerieux (Paulsen *et al.*, 2006; biomerieux, 2008), an automated quality indicator system, employs a miniaturized most probable number (MPN) technique on a multi-well card to enumerate bacteria in food samples. A fluorescent indicator is present in the media for easy and fast detection and calculation of colony forming units (cfu/g) by a reader, 500 samples can be processed within 24-48 hours. Soleris™ system by Neogen® Corporation (http://www.neogen) also monitors colour changes caused by bacterial growth, using a specially designed vial containing growth medium and colour indicators which respond to pH or other biochemical parameters. The system utilises an LED and a photo detector to monitor the vials and record the time taken to produce a detectable colour change. A result for the initial microbial count can be produced within 18 hours. The RABIT® system by Don Whitely Scientific (http://www.dwscientific) and BacTrac® by Sy-Lab (Hattula *et al.*, 2002; http://www.sylab) both apply impedance-based methods. When the microbial amount increases in the growth medium the impedance is changing, measured by a pair of electrodes. The direct epifluorescent filter technique (DEFT) by Perceptive Instruments Ltd (http://www.perceptive) uses a polycarbonate filter, which is stained with fluorescent dye. Liquid sample is filtered through and then examined by epifluorescent microscopy. The flow cytometric BactiFlow® ALS real time analyzer by AES Chemunex (Vollmer *et al.*, 2011; http://www.aeschemunex) uses fluorescent labelling technique. This method detects directly viable cells, but is limited to liquid samples and

to medium to high microbial populations. Results can be obtained within minutes or hours.

1.3.2 Rapid Microbial Tests and Biosensor Systems

Some biosensor systems for quick determination of microorganisms in food samples based on fluorescent dye technology are available. MicroFoss^{TM} by Biosys, Inc., developed by Ann Arbor, includes a computerized instrument with disposable vials based on the detection of metabolic processes of organisms. An optical sensor allows screening results in as little as 7-18 hours, depending on microbial contamination (Odumeru and Belvedere, 2002; http://www.foodsafetymagazine).

A microtitre-plate TVC test based on monitoring of bacterial respiration using phosphorescent oxygen sensing probes and fluorescent plate reader detection (Fig 1.9) was described by O'Mahony *et al.* (2006) and applied to analysis of aerobic bacteria in complex samples such as broth and food homogenates (O'Mahony and Papkovsky, 2006).

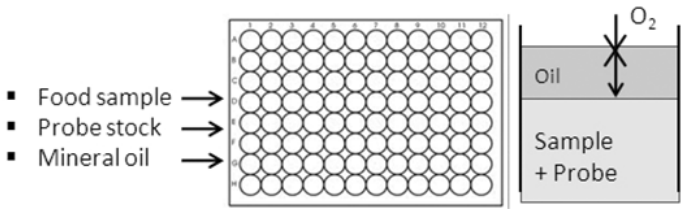

Fig. 1.9: Microtitre-plate assay format.

Initially (at relatively low cell numbers) the sample remains oxygenated and the probe fluorescent signal stays flat and low as it is quenched by dissolved oxygen. As bacteria grow the sample undergoes rapid deoxygenation (seen as steep increase of probe fluorescence) followed by leveling off when dissolved oxygen is depleted (unquenched probe). These prominent changes in probe fluorescence are due to

microbial growth and allow unambiguous identification of positive samples and quantification of their microbial load (TVC or selective) on the basis of measured threshold times (TT). At this threshold the sample containing rapidly proliferating micro-organisms starts to rapidly deplete the dissolved oxygen (producing typical profiles as seen in Fig. 1.10). The TT is related to the initial microbial population and can be used for microbial determination within 1-12 hours after instrumental calibration.

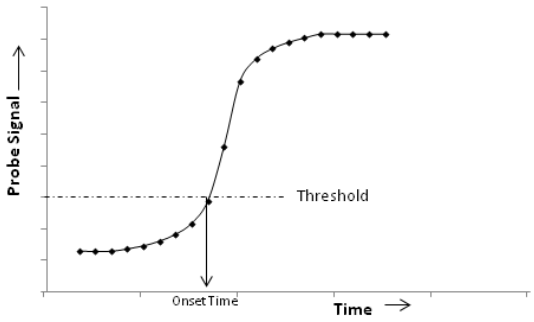

Figure 1.10: Typical profile of oxygen depletion in a food homogenate.

These assays are validated in aqueous media with different bacteria including E. *coli*, M. *luteus* and P. *fluorescence* (O'Mahony and Papkovsky, 2006), and with the enumeration of total viable counts in different food matrices such as meat (O'Mahony *et al.*, 2009), fish (Hempel *et al.*, 2011) and salad (Borchert *et al.*, 2012) (see chapter 4). This approach has been commercialised by Luxcel Biosciences^{TM} and Mocon Inc. and is now sold as GreenLight™ system.

Chapter 2: Development of a O_2/pH Multi-Parametric Sensor

2.1 Introduction

Optochemical sensors have advanced remarkably in recent years, many of them are used in different areas and applications (McDonagh *et al.*, 2008; Wolfbeis, 2008). Sensor research is now shifting towards the development of multi-parametric sensing, particularly of core analytes such as O_2, pH, CO_2, temperature, humidity, ions, as well as of more simple, robust, versatile and cost-efficient systems tailored to specific applications (Stich *et al.*, 2010). Internal referencing schemes, such as the ratiometric absorbance/reflectance/fluorescence and luminescence lifetime based sensing represented by direct quenching, DLR or FRET formats, are preferred detection modalities for such systems (Stich *et al.*, 2010). Rapid development of imaging techniques and low-cost optoelectronics provide information-rich data, miniaturization and integration, while still retaining sensor accuracy, reliability and affordable costs (Sax *et al.*, 2009; Schröder *et al.*, 2007; Wang *et al.*, 2010).

On the chemistry side, the use of arrays of discrete sensors and/or composite materials with several indicator dyes has proved efficient for O_2/T, O_2/pH, O_2/T/CO_2, O_2/T/pH and some other analyte panels (Stich *et al.*, 2010; Tian *et al.*, 2010). However, increased number of ingredients, wide bands of most of the indicators which tend to overlap in the usable spectral region (350-1000 nm), cross-sensitivity and multiple practical restrictions, limit multiplexing potential, compromise performance and boost manufacturing costs of such sensors.

One way to overcome these bottlenecks is to apply multi-functional reporter molecules together with multiple detection modalities. Here, supramolecular structures possessing long-decay luminescence, large spectral shifts, and internal referencing

capabilities are particularly advantageous, providing greater scope for multiplexing. We demonstrate this concept with a dual-analyte O_2/pH sensor based on a single phosphorescent porphyrin dye.

Porphyrins have attractive photophysical properties for use in sensor systems (Borisov *et al.*, 2010; Briñas *et al.*, 2005; Dolphin, 1978; Kadish *et al.*, 2010; Khalil *et al.*, 2010; Papkovsky, 2004; Papkovsky and O'Riordan, 2005; Zhang *et al.*, 2007), especially platinum(II) and palladium(II) complexes are known to exhibit strong phosphorescence at room temperature and quantum yields of >10%. Their aromatic tetrapyrolic macrocycle can be modified by different peripheral substituents in pyrrole and *meso*-positions. These features provide flexibility in tuning the optical and physical-chemical properties of porphyrin dyes. In particular, *meso*-substituted porphyrins have been actively exploited in phosphorescence lifetime based O_2 sensing, providing robust and versatile systems (Borisov *et al.*, 2011; Vasil'ev and Borisov, 2002).

Herein, we present new solid-state materials based on the bi-functional phosphorescent porphyrin dyes, which provide simultaneous, reversible sensing of the two principal analytes - dissolved O_2 and pH, and potential for further multiplexing.

2.2 Experimental

2.2.1 Materials

Pt-octaethylporphyrin Schiff-base (PtOEP-SB) and Pd-coproporphyrin-I tetraester Schiff-base (PdCP-SB) were synthesized at the Institute of Biomedical Chemistry, Moscow as described previously (Papkovsky *et al.*, 1997). Tetrahydrofuran (THF), chloroform, high molecular weight poly(vinyl chloride), bis(2-ethylhexyl) sebacate (DOS), sodium sulfite were from Sigma Aldrich. The PTAs TCPB, TBPB and TTB were from Fluka. Standard gas mixtures (O_2 balanced with N_2) were from Irish Oxygen.

2.2.2 Methods

2.2.2.1 Sensor Fabrication

Sensors were fabricated by dissolving 120 mg of PVC and 240 mg DOS in 3 g THF, and adding PtOEP-SB or PdCP-SB dye and PTA (borate salt) in the required quantities (Table 2.1). The cocktail was spotted in 2 µl aliquots on polyester film Mylar® and dried to produce thin film sensors of ~10 mm in diameter.

Table 2.1: Sensor cocktail and coating composition.

Components	**Cocktail**	**Sensor Coating [%]**
Solvent	~94,75% (w/w)	-
PVC	1.75% (w/w)	30.8-32.55 (w/w)
Plasticizer	3.5% (w/w)	61.6-65.09 (w/w)
PtOEP-SB or	0.25 mM	0.36 (w/w)
PdCP-SB	0.1 mM	0.16 (w/w)
PTA	2.5-8 mM	2.36-7.6 (w/w)

2.2.2.2 Optical Measurements

UV-Vis absorption spectral measurements (range 350 – 700 nm) were carried out on a HP8453 diode-array spectrophotometer (Agilent). Phosphorescence spectral measurements (range 350 – 600 nm for excitation and 600-750 nm for emission) were carried out on Cary Eclipse fluorescence spectrometer (Varian). Time resolved fluorescence (TR-F) measurements were performed on Victor^2 multilabel reader (Perkin Elmer), using 340 nm excitation and 665 nm emission filters. Phosphorescence lifetime measurements on the Victor reader were carried out by taking TR-F intensity readings at two different delay times, 30 and 70 µs with a window time of 30 µs and calculating the lifetime according to following formula: $\tau = t_1\text{-}t_2/\ln(F_1/F_2)$ (O'Riordan *et al.*, 2007).

Measurements on a Cary Eclipse fluorometer were made using a built-in short phosphorescence decay option and lifetime determination by single or double exponential fits.

2.2.2.3 Sensor Preparation

Measurement of optical responses of the dual-analyte sensors to pH and O_2 were conducted using 13 x 60 mm pieces of sensor membranes inserted diagonally in a standard 1 cm quartz cell or placed in the wells of a 24-well plate (Costar) and submerged in an aqueous buffer.

2.2.2.4 pH Calibrations

pH calibrations were conducted by adjusting the pH of the buffer inside the cuvette or micro-well to different pH values (using calibrated pH meter Jenway 3310) and measuring after ~10 min equilibration changes in sensor absorption on the UV-Vis spectrophotometer or changes in emission intensity on the Victor^2 reader. From this data, sensor pKa values were determined by plotting intensity vs. pH and to find the inflection point that will point to the pKa value. This is done at a certain wavelength after correcting the intensity values. To reduce influence of the sensor matrix, control sensors were prepared and a blank reading without dye was performed. Sensor response time to changes in pH was typically around 3 min.

2.2.2.5 Oxygen Calibrations

Oxygen calibrations were performed on Cary Eclipse spectrometer. The cuvette with sensor and buffer of known pH was bubbled with standard O_2/N_2 gas mixtures (0-21 kPa oxygen) produced and delivered by precision gas mixing unit (LN Industries SA). Temperature control was set at 30 or 37˚C. Upon gas equilibration, phosphorescence decay was measured and lifetimes calculated from double exponential fits with subsequent calculation of average lifetime.

2.3 Results & Discussion

2.3.1 Spectral Properties

The reporter dyes comprise the derivatives of hydrophobic Pt-octaethylporphyrin (PtOEP) and Pd-coproporphyrin-I tetraester (PdCP) which contain an additional pH-responsive moiety - Schiff-base group (SB) at one meso-position proximal to the macrocyle (Fig. 2.1A). In unprotonated state these dyes display normal porphyrin type of electronic spectra, with intense Soret and several minor visible absorbance bands, and bright room temperature phosphorescence in the red region which is readily quenched by O_2. Like for normal porphyrins, the spectra of PdCP-SB are slightly red-shifted compared to PtOEP-SB (Fig. 2.1B), and the emission lifetime is several-fold longer (Table 2.2). At the same time, protonation of the peripheral SB group is accompanied by a major change in electronic spectra due to the formation of a delocalised carbocation (Papkovsky *et al.*, 1997). This process shifts absorption maximum from approximately 398 nm to 443 nm, with the disappearance of porphyrin-type spectra and phosphorescence. The protonation is reversible (though very high pH can degrade the dye), thus allowing sensing of pH by absorbance or phosphorescence measurements.

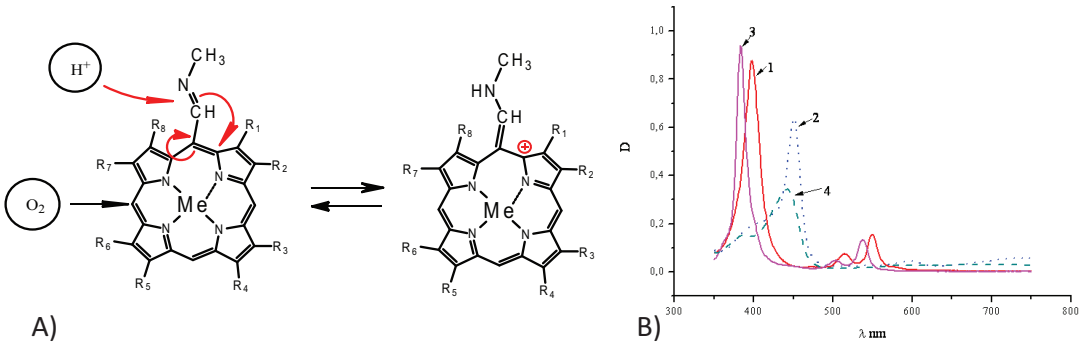

Figure 2.1: A) General chemical structures of the PtOEP-SB (Me = Pt^{2+}, R_1-R_8= CH_2CH_3) and PdCP-SB (Me = Pd^{2+}, R_1,R_3,R_5,R_7=CH_3, R_2,R_4,R_6,R_8 = $CH_2CH_2COOCH_3$) showing interaction sites for H^+ and O_2. B) Changes in absorption spectra in methylene chloride upon the addition of trifluoroacetic acid (1-PdCP-SB, 2-PdCP-SB + TFA, 3-PtOEP-SB, 4-PtOEP-SB + TFA).

2.3.2 Oxygen & pH Sensing

For optochemical sensing of physiological O_2 concentrations (range 0-25 kPa or 0-250 μM) and pH (range 5-9) in a convenient format, the reporter dye has to be embedded in a polymeric matrix which provides the desired sensitivity and selectivity for the two analytes and robust optical responses (McDonagh *et al.*, 2008; Wolfbeis, 2008). Hydrophobic polymers with moderate O_2 permeability commonly used in O_2 sensors (e.g. polystyrene and alike) are not very suitable as they are impermeable to protons. Likewise, many polymers employed in conventional pH sensors show inadequate O_2 quenching (in ethyl cellulose Pt-porphyrins are quenched too much by ambient O_2 producing low phosphorescent signals). After testing several different polymeric matrices, we found plasticized PVC to possess the required characteristics, and selected it as sensor matrix. Plasticizer content is known to affect O_2 quenching in polymers (Hartmann and Trettnak, 1996), therefore it was maintained constant (63±1.5% w/w). The availability of two phosphorescent dyes with different lifetimes and sensitivity to O_2 facilitated the development of O_2/pH sensitive materials and tuning their characteristics. Possible self-quenching in semi-liquid PVC membranes was also

assessed to optimize dye concentration. Phase transfer additive such as potassium tetrakis(4-chlorophenyl)borate (TCPB) was introduced to allow proton transfer (McDonagh *et al.*, 2008; Wolfbeis, 2008). Following the initial selection, sensors of different composition were prepared and studied with respect to their photophysical, O_2 and pH sensing properties and operational performance. Sensors were made by dissolving their components in organic solvent (THF and $CHCl_3$) and casting the cocktail on polyester Mylar® film, to produce ~5 μm thick coatings (Table 2.1).

Table 2.2: Main characteristics of the PtOEP-SB and PdCP-SB sensors.

Reporter Dye/sensor No	**Absorbance Maximum** [nm]	**Phase Transfer Agent** [%] (w/w)	**pK ***	**Emission Lifetime **** [μs]
PtOEP-SB	398 (pH 8.0)			
N1	443 (pH 2.0)	2.4 (TCPB)	5.9	32.8
N2		4.1 (TCPB)	6.5	31.0
N3		5.7 (TCPB)	7.0	n.m.
N4		7.6 (TCPB)	6.1	n.m.
N5		7.6 (TBPB)	<4.0	n.m.
N6		7.6 (TTB)	<4.0	n.m.
PdCP-SB	398 (pH 8.0)			
N7	443 (pH 2.0)	4.1 (TCPB)	6.9	60.3
N8		5.7 (TCPB)	7.2	n.m.

* Phosphorescent measurements in 0.1 M K_2HPO_4, 21 kPa O_2, 30˚C; Standard deviations were ~0.2 μs or 0.1 pH, respectively, (N = 3); n.m. – not measured.

** Quenched emission LTs.

When embedded in plasticized PVC membranes, the two dyes showed similar spectral characteristics (absorption and emission), while their sensitivity to O_2 was different. Both sensor types produced the anticipated spectral response in the useful range of pH. Fig. 2.2A shows absorption spectral changes associated with dye protonation and Fig. 2.2B - pH calibration produced by ratiometric absorption measurements (443/397 nm). The nature and concentration of PTA (and temperature)

had a profound influence on sensor response to pH. Thus, PtOEP-SB sensors increased their pKa from 5.9 to 7.0 when TCPB content increased from 2.4 to 5.7 %, but then decreased to 6.1 at 7.6 % TCPB. Two other phase transfer reagents - potassium tetrakis (4-tert-butylphenyl)borate (TBPB) and sodium tetra(p-tolyl)borate (TTB) - produced significantly lower pKa values. Similar dependence was observed for PdCP-SB sensors with slightly more basic pKa than for PtOEP-SB. Such dependence of calibration on the nature and concentration of PTA can be due to different access of protons to the dye (also seen in other ion-selective membranes) (Hartmann and Trettnak, 1996; Papkovsky *et al.*, 1997). Therefore, by selecting the indicator dye and PTA, pH sensitivity of the sensor can be tuned, to cover the range of practical interest (pH5-8 in this case). Based on these results, PtOEP-SB *N2* and *N3* and PdCP-SB *N7* and *N8* sensors (Table 2.2) were selected for further testing of their O_2 sensitivity and phosphorescent characteristics.

According to the mechanism of protonation (Fig. 2.1), the changes in absorption were accompanied by a marked reduction in phosphorescence intensity signals (Fig. 2.2B). At low pH values in air-saturated buffer at 30˚C, the intensity of the PtOEP-SB sensors decreased by almost 70%. Residual phosphorescence was attributed to incomplete protonation of the dye in polymer membrane.

With respect to the sensitivity to dissolved O_2, the PtOEP-SB sensors showed a moderate response. Phosphorescence lifetime of the sensor with unprotonated dye in O_2-free buffer was 84 μs at 30˚C (92 μs at 24˚C), and reduced by ~70% in air-saturated solution.

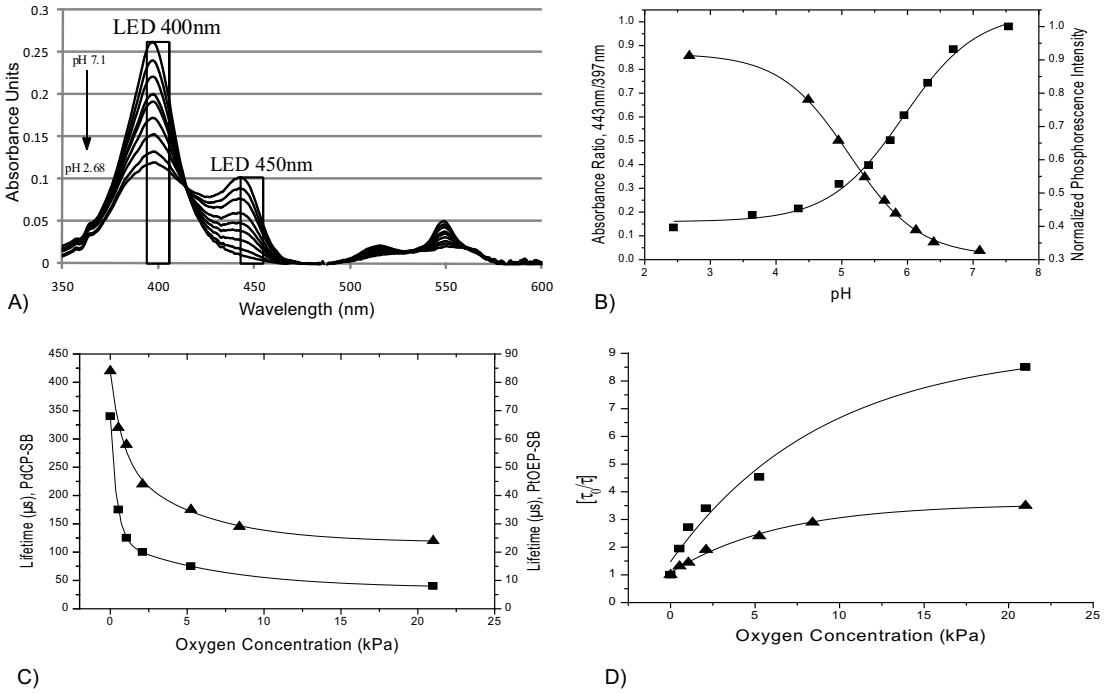

Figure 2.2: A) Absorption spectra of PtOEP-SB *N1* sensor at different pH, 24^{o}C. The bars show the bands of standard 400 nm and 450 nm LEDs. B) pH calibrations for the PtOEP-SB sensor in ratiometric absorbance (▲) and phosphorescence intensity (■) scale, 0.1M acetate buffer, 24˚C and 30˚C, respectively. C) O_2 calibrations of the PdCP-SB (■) and PtOEP-SB (▲) sensors in phosphorescence lifetime scale, 23°C. Lifetime values were produced from double-exponential fits. D) Stern-Volmer O_2 calibrations for the PtOEP-SB (▲) and PdCP-SB (■) sensors, in 0.1M K_2HPO_4, pH 8.5, 30˚C.

The PdCP-SB sensors showed several-fold longer unquenched lifetimes (360 μs at 24˚C and 340 μs at 30˚C) and therefore stronger quenching by O_2. Phosphorescence of the PtOEP-SB and PdCP-SB sensors showed double-exponential decay and a pronounced non-linearity of Stern-Volmer calibrations (Fig. 2.2D and 2.2C). Such behavior is similar to the other O_2 sensors based on Pt and Pd porphyrins (Hartmann and Trettnak, 1996; Papkovsky, 2004; Papkovsky and O'Riordan, 2005). Both sensor types were deemed suitable for lifetime-based sensing of physiological O_2 concentrations (0-250 μM), while PdCP-SB sensors better suited for the low O_2 range. Importantly, upon

protonation the sensors showed practically no changes in emission lifetime, variations were within measurement error (2-3%).

2.3.3 Cross-Sensitivity & Signal Changes

Like for the traditional pH and O_2 sensors based on similar principles (Leiding *et al.*, 2009; Niu *et al.*, 2005), operational performance of the new sensors was seen to be influenced by a number of factors. Temperature has a prominent effect on both pH and O_2 calibrations, while pH calibrations were also influenced by ionic strength. These are inherent features of the sensing schemes, which need to be considered during sensor operation. Sensor photostability was moderate: bleaching under illumination with 150 W Xe-lamp was in the region of 4% per hour (Fig. 2.3). Although not as good as for traditional O_2 sensors based on highly photostable dyes, this parameter is not critical for the sensing schemes used. Response times to pH and O_2 were within the anticipated range (2-3 min).

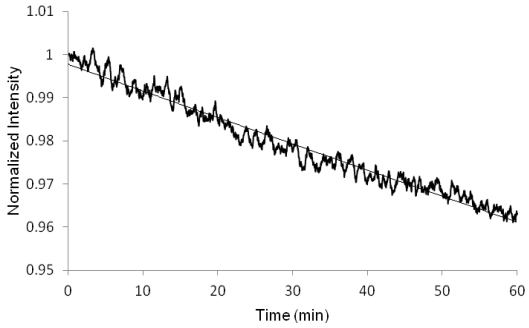

Figure 2.3: Kinetics of photobleaching of PtOEP-SB sensor. Excitation – 398 ± 5 nm, emission – 670 ± 10 nm, 0.1M phosphate buffer, pH 8.5, 23˚C.

2.3.4 Dual-Analyte Sensing Schemes

The above results show that PtOEP-SB and PdCP-SB sensors perform very satisfactory covering the ranges of high practical significance (pH 6-8 and 0-200 μM O_2). In absorbance (or reflectance) modality, sensor response to pH is independent on O_2, while ratiometric measurement (400/450 nm) provide internal referencing with stable calibration, reduced dependence on sensor alignment, measurement geometry and dye concentration. Likewise, in phosphorescence lifetime modality sensing of dissolved O_2, with internal referencing and no cross-sensitivity to pH was secured. Thus, the two analytes can be measured independently and continuously with one sensor.

Practical realization of such dual O_2/pH sensor system can be achieved with relatively simple optical schemes. Fig. 2.4A shows a setup with one LED and one photodiode with an optical filter to monitor phosphorescence intensity and lifetime (in time or frequency domain (McDonagh *et al.*, 2008; Wolfbeis, 2008)) signals from the sensor. By applying known relationships (calibrations for each analyte, compensation algorithms which account for dual sensitivity of the intensity signal), the two readings can be related to pH and O_2. Since the intensity signal is not referenced, this scheme requires fixed alignment and consideration of possible signal fluctuations (detector, sample optical properties, dye photobleaching (McDonagh *et al.*, 2008; Wolfbeis, 2008)).

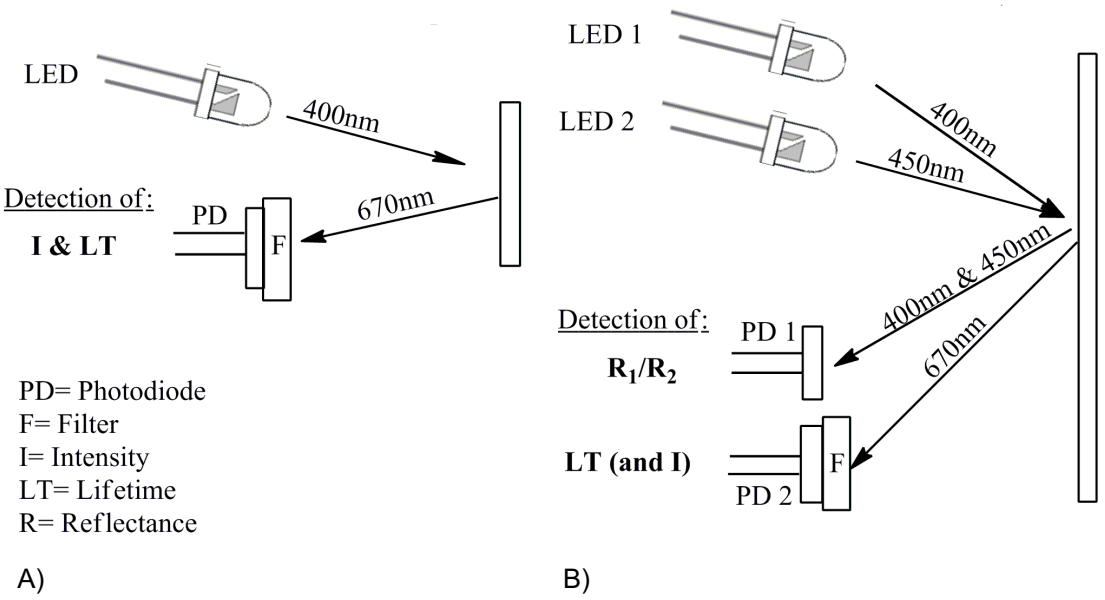

Figure 2.4: Proposed optical setups for the dual-analyte pH/O_2 sensing. A) Phosphorescence intensity (O_2, pH) and lifetime (O_2) measurements via one optical channel. B) Alternating ratiometric absorption/reflection (pH) and phosphorescence lifetime (O_2) measurements.

The alternative scheme (Fig. 2.4B) involves two LEDs shining sequentially coupled with ratiometric absorbance/reflectance based sensing of pH via PD1 and phosphorescence lifetime based sensing of O_2 via PD2. This scheme does provide interference-free, dual-analyte O_2/pH sensing with internal referencing being more advantageous than the first one. It can be implemented with two common LEDs matching the excitation and absorption maxima of the neutral and protonated forms of the dye (see e.g. Fig. 2.2A and http://www.roithner-laser).

2.4 Conclusions

This study demonstrates realization of a simple dual-analyte optochemical sensor for dissolved O_2 and pH with one bi-functional reporter dye - meso-substituted Pd- or

Pt-porphyrin Schiff-base derivative - embedded in plasticized PVC membrane. Such sensor chemistry allows sensing of each analyte in internal referencing mode and with no cross-sensitivity. Moreover, it leaves wide spectral windows (500-650 nm and 800-1000 nm) for further multiplexing with other indicator dyes including fluorescent lanthanide chelates (Fu *et al.*, 2005) and inorganic phosphors (Chen *et al.*, 2008). This approach can be applied to other types of sensor materials (e.g. nanosensors (Borisov and Klimant, 2008; Peng *et al.*, 2010), magnetic particles (Mistlberger *et al.*, 2010)), analytes (temperature, CO_2, NH_3, ions, enzyme biosensors based on O_2 and pH transducers (McDonagh *et al.*, 2008)), sensing schemes (de Silva *et al.*, 2009; McDonagh *et al.*, 2008; Wolfbeis, 2008); and also integrated with optical imaging systems.

Chapter 3: A CO_2 Sensor Based on Pt-Porphyrin Dye and FRET Scheme for Food Packaging Applications

3.1 Introduction

Several analytical techniques for CO_2 detection are available, which provide accurate and reliable data, including the Severinghaus type electrode, infrared (IR) spectroscopy, gas chromatography (GC) and mass spectrometry (MS). Their main drawbacks however are slow response time, high complexity and cost, destructiveness, limited throughput and the requirement of sampling and calibration (Severinghaus, 1958; Schulz *et al.*, 2004; Sipior *et al.*, 1996; Thrall *et al.*, 1996).

Optochemical CO_2 sensors can overcome these limitations demonstrating simplicity, portability, low cost, fast response and flexibility (Neurauter *et al.*, 1999). The working principle is described in detail in chapter 1.2.4. They show high potential for food packaging and require the sensitivity to cover the range 0-100% CO_2 (McMillin, 2008) which can be realized using indicator dyes with relatively high pK_a values. In contrast, for environmental applications and process control high sensitivity to CO_2 is usually required. To achieve fast diffusion of CO_2 and response time, a plasticizer can be added to the polymeric membrane (Schröder and Klimant, 2005).

With respect to signal readout from a CO_2 sensor, basic qualitative and semi-quantitative systems can use simple visual detection via colour change. However for accurate quantitative detection instrumental readout is usually required and in this case photoluminescence based sensors offer a significant potential. Classical approaches rely on fluorescence intensity measurements (Neurauter *et al.*, 1999), but these are affected by drifts in optoelectronic system, dye photobleaching, sample properties and measurement geometry. This can be circumvented by the schemes with internal referencing (Oter *et al.*, 2008; Petrova *et al.*, 2007; Wencel *et al.*, 2010). Thus, in ratiometric luminescence intensity scheme signals at two different wavelengths are measured, one is analyte-sensitive while the other is analyte-insensitive, and related to

each other. This improves system performance and stability but still cannot fully compensate for light scattering, reflection and differential sample absorbance influencing the measurement.

Instead of measuring changes in fluorescence intensity (Amao and Komori, 2005; Bültzingslöwen *et al.*, 2003; de Vargas-Sansalvador *et al.*, 2009; Lakowicz *et al.*, 1993), the use of long-decay phosphorescent indicator dyes and analyte-dependent changes in luminescence lifetime (LT) of the sensor (Neurauter *et al.*, 1999) can provide accurate CO_2 quantification with relatively simple instrumentation similar to the one developed for O_2 measurement. Such systems are demanding for many industrial applications, particularly food packaging (Papkovsky *et al.*, 2005). The FRET scheme for CO_2 detection is based on sensor materials with microsecond lifetimes, such as a long-decay Ru(II) complex as fluorescent donor (CO_2 insensitive) and a pH/CO_2-sensitive acceptor dye co-immobilized in a host matrix together with a PTA (Amao and Komori, 2005; Bültzingslöwen *et al.*, 2003; de Vargas-Sansalvador *et al.*, 2009; Lakowicz *et al.*, 1993). To produce optimal FRET, the two chromophores should be in close proximity and have good overlap of acceptor excitation and donor emission spectra. In this case, LT based detection with a single excitation source and photodetector can be realized (Burke *et al.*, 2006). However, systems accomplished with Ru(II) complexes have relatively short lifetimes and lifetime changes (Kosch *et al.*, 1998; Neurauter *et al.*, 1999).

In this work, we describe a polymeric solid-state CO_2 sensor which uses phosphorescent Pt-porphyrin (PtTFPP) reporter and pH-sensitive acceptor (NP) dye pair, solution FRET scheme and LT measurements. The sensor material was optimized for food packaging applications and underwent detailed characterization with respect to its CO_2 sensitivity, response and recovery times, stability, cross-sensitivity to oxygen and temperature. Sensor behaviour upon storage and operational stability in packaged foods were evaluated, and migration of sensor compounds into food was examined using standard panel of food simulants.

3.2 Experimental

3.2.1 Materials

PtTFPP dye was from Frontier Scientific (Carnforth, UK). α -naphtholphthalein (NP), poly(Isobutyl methacrylate) (P(IBM)), ethyl cellulose (EC), cetyltrimethylammonium hydroxide (CTA-OH), tetraoctylammonium hydroxide (TOA-OH), tributyl phosphate, acetic acid, lactic acid, $NaHCO_3$, NaCl, sucrose, olive oil, ethanol, hexane, ethyl acetate, trifluoroacetic acid (TFA), toluene, acetonitrile were from Sigma- Aldrich. Mylar® polyester film was from Du Pont. 1.5 ml HPLC vials with caps were from Agilent (Ireland). Aqueous solutions were prepared using Milli-Q grade water (Millipore). White trays for MAP with the dimensions 203 mm x 146 mm x 47 mm (L x B x H) made of polystyrene-EVOH- polyethylene were from Bachmann Forming AG (Hochdorf, Switzerland) and Satina® sealing film was from Cryovac (UK). Oxygen, nitrogen and carbon dioxide gases were supplied by BOC (Cork, Ireland).

3.2.2 Sensor Fabrication

Optimized CO_2 sensors were prepared by mixing 0.05 mM PtTFPP and 2.8% w/w P(IBM) dissolved in toluene with NP (13.44 mM and 36 mM) dissolved in methanol containing TOA-OH and CTA-OH (2.4% and 3.0% w/w, respectively). The resulting cocktail was applied with a micropipette in 2 μl aliquots on Mylar foil and allowed to dry overnight in a fume hood. Thus, uniformly coloured sensor spots (approximately 8 mm in diameter and ~2 μm thick) were produced. Other CO_2 sensor formulations were produced using the same fabrication method and different concentrations of the ingredients (specified in the text).

3.2.3 Sensor Characterization

Sensor spots on Mylar support were cut out as 13 mm x 30 mm pieces and fitted inside a quartz cuvette or in 13 mm x 13 mm pieces and fitted in a metal flow cell connected with PEEK tubing to a precision gas mixing unit (LNI Industries, Switzerland). The flow-cell with the sensor was inserted in an absorbance or fluorescence spectrometer where optical measurements were conducted. Absorbance measurements were carried out on a HP8453 diode-array UV-Vis spectrophotometer (Agilent). Phosphorescence excitation and emission spectra and lifetimes were recorded on a fluorescence spectrometer Cary Eclipse (Varian). Phosphorescence decay was measured under the following settings: excitation wavelength - 390 nm, emission wavelength – 647 nm, slits – 5 nm, and lifetimes were determined from single exponential fits. For calibration, sensors were flushed sequentially with 0%, 1%, 2%, 5%, 10% and 100% of CO_2 (correspond to 0 kPa, 1 kPa, 2 kPa, 5 kPa, 10 kPa, 100 kPa; in the following text percentage values will be given) at constant temperature (4°C, 14°C or 24°C). After sample equilibration with CO_2, a standard phosphorescence decay curve was recorded and then fitted.

3.2.4 Stability Studies

In shelf-life stability studies, sensors were stored at -20°C, 4°C and 22°C (RT) for the specified time, then brought to RT for 30 min, measured at this temperature and compared with freshly made sensors. Each sensor was measured repeatedly at several different storage times and then average signals were used to construct profiles.

In the food trials sensors were exposed to ready-to-eat mixed salads in white polystyrene-EVOH- polyethylene trays (dimension: 203 mm x 146 mm x 47 mm (L x B x H), volume: 750 ml). The commercially Florette salad pouch, contained the leaves frisee, lambs, lettuce and radicchio, was purchased from a local retailer. After incorporation in packs (3 sensors and 30 g of salad in each pack) the packs were sealed with Satina film under O_2 = 21.55% and CO_2 = 6.6%, 100% humidity and stored at

3.5°C. During storage gas composition inside the packs was controlled with a needle-type Checkmate 9900 O_2/CO_2 gas analyzer (PBI Dansensor). On days 0, 11 and 26, one pack was sacrificed, sensors were extracted and their characteristics were analyzed under standard conditions on the Cary spectrometer.

Migration of sensor components was studied as described previously (O'Riordan *et al.*, 2005), using standard set of food simulants and analysis of migrating components (PtTFPP and NP) by HPLC. Sensors were submerged in 1 ml of each simulant and incubated in a capped vial for up to three weeks at 37°C on a shaker. From aqueous simulants hydrophobic PtTFPP was recovered by extraction with equal volume of hexane: mixing 600 µl of each, agitating on a shaker overnight, separating the organic layer and analyzing it by normal phase HPLC. The more polar NP dye was analyzed directly by reversed phase HPLC.

An HPLC 1100 series system (Agilent) consisted of a quaternary pump, autosampler, and diode-array UV-Vis detector was used. PtTFPP was analyzed on a normal phase column SGMS-250 HILIC WPSD (4.5 mm x 100 mm, 2 µm) equillibrated with hexane, in which 5 µl aliquots of samples were injected and eluted with an ascending gradient of ethyl acetate (0-20% over 15 min). PtTFPP peak was identified by spectral analysis and quantified based on the peak hight and calibration produced with the standard.

Similarly, NP migration was assessed on a reversed phase column ZORBAX eclipse XDB –C18 (4.6 mm x 50 mm, 5 µm) (Agilent), in which 5 µl aliquots were injected in water/1% TFA (solvent A) and eluted with an ascending gradient of acetonitrile: 0-100% over 15 min.

3.3 Results & Discussion

3.3.1 FRET Scheme of CO_2 Sensing

In the FRET scheme of CO_2 sensing, PtTFPP is acting as a donor from which emission energy (band at 650 nm) is transferred to the deprotonated form of NP absorbing in the same region (Fig. 3.1). The NP dye, which has pK_a of about 8.0, is combined with a PTA such as TOA-OH to form ion pairs, as it has previously been used in CO_2 sensors (Amao and Komori, 2005; de Vargas-Sansalvador *et al.*, 2009). The interaction with CO_2 is described as: $A^-Q^+ xH_2O + CO_2 \Leftrightarrow AH + Q^+ HCO_3^- (x-1)H_2O$, were AH is protonated indicator form, A^- - deprotonated form, Q^+ - quaternary ammonium base. Thus, A^- gets stabilized in the matrix by Q^+, whereas CO_2 neutralizes Q^+ and forms a lipophilic hydro carbonate in the polymer.

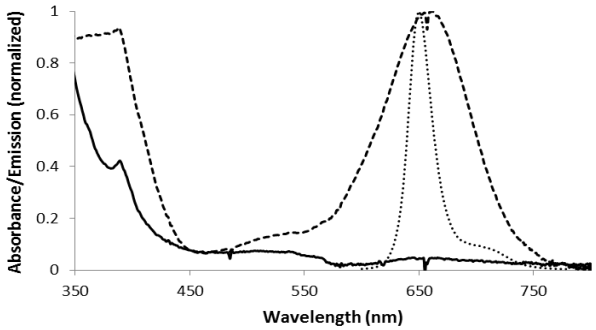

Figure 3.1: Overlap of the absorption spectrum of NP (dashed line - in 100% N_2 and solid line – in 100% CO_2) with emission spectrum of PtTFPP (dotted line).

For this system acceptor absorption is high when NP is ion-paired with TOA-OH (A^- which exists at low CO_2 concentrations), while at high CO_2 NP converts into protonated neutral form AH which does not absorb at 650 nm. Therefore FRET from PtTFPP to NP is highest in the absence of CO_2 and decreases to negligible values at high CO_2 concentrations. Such ion-pairing sensor design usually shows optical response to CO_2 and allows tuning of sensitivity by changing pH-sensitive dye or their pK_a value,

the PTA (Bültzingslöwen *et al.*, 2002), readout modality (absorbance or fluorescence) and spectral characteristics by selecting the reporter dye.

3.3.2 Optimization of Sensor Composition

For the new FRET based CO_2 sensing scheme PtTFPP was chosen as reference dye. Ruthenium dye, although showing a good spectral overlap with the indicator and reduced cross-sensitivity to O_2, has much shorter LT, smaller response to CO_2 (< 2 μs) (Bültzingslöwen *et al.*, 2002; Kosch *et al.*, 1998), and higher hydrophilicity which may result in significant leaching. Firstly, it was necessary to optimize sensor composition to produce sufficiently high phosphorescent signals, significant LT changes which are easy to measure and which occur within the desired CO_2 range (ideally 0% - 100%). Very high concentrations of the dyes can interfere with reporter emission (PtTFPP) due to excessive FRET or self-quenching. Whereas at low concentrations, phosphorescent signals, FRET efficiency and lifetime changes become small and hard to measure. We therefore prepared sensor formulations with different concentrations of PtTFPP, NP and quaternary ammonium base. Two different polymers: P(IBM), with and without tributyl phosphate plasticizer and EC were assessed.

From this screening (results not shown), P(IBM) was chosen as preferred encapsulation matrix, (one component matrix), hydrophobic and producing reproducible results. The use of plasticizers was abandoned as they produced sticky, semi-liquid structures, not very suitable for food and packaging applications. We then produced P(IBM) based sensors having different composition (Table 3.1) and examined their spectral characteristics, response to CO_2 (at room temperature and constant O_2 = 0%) and physical properties (appearance, liquidity, etc.).

Table 3.1: Composition of optimal sensor formulation (sensor 1) and sensors with altered PtTFPP (sensors 1, 2, and 3), NP (sensors 1, 4 and 5) and TOA-OH (sensors 1, 6 and 7) content in dry material.

Solid state sensor	Sensor 1 [mM]	Sensor 2 [mM]	Sensor 3 [mM]	Sensor 4 [mM]	Sensor 5 [mM]	Sensor 6 [mM]	Sensor 7 [mM]
PtTFPP	1.0	2.0	6.0	1.1	0.9	1.0	1.0
NP	270	270	270	74	444	270	270
TOA-OH	789	763	759	835	725	395	1578

In the first place the response to CO_2 can be seen as a colour change from blue to colourless (Fig. 3.2). This feature is advantageous for semi-quantitative visual detection of CO_2 leaks in packages. Notably, most of the changes in sensor absorption occurred within 0% - 10% CO_2 range, at higher CO_2 levels no further color changes were seen (flat response).

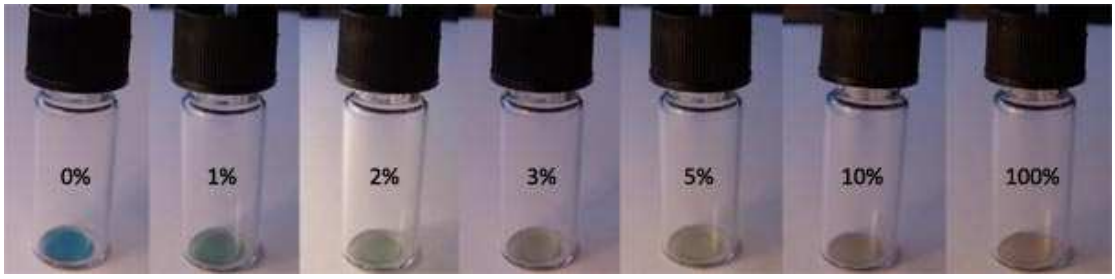

Figure 3.2: The colour change in Sensor 1 mainly takes place in the range of 0 – 10% CO_2, but is depicted for the entire range up to 100% CO_2.

Fig. 3.3A shows phosphorescence intensity signals at 650 nm under 390 nm excitation (correspond to PtTFPP, NP is non-luminescent) from Sensor 1 at different CO_2 %. The phosphorescence intensity is increasing at higher CO_2 concentrations and higher PtTFPP concentrations. The sensors were also exposed to alternating CO_2 concentrations (100% and 0% CO_2, at RT) while monitoring their phosphorescence

intensity signal. Fig. 3.3B shows that they responded in a reversible manner changing its phosphorescent signal from 32.5 to 6.5 intensity units. Sensor response time when changing from 0% to 100% CO_2 was 1 min (99.9%) and recovery time - 4 min (99.9%). Smaller steps of CO_2 concentration were seen to produce similar response times (not shown). Signal drift during the measurement was minor. Under intense constant illumination the sensor showed a drift of 6.5% per hour, which was quite acceptable for the application.

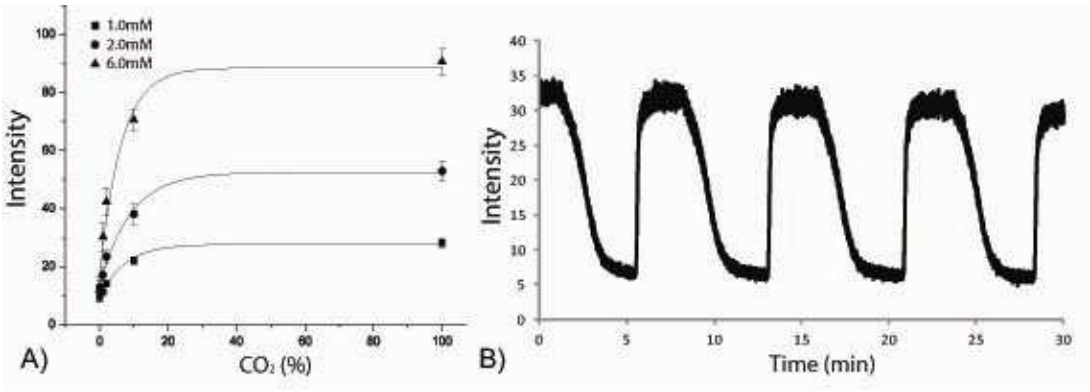

Figure 3.3: A) Changes in phosphorescence intensity (λ = 650 nm) in response to CO_2 concentration for three different sensor formulations, R^2■ = 0.946, R^2● = 0.961, R^2▲ = 0.921 (exponential fit). B) Response and recovery time of sensor 1 to alternating of 100% CO_2 and 100% N_2.

The observed changes in phosphorescence intensity signal can be due to FRET and/or reabsorption of PtTFPP emission by NP. The contribution of FRET to the quenching can be devised by measuring changes in phosphorescence lifetime at different CO_2 levels (reabsorption does not affect the lifetime). And indeed, this system showed significant changes in the LT of PtTFPP in response to changing CO_2 concentration. Fig. 3.4A illustrates the changes in phosphorescence LT for the different sensors from Table 1 measured at 100% CO_2 and 100% N_2. One can see, that increased PtTFPP concentration (sensors 1,2,3) had a small effect on the sensor, causing a moderate increase in LTs at 100% CO_2 and 100% N_2 but changing substantially the

sensitivity. The NP (sensors 1,4,5) and TOA-OH (Sensors 1,6,7) concentration dependence of the response produced a bell shape, with the optimum close to Sensor 1 composition. From Fig. 3.4B one can conclude that a PtTFPP concentration of 1.0mM provides the most appopriate sensitivity and phosphorescent signals. Based on these results, sensor 1 formulation was selected for more detailed investigation.

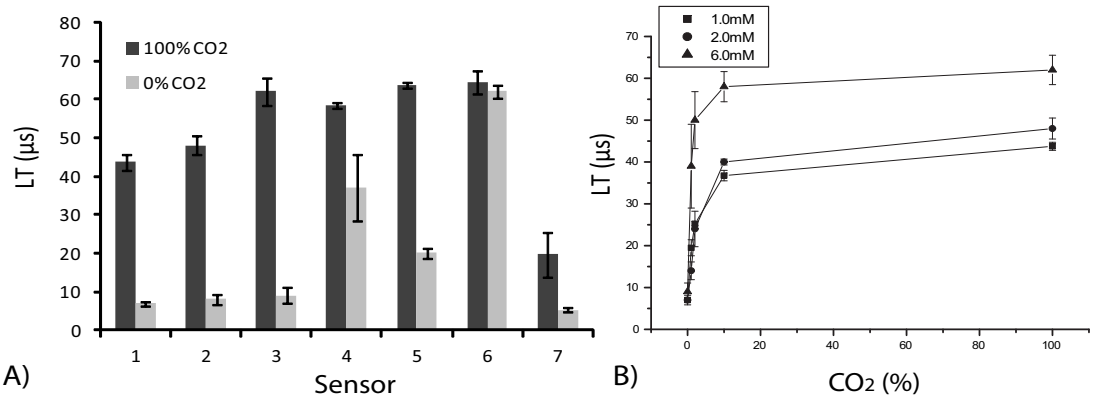

Figure 3.4: A) LTs of different sensor formulations (see sensor 1-7 in Table 1), measured in 100% CO_2 and 0% CO_2 (T = 24°C) and B) Calibrations for sensor 1, 2 and 3. N = 3.

3.3.3 Detailed Characterization and Stability Study of Sensor 1 Formulation

Sensor UV-Vis absorption and spectral changes at increasing CO_2 concentrations in the gas phase are shown in Fig. 3.5. One can see that absorption is dominated by NP which produces a large reduction in absorbance in the region of PtTFPP emission (650 nm) by converting from the charged deprotonated form into uncharged protonated form: A^- (coloured) + H^+ ↔ AH (colourless). The changes in absorbance at varying CO_2 concentrations are concurrent with the changes in phosphorescence intensity of the sensor. Soret absorption band of PtTFPP can also be seen as a small shoulder at 390 nm.

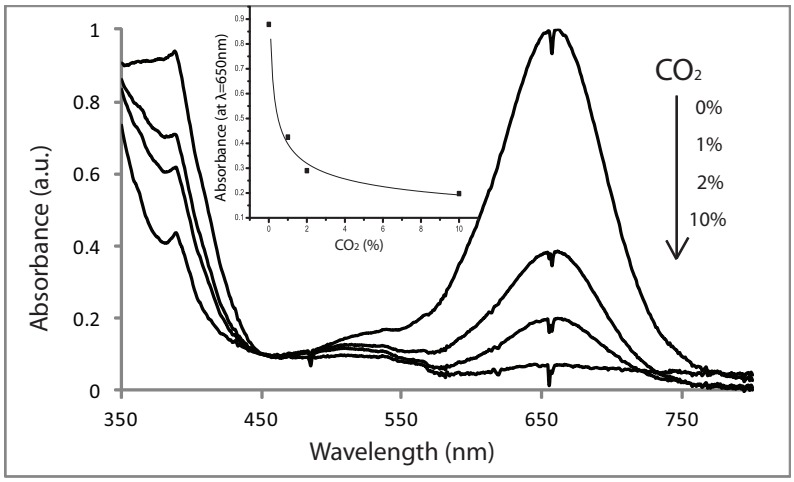

Figure 3.5: Changes in UV-Vis absorption for Sensor 1 formulation at different CO_2 concentrations. Inset shows A_{650} as a function of CO_2 %.

For the long-decay emitting PtTFPP, we anticipated cross-sensitivity to O_2, which can penetrate the polymer matrix and quench the phosphorescence lifetime. Phosphorescence lifetime-based sensing of CO_2 was the main goal of this study. We therefore conducted detailed lifetime calibrations of the CO_2 sensor at several different temperatures (4, 14 and 24°C) and O_2 concentrations (0-21%). This allowed us to reconstruct the 3-dimensional calibration map. The results are shown in Fig. 3.6.

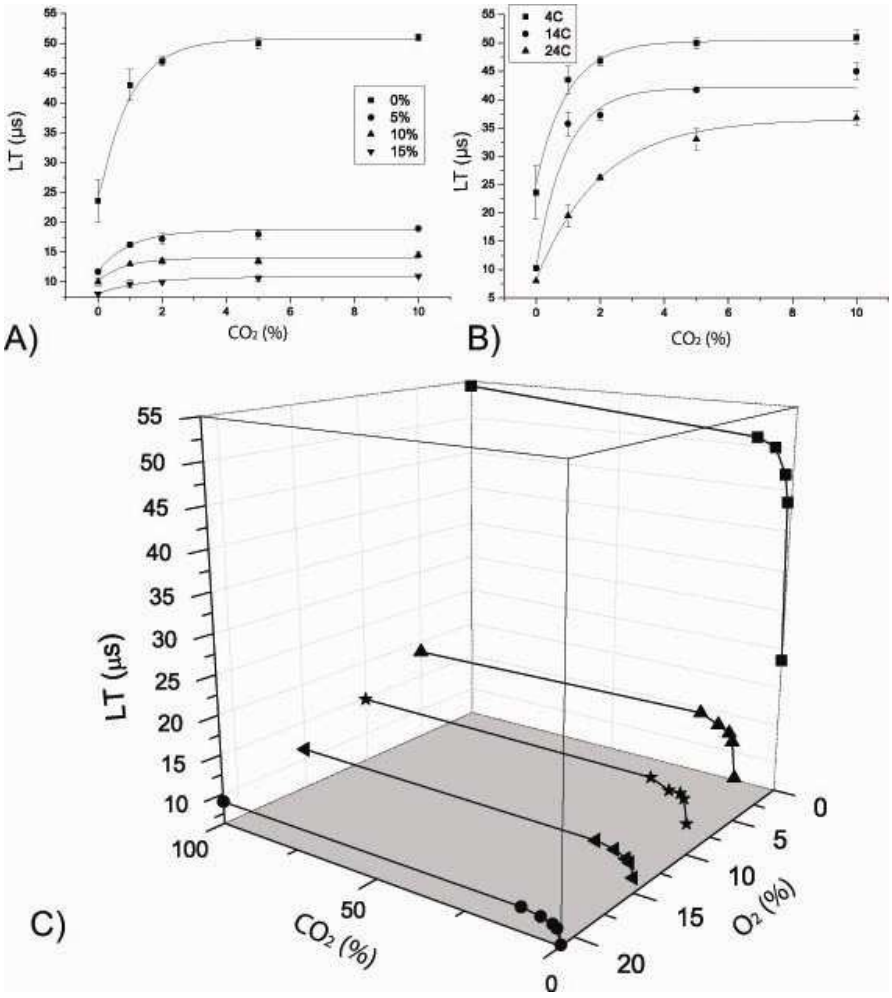

Figure 3.6: Lifetime calibrations for Sensor 1: A) At different O_2 levels (T = 4°C), exponential fit: R^2■ = 0.983, R^2● = 0.989, R^2▲ = 0.945 and R^2▼ = 0.981; B) At different temperatures (O_2 = 0%), exponential fit: R^2▲ = 0.998, R^2● = 0.995 and R^2■ = 0.983; and C) CO_2 3-D surface for different CO_2 & O_2 concentrations (T = 4°C). All points represents N = 3.

The majority of existing CO_2 sensors are known to have limited shelf-life, and the reason of that is not very well understood (Fernandez-Sanchez *et al.*, 2007; Mills and Skinner, 2010). We therefore investigated this feature for the new sensors under different storage conditions. Firstly, batches of sensors were incubated at different temperatures over several weeks in air atmosphere and tested measuring their basal

lifetime and CO_2 calibration every 3 days for the first 3 weeks, then once a week. Increased basal lifetime in pure nitrogen and visual color change can be used for the assessment of sensor deterioration. Figure 3.7A shows that at RT the sensors are stable for up to 8 days, but then quickly go off within ~3 days. At 4°C they were usable for up to 2 weeks and then started to deteriorate but at a much slower rate (several weeks). Finally, at -20°C no deterioration occurred and even after 50 days the sensors remained usable.

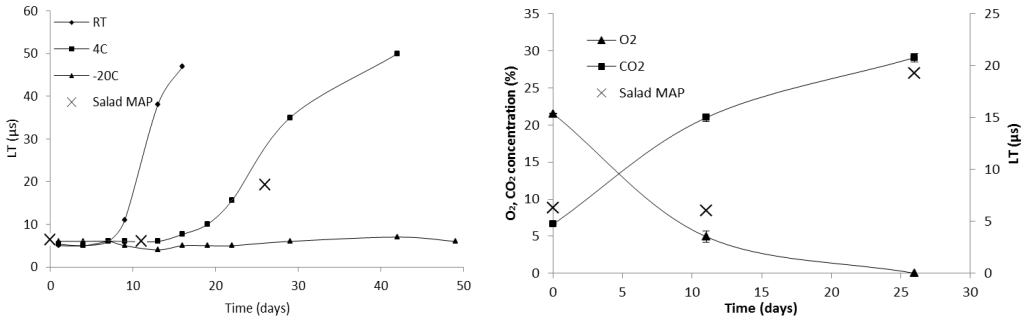

A) B)

Figure 3.7: A) Storage stabilityof the FRET CO_2 sensors at RT, 4°C and -20°C. B) Headspace gas composition in food packs during the food trial. X symbols show in both figures the sensor characteristics during the food trial (in µs).

Secondly, the sensors were brought in gas contact with food products (green salad leaves), sealed under the defined O_2 and CO_2 composition and monitored over 3 week period (Fig. 3.7B). Gas composition inside the packs was monitored by means of a needle-type Dansensor analyzer (residual O_2 and CO_2). At certain time intervals the sensors were extracted from the packs and tested. The results on day 0 and 11 showed no loss in CO_2 sensitivity, and even on day 26 the lifetime signal, measured in pure N_2, was only slightly increased (see symbol X in Fig. 3.7A). These results demonstrate that exposure of the sensors to food and standard packaging conditions (at least the ones used in this particular trial) did not affect much the sensors which remained operational even after several weeks. This is a promising result for food packaging application

which typically requires the same time scale. At the same time, more detailed investigation with other product types, packaging and storage conditions is deemed necessary.

Sensors inside the packs can have contact with the food. Therefore, migration of sensor components into food was evaluated. For this purpose a representative panel of food simulants suggested by FDA/EU guidelines (Food and Drug Administration, 2002; European Economic Community, 1985 and 1997) was taken in which simulants the sensors were incubated for a period of up to 3 weeks while monitoring their characteristics. The two main components of the sensor - PtTFPP and NP- were analyzed by HPLC to determine the amounts migrating into these simulants (Table 3.2). Prior to this analysis, retention times were determined for these materials and calibrations were generated resulting in linear functions: Intensity[PtTFPP] = 3.4538*[Concentration in μg/ml] (R^2 = 0.9896, 3.4 min at 390 nm) and Intensity[NP] = 1.5517*[Concentration in μg/ml] (R^2 = 0.9969, 7.5 min at 310 nm).

In all six aqueous simulants no traces of test substances were detected over the 21 day incubation period. Both components were tested positive in 95% ethanol, and PtTFPP was less prone to migrate than NP. In olive oil and 95% ethanol PtTFPP was found to leak out progressively reaching a maximum of about 70% (0.12-0.13 μg/ml) of the total amount in the sensor on day 21. Similar results were obtained for NP in 95% ethanol, starting at a slightly higher level of 74% (16.08 μg/ml) on day 7 and reaching 100% (21.65 μg/ml) on day 21. In 50% ethanol it kept constant over the 21 day period at about 50% (9.86-10.57 μg/ml). At the same time, according to the directives alcoholic food is usually represented by 10% ethanol, and in such simulant no sensor leaching of sensor components. It is worth noting that 95% ethanol was used as positive control and as a substitute simulant to assess the migration into fatty food since olive oil was not possible to use in reversed phase cromatography analysis.

Table 3.2: Migration of PtTFPP and NP into different media over a period of 21 days. The values in brackets represents the percentage of the component migrated.

Dye	**PtTFPP, [µg/ml, %]**			**NP, [µg/ml, %]**		
Incubation time [days]	**7**	**14**	**21**	**7**	**14**	**21**
Simulants						
EtOH, 95%	0.07 (41)	0.06 (35)	0.12 (69)	16.08 (74)	18.66 (86)	21.65 (100)
EtOH, 50%	ND	ND	ND	9.86 (46)	10.57 (49)	10.15 (47)
EtOH, 10%	ND	ND	ND	ND	ND	ND
Olive oil	0.10 (59)	0.11 (65)	0.13 (72)	NM	NM	NM
Acetic Acid, 5%	ND	ND	ND	ND	ND	ND
Lactic Acid, 3%	ND	ND	ND	ND	ND	ND
$NaHCO_3$, 3%	ND	ND	ND	ND	ND	ND
NaCl, 3%	ND	ND	ND	ND	ND	ND
Sucrose, 20%	ND	ND	ND	ND	ND	ND
H_2O	ND	ND	ND	ND	ND	ND

ND- Not detectable, NM- Not measured

The risk of exposure to chemicals has been well documented and LD_{50} values of 6400 mg/kg (oral intake of rats) are stated (www.chemyq.com). For humans, EU guidelines (Commision Directive 2002/72/EC, 2002) do not give a specific migration limit (SML) specifically for IBM monomer, however, methacrylic acids have an SML = 0.05 mg/kg. The amount of P(IBM) in one sensor is only 80 µg, hence the level of IBM that can potentially migrate into food is too low to be significant (even when assuming that all P(IBM) converts into its monomer IBM). Dyes are normally not used in food packaging so there are no guidelines for SML or specifications regarding daily tolerable intake or LD50. The amounts leaching from the sensor in 95% (50%) ethanol and olive oil were quite high, however such conditions do not occur in practice as the developed sensors are not intended to have much contact with food. They are normally used in the headspace and can be protected from food with a gas-permeable membrane or coating.

3.3.4 Sensor Fine-Tuning for Packaging Applications

Temperature sensitivity, although representing a major issue for sensor operation, can be dealt with by conventional means. For example maintaining samples at known temperature or measuring temperature with a T-probe or a built-in contactless IR sensor (Buydens *et al.*, 2006). Sample O_2 content is another variable parameter which can affect the signals from the CO_2 sensor . For example in food products packaged under modified atmosphere residual O_2 can fluctuate over time (Fig. 3.7B) as a result of O_2 permeation through the package (Kim *et al.*, 2005; Wang *et al.*, 2010), uptake by the product (Simpson *et al.*, 2009), microbial spoilage (Kim *et al.*, 2011) or package damage. The strong dependence of sensor response on O_2 concentration therefore necessitates its parallel assessment and compensation during operation of the CO_2 sensor. In particular, this can be realized as a tandem sensor, in which the CO_2 sensor is paired with the PtTFPP based O_2 sensor that can be measured with the same instrument. Phosphorescence lifetime based O_2 sensing is a well-established approach and therefore we produced PtTFPP-P(IBM) sensor and calibrated it at different temperatures. The calibrations are shown in Fig. 3.8, both in lifetime scale and Stern-Volmer plots.

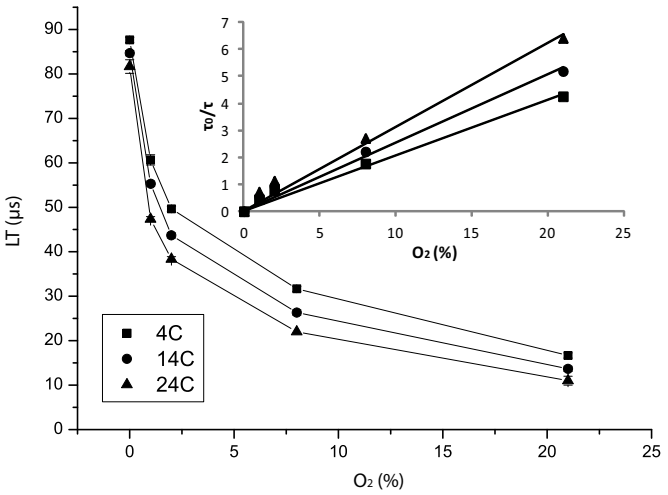

Figure 3.8: O_2 calibrations at temperatures of 24, 14 & 4°C. Inset: Stern Volmer plots show good linearity, R^2▲ = 0.9813, y = 0.3129x; R^2● = 0.9818, y = 0.2534x; R^2■ = 0.9827, y = 0.207x.

Based on these experiments, algorithms for the calculation of CO_2 levels in unknown samples can be worked out for the tandem CO_2/O_2 sensor. As a result, from lifetime readings from the two sensors and respective calibrations (e.g. those shown in Fig. 3.6C and 3.8), both O_2 and CO_2 levels can be determined. At the same time, one should keep in mind that performance of the CO_2 sensor deteriorates at high O_2 levels (above 10%), and CO_2 concentrations above 10%, since in these conditions calibration functions become flat. Furthermore, the lifetime of the sensor stored at higher temperature (RT) was significantly reduced.

Trying to extend the range of CO_2 concentrations that can be measured accurately and reliably, we produced sensors with CTA-OH additive. The size and shape of the ammonium cation may influence the sensitivity of the sensor depending on how strongly the positive charge is shielded from the protonable group. By applying a PTA with a smaller or less spherical group (Bültzingslöwen *et al.*, 2002), for example using CTA-OH instead of TOA-OH, the sensitivity can be reduced like it was reported for CO_2 sensors consisting of 1-hydroxypyrene-3,6,8-trisulfonate (HPTS). Fig. 3.9A and B depicts that the use of CTA-OH in the FRET sensor formulation (CTA-OH: 1230 mM,

PtTFPP: 0.8 mM, NP: 564 mM in solid sensor) broadened the range of measurable LT values reduced the sensitivity to CO_2. This comes along with a lower sensitivity in the 0 - 2% region but a broader measurable CO_2 range spanning up to 40%. The response and recovery time to CO_2 for this sensor were 3.5 min (99.9%) showing an increase of 2.5 min and decrease of 0.5 min with respect to sensor 1. When stored at RT these sensors remained stable for up to 2 days and then quickly went off within a few days. At 4°C the sensors were usable for up to 9 days and then went off gradually until day 19. Finally, at -20°C no deterioration occurred and even after 85 days the sensors remained usable (Fig. 3.9D). The CO_2 sensitivity possessed by the TOA-OH sensors is suitable for MAPed fruits and vegetables (0-10% with some exceptions), fresh pasta (0%), dairy cakes (0%), dried/roasted foods (0%). On the other hand, high CO_2 levels of above 50% CO_2 normally used red meat, poultry, white and oily fish (McMillin, 2008; Parry, 1993; Sandhya, 2010; Sivertsvik *et al.*, 2002) are not possible to analyse with the current sensors. It is still desirable to extend the measurement range furter to 100% CO_2, however the current FRET system suffers from the lack of suitable acceptor dyes for covering the whole range of CO_2 concentrations 0-100%.

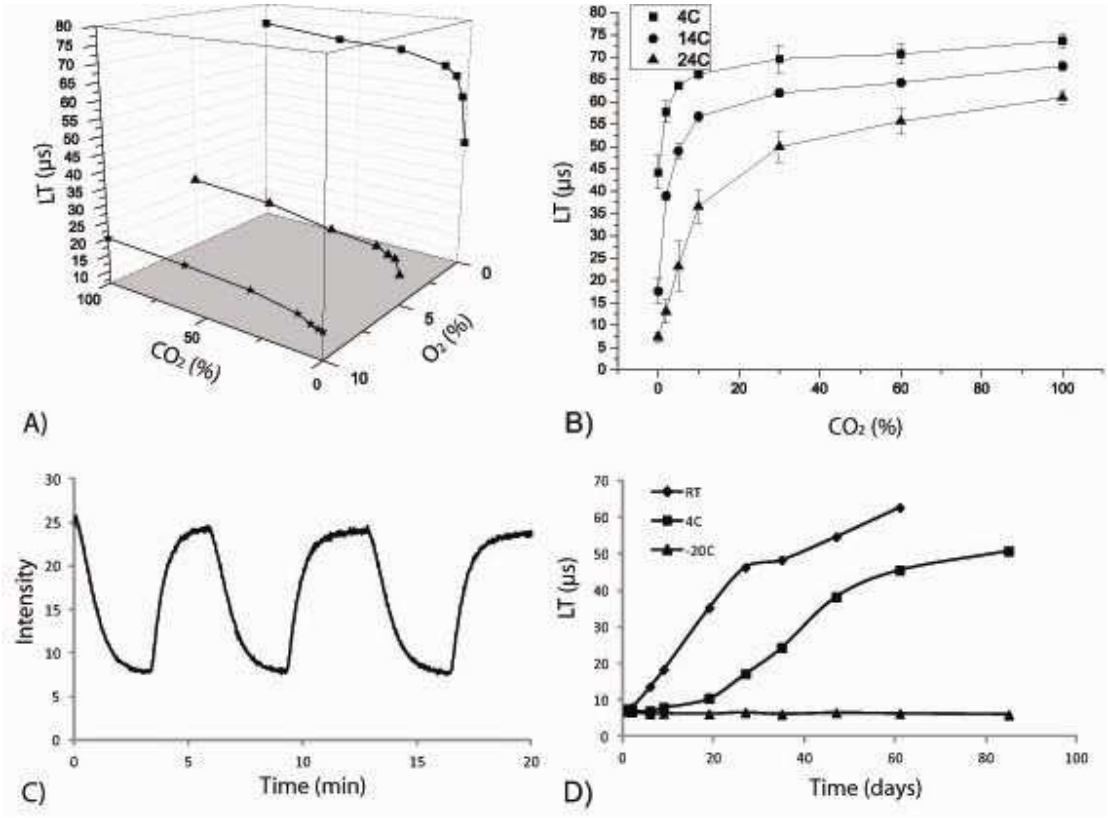

Figure 3.9: A) Calibrations of the CTA-OH sensors at different CO_2 and O_2 concentrations, at 4°C; B) Calibration at differnt temperatures 4°C, 14°C and 24°C, 0% O_2. (N = 3); C) Response and recovery time of CO_2 sensor with CTA-OH to alternating of 100% CO_2 and 100% N_2; D) Storage stabilityof the CO_2 sensor with CTA-OH at RT, 4°C and -20°C.

3.4 Conclusions

The new FRET based CO_2 sensor (with TOA-OH) is described which shows potential for food packaging applications on disposable basis. When the sensors are stored at -20°C their shelf-life exceeds 50 days but decreases gradually at higher temperatures to a few weeks at +4°C and less than a week at room temperature. Because of its intended use in packaged foods the sensor was tested for migration of its components which was undetectable for both dyes in water based simulants and

detectable only in olive oil and high percentage ethanol. These disposable sensors show robust changes in phosphorescence LT of the PtTFPP dye in response to CO_2 concentration, fast response and recovery times. Compared to the absorbance or fluorescence intensity based CO_2 sensors, the long-decay FRET system is advantageous since it enables stable calibration and simple readout of the optical signal. The use of a long-decay phosphorescent indicator dye, such as PtTFPP, and an absorbance pH indicator dye, like α-naphtholphthalein, provides accurate readout of CO_2 content with relatively simple instrumentation. At the same time, it shows significant cross-sensitivity to O_2 and temperature, which can be compensated by parallel measurements with a tandem O_2 sensor or a T-probe. By changing the PTA from TOA-OH to CTA-OH it is possible to shift the sensitivity of the sensor from high to low tuning it to the desirable range. These sensors possesses slightly changed response and recovery times and shelf-lifes at different storage conditions. They also produce a colour change, which can be detected visually.

Chapter 4: Development of Rapid TVC Tests for Different Food Matrices Using Phosphorescent O_2 Sensitive Probes

4.1 Introduction

Food is generally a highly perishable product owing to its high a_w (Abbas *et al.*, 2009), relatively high pH and the presence of autolytic enzymes (Robertson, 2006). Microbiological criteria for all packaged food products are subject to health and safety regulations. In particular, shelf-life of food products is controlled by the Regulation (EC) No 2073/2005 (Ireland) by applying the total aerobic viable counts (TVC) method which provides quantification of viable microorganisms in a sample. Traditionally, TVC has been done by agar plating technique which normally takes 24-48 h to generate results (ISO:4833:2003, 2003). This macro-method involves multiple dilutions of sample and manual or semi-automated readout (counting of grown colonies). When dealing with rapidly deteriorating products such as raw meat, fish or green produce, a more rapid, simple and automated micro-method which provides determination of TVC in large number of samples is highly desirable.

A number of tests and systems for TVC determination alternative to the conventional agar plating method (ISO:4833:2003) have been described. These methods utilize different chemistries, detection principles and instrumentation, and include Petrifilm TEMPO® by bioMerieux (Blackburn *et al.*, 2008), Simplate® by BioControl (Townsend and Naqui, 1998), impedance based systems RABIT® by Don Whitely Scientific and BacTrac® by Sy-Lab (Hattula *et al.*, 2002); and optical MicroFoss (Odumeru and Belvedere, 2002) and oxygen respirometry (O'Mahony *et al.*, 2005; Papkovsky, 2004).

In particular, optical micro-respirometry uses phosphorescence based oxygen sensing probes, standard 96-well plates and fluorescent reader detection to monitor growth of aerobic cells and micro-organisms via their respiration. Its initial food safety application has been developed for raw meat (O'Mahony *et al.*, 2009), in which TVCs

of meat samples are determined directly in crude homogenates prepared in peptone buffered water (PBW) medium by standard stomaching method. This screening assay has been successfully validated with different types of meat samples (raw beef, pork, lamb and poultry) and also certified by the American Organization of Analytical Chemists (AOAC) for use in food industry. It has now been adopted by a number of meat producing companies and food safety labs.

Fresh fish by nature has a low microbial load both internally and externally. The muscle tissues are usually sterile in healthy fish, while large populations of bacteria are present on the external surfaces, gills and intestines. There may be as many as 10^2-10^6 bacteria per cm^2 on skin surfaces (Gram and Dalgaard, 2002; Robinson, 2000). As soon as fish is caught and processed, a series of bacteriological, chemical, physical, and histological changes develop in the muscle tissue (Jeremiah, 1996). Significant microbial spoilage and chemical changes in fish cause sensory changes to a degree that it becomes unacceptable to the consumer. Autolytic, chemical and microbiological processes produce undesirable sensory changes in fish, which include discoloration, changes in texture, odour and flavour as well as slime and gas formation. Microbial growth is the main reason for the development of off flavours and odours rendering fish products unacceptable or spoiled (Gram and Huss, 1996; Robinson, 2000). The high degree of perishability of fish has limited its consumption in a fresh state to areas close to capture. To preserve the freshness of fish products, especially during prolonged transportation and storage, and extend their shelf-life, various packaging and holding temperature techniques are used, including freezing, cooling, refrigeration (Davies *et al.*, 2009), vacuum and modified atmosphere packaging (Ibrahim *et al.*, 2008; Sivertsvik *et al.*, 2002). At the same time, prolonged storage and transportation requires efficient control measures, to ensure high quality and safety of fish products (whole fish and cut pieces). In particular, their microbial load has to be carefully controlled and maintained below the acceptable threshold levels.

The fresh produce market has changed dramatically over the last 2 decades, reflecting the new consumer demands and technological innovations in harvesting, production and packaging. Consumers are eating more fresh produce, purchasing a

broader variety and demanding more convenience products such as ready to eat salads (Dimitri *et al.*, 2003). Since fresh produce is still alive and respiring post harvest, it requires rapid processing, adequate packaging and controlled storage conditions. A number of techniques can be applied to increase the shelf-life and sensory quality and reduce microbial degradation, including genetic variation (Hayes and Liu, 2008), chilling (Lee, 2008), rational choice of packaging materials (Kim *et al.*, 2005, Lee, 2008, Seglina, 2009), the use of biodegradable films (Del Nobile *et al.*, 2008),warm chlorinated water treatment (McKellar *et al.*, 2004) and modified atmosphere packaging (MAP) (Allende *et al.*, 2004; Jacxsens *et al.*, 2001; Rojas Graü *et al.*, 2009; Wang *et al.*, 2010). MAP, in combination with refrigerated temperature, seems to be the most efficient and well understood strategy to maintaining product quality and enhancing shelf-life. Traditionally, reduced O_2 (1-5%) and elevated CO_2 (5-10%) levels are used to reduce respiration, product transpiration and ethylene production (Rojas Graü *et al.*, 2009). In recent years, elevated O_2 levels (>70%) combined with elevated CO_2 concentrations (10-20%) (Amanatidou *et al.*, 1999; Jacxsens *et al.*, 2001; Van der Steen *et al.*, 2002) have been applied to inhibit growth of naturally occurring spoilage microorganisms, prevent undesired anoxic processes and maintain freshness. Using optimized packaging material it was possible to control tissue browning and senescence by matching the oxygen transmission rate (OTR) of the package and oxygen consumption by the product (Kim *et al.*, 2005). On the other hand, to assure good taste, visual appearance and low microbial load (total viable counts, TVC) of MAP green produce, it is necessary to deploy adequate control systems. In particular, headspace gas composition and TVC are the key quality parameters which can inform on the physico-chemical and microbiological status of individual packs, respectively.

In this study we applied the optical oxygen micro-respirometry assay methodology (Papkovsky *et al.*, 2006) using a commercial GreenLight^{TM} probe to develop a similar TVC test for fresh fish and salad samples. In such a test, the probe produces a large increase in phosphorescence upon the depletion of dissolved oxygen by growing microorganisms, which occurs when a certain level of respiration is reached (threshold). For different samples fluorescent profiles are expected to be similar in shape, but shifted

with respect to each other according to their initial TVC load: samples with higher TVC values break the signal threshold earlier, with low TVC - later. The samples are partially sealed with mineral oil to reduce back diffusion of atmospheric oxygen. Using different food matrices, we investigated matrix effects on assay performance, performed optimization of assay parameters (dilutions, volumes, timing) and generated calibrations for each type of food matrix. The assays were validated with a panel of unknown fish and salad samples and benchmarked against conventional agar plating TVC test.

4.2 Experimental

4.2.1 Materials

Samples of salmon, cod, whiting, plaice and mackerel filets were purchased from local retailers in Cork. Salad samples were provided by a local fresh fruit and vegetable company based in Dublin, Ireland. Sterile PBW was prepared fresh using the ingredients from Sigma-Aldrich Corp. (St Louis, MO) and Milli-Q water (Millipore, Billerica, MD). A Stomacher machine and sterile stomacher bags were from Seward, Ltd (London, UK). Sterile 96-well flat-bottom microplates with lid made of clear polystyrene were from Sarstedt (Nümbrecht, Germany). The GreenLight^{TM} oxygen probe and mineral oil were from Luxcel Biosciences (Cork, Ireland). Plate Agar was from Merck (Darmstadt, Germany). White trays for MAP (203 x 146 x 60mm) made of polystyrene-EVOH-polyethylene were from Bachmann Forming AG (Hochdorf, Switzerland) and the Satina® sealing film was from Cryovac (St Neots, UK). Oxygen, nitrogen and carbon dioxide gases supplied by BOC (Cork, Ireland) were fed into the MAP tray sealer (type: VS100BS) from Gustav Müller & Co. KG (Bad Homburg, Germany) connected through a gas mixer (type: KM1003MEM) from WITT-GASETECHNIK GmbH & Co. KG (Witten, Germany).

4.2.2 Methods

4.2.2.1 Respirometric TVC Assays

The assay was performed as follows: A GreenLight^{TM} probe was reconstituted in 10 ml of sterile PBW to produce stock solution. Food samples (10 g) were placed in a stomacher bag together with 90 ml of PBW and homogenized for 1 minute. After this, 100 µl aliquots of the homogenate were transferred to the wells of a 96 well plate. Subsequently, 100 µl aliquots of probe stock and 100 µl of mineral oil (seal from ambient oxygen) were dispensed in each well. The plate was then placed in the fluorescent reader and monitored at 30ºC using the settings recommended for each instrument (see below) to determine threshold time (TT) for each sample. The Phosphorescence intensity threshold was set to be 400 FU (fluorescence units) and lifetime threshold - 32 µs. To summarize, the respirometric TVC assay includes six simple steps according to the flow chart shown in Scheme 4.1. Compared to the previously described assay for raw meat (O'Mahony *et al.*, 2009) the procedure has been rationalized to three 100 µl pipetting steps requiring just one micropipette. The homogenization step and medium used are the same as in conventional agar plating TVC method. Plate preparation time should be kept to a minimum (typically 15-20 minutes).

1. Take 10 g of each **Food Sample** and 90 ml of sterile PBW,

homogenize in stomacher bag for 1 minute

↓

2. Dispense 100 µl aliquots of **homogenates** into wells of a sterile 96WP

↓

3. Reconstitute a vial of **GreenLight™ probe** in 10 ml PBW and

dispense 100 µl into sample wells (negative control is usually included)

↓

4. Dispense 100 µl of **mineral oil** to each well (seal from air oxygen)

↓

5. Read the plate on **Fluorescent reader** at 30ºC for 2-12 hours

↓

6. **Analyze** measured fluorescence profiles, determine (using software)

the TT values and cfu/g load for each sample

Scheme 4.1: Flow chart of the respirometric TVC assay.

The respirometric assay can be run on different fluorescent readers, for example Safire (Tecan), Victor2 (Perkin Elmer) and Omega (BMG) readers which are spectrally compatible with the probe and allow temperature control and measurements in kinetic mode in 96 well plates. To generate TT data with food matrices, we used the first 2 plate readers with the following settings:

A) Safire (Tecan, Switzerland): measurement mode - fluorescence; excitation filter – 380 nm; emission filter – 650 nm; gain - 60.

B) Victor2 (Perkin-Elmer): emission filter - D642, excitation filter - D340, delay time 1 – 30 μs, delay time 2 – 70 μs, window time – 100 μs, integration time – 1000 μs.

4.2.2.2 Conventional TVC Test

Conventional TVC test on agar plates was performed according to the standard ISO: 4833:2003 method, using PBW medium, incubation at 30ºC and counting the colonies of bacteria after 48 hours (ISO:4833:2003, 2003).

4.3 Food Matrix: Fish

4.3.1 Experimental Design

During the initial set-up of the assay, positive controls (medium spiked with *E.coli)* and blanks (medium without probe) were included to ensure sufficient sensitivity and proper operation of the instrument. At later stages these controls are not necessary. Plate preparation time should be kept to a minimum (< 20 minutes). Where appropriate, the same homogenates were also used in agar plating TVC test (see below).

To determine possible matrix effects, respirometric measurements were conducted at several different dilutions of fish homogenates: 1:20, 1:40, 1:80 and 1:160 dilutions. Spiking with *E.coli* was also used to assess matrix effects on microbial growth and calibration. In this case, frozen cod filet (has low TVC as tested by agar plating) was thawed for 3 hours at room temperature, homogenized in PBW, then spiked with *E.coli* stock to produce concentrations between $5*10^1$ and $5*10^7$ cfu/g, and measured as above.

To generate TVC calibration, sets of samples of the different types of fish were prepared and analyzed in parallel by the respirometric test (using 1:20 dilution of homogenates) and by conventional ISO test. The results were plotted against each other (TT vs cfu/g) and fitted with linear regression function to produce combined calibration.

To validate the new TVC assay, a panel of fresh fish samples with unknown levels of microbial contamination (salmon, cod, mackerel, whiting, N = 169) was obtained from local retailers on different days, several samples each day. Each sample was tested by the new respirometric test and their cfu/g values were determined by applying the combined calibration. In parallel, the samples were analyzed by the conventional TVC test (ISO:4833:2003 method) and the results were compared and plotted against each other to establish correlation.

To test the ruggedness of the respirometric assay, two different types of errors were introduced: pipetting volume and probe concentration (Table 4.1). Since standard protocol involves 3 consecutive additions of 100 µl volumes (Probe + Sample + Oil), an error in each was introduced applying a lower (70 µl) and higher (120 µl) pipetting volume. An error in probe concentration was introduced using a lower (50%) and higher (150%) probe dilution compared to the standard conditions. The effects of these errors were tested at two different contamination levels: 10^4-10^5 cfu/g (low) and 10^6 cfu/g (high), with negative controls (media only, < 10^3 cfu/g) included in each test. Samples were taken from cod filets which were stored at 24ºC for 2 days (high cfu/g) and at 4ºC (low cfu/g), and analyzed in 5 repeats (N = 5).

Table 4.1: Ruggedness test parameters.

No.	**Assay Variable**	**Standard Protocol**	**Test Parameters**	
1	Pipetting volume (µl)	100+100+100	70+70+70	120+120+120
2	Probe concentration (%)	100	50	150

In the storage trials, fish samples were kept at 4ºC, 14ºC and 24ºC, and analyzed periodically by the respirometric and conventional TVC test: daily for 4ºC and 14ºC tests and hourly for 24ºC (due to fast deterioration).

4.3.2 Selection and Preparation of Fish Samples

Fish samples (stored at 4˚C, 14˚C or 24˚C) were taken by cutting 10 g squares from the edges of each fillet containing skin on the outside. One fillet per type of fish represents a fish sample (one 10 g replicate) and was used per testing day, analyzed in triplicate by the respirometric method and in duplicate by conventional TVC. Negative controls (PBW with probe) and blanks (PBW without probe) were also included.

4.3.3 Statistical Analysis

The possibility of the calibration relation between TVC (cfu/g) and TT (h) being modulated by other factors such as species of fish or trial effects was investigated by fitting a general linear model in the form:

$$th_{ijk} = \mu + b\log\left(TVC_{ijk}\right) + \alpha_i + \beta_j + \gamma_i \log\left(TVC_{ijk}\right) + \delta_j \log\left(TVC_{ijk}\right) + \phi_{ij} + \varphi_{ij} \log\left(TVC_{ijk}\right) + \varepsilon_{ijk} \quad \text{Eqn. 4.1}$$

Where th_{ijk} stands for the threshold recorded on the k-th sample on the j-th trial for the i-th species and similarly for TVC_{ijk}. Here μ stands for overall mean TT values, b (TVC) for the overall slope of the regression of TT and log(TVC), a_i (Species) and β_j (Trial) for the main effect on the mean of the i-th species and j-th trial respectively, γ_i (TVC:Species) and δ_j (TVC:Trial) for the effect on the slope of the i-th species and j-th trial respectively, Φ_{ij} (Species: Trial) for the interaction (combined) effect on the mean of the i-th species and j-th trial, φ_{ij} (TVC:Species:Trial) for the interaction (combined) effect on the slope of the i-th species and j-th trial; and ε_{ijk} (Error) for measurement error. For estimation and hypothesis testing, measurement errors were assumed to have a Gaussian distribution with identical variance and be mutually independent. The significance of effects in model (Eqn 4.1) was measured using F-tests computed by a three factor analysis of variance (ANOVA) (Zar, 2000). The acronyms in parentheses are used to represent each effect in the ANOVA table. Based on the significant terms identified by the ANOVA procedure, a reduced model of the form:

$$th_{ijk} = \mu + b\log\left(TVC_{ijk}\right) + \varepsilon_{ijk} \qquad \text{Eqn. 4.2}$$

was fitted to the data by the least square method. The fitted calibration model was examined for adequacy by examining the residuals (estimated errors) for outliers and constancy of variability. Outliers identified by this process were removed for estimating the final calibration model. The assumption of Gaussianity of measurement error was checked using a quantile quantile plot (Venables and Ripley, 2002). The quality of fit was quantified by the R^2 statistic.

The respirometric TVC assay (TVC_R) was computed using the relation:

$$TVC_R = \frac{th - \mu}{b} \qquad \text{Eqn. 4.3}$$

Where *th* is the observed TT. The quantities μ and b are obtained from the final calibration model in (Eqn 4.2). For validation, we compare TVC_R values against standard *TVC* values using agar plating across a range of validation samples i = 1,..., 169, by linear regression:

$$TVC_{Ri} = c + mTVC_i + \varepsilon \qquad \text{Eqn. 4.4}$$

For a perfect validation, we would expect $c = 0$ and $m = 1$ (the line y = x), but the actual values are likely to be different due to sampling variability. However, we can check for adequacy of the validation by checking if 95% of the data values are within ± 1.96 standard deviation (SD) of the ideal line, where SD due sampling variability is estimated from the residual error of the fitted regression model in (Eqn 4.4) (Zar, 2000).

Analysis of ruggedness testing was performed using a two factor ANOVA (Zar, 2000) where the factors were: 1) the level of sample contamination (high and low cfu/g), and 2) either the assay volume (70, 100 and 120 μl) or the probe concentration (50, 100 and 150 ml). Significance of effects was measured by standard ANOVA F-tests (Zar, 2000). Statistical analysis was done using the R package (cran.r-project.org).

4.3.4 Results & Discussion

4.3.4.1 Analysis of Fish Matrix Effects and Optimization of Assay Conditions

To assess matrix effects in the respirometric assay, fish samples with relatively low level of contamination (10^5-10^4 cfu/g range, verified by conventional TVC) were initially measured at different dilutions of the homogenates. Representative respiration profiles for one such salmon sample are shown in Fig. 4.1A. As with pure microbial cultures (O'Mahony and Papkovsky, 2006) and raw meat homogenates (O'Mahony *et al.*, 2009), the samples showed characteristic sigmoidal profiles. In contrast, negative samples produce flat profiles, as their oxygen concentration is not changing.

From these profiles a good linearity between measured TT values and sample dilution is seen (Fig. 4.1B processed data). The threshold is the point at which the fluorescence signal shows a sharp increase above the basal level. Corresponding TT is compared with the results of conventional TVC cfu/g results which show that sample matrix has no significant effect on assay performance and that at different sample dilutions the microorganisms proliferate at about the same rate (exponential growth).

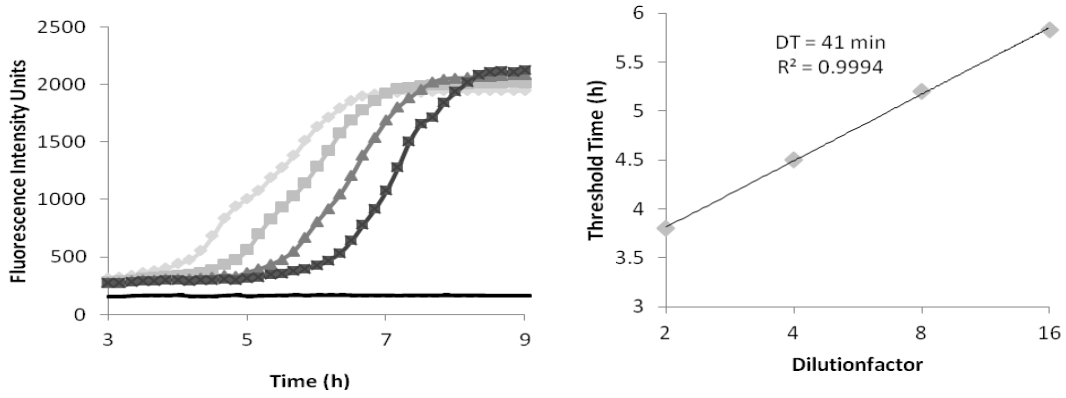

A) B)

Figure 4.1: A) Typical profiles of food samples (e.g. salmon homogenate) measured at different dilutions: 1:20, 1:40, 1:80 and 1:160 (from left to right) and negative control (flat line), B) relationship between TT (at 400 FU) and sample dilution. Doubling time (DT) calculated from the slope is shown on the graph.

To mimic the responses at different initial microbial load, homogenate of cod sample with low levels of microbial contamination (< 10^2 cfu/g, 1:20 homogenate dilution) was spiked with increasing concentrations of *E.coli* and measured. Fig. 4.2 shows that spiked homogenates produce consistent profiles in the assay and give a linear relationship between TT and *E.coli* concentration (cfu/ml). In this matrix, doubling time of *E.coli*, the limit of detection and maximal monitoring time were determined: 25.6 minutes, 50 cfu/g, and 10-12 hours, respectively.

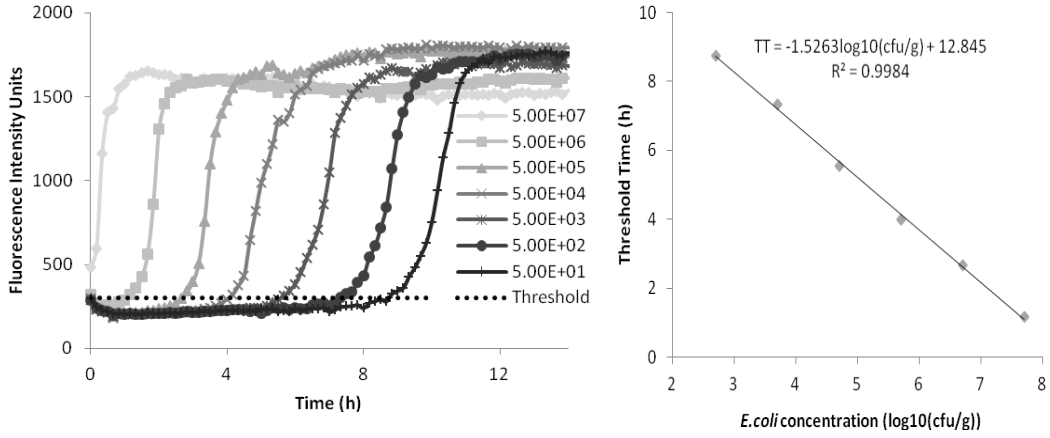

A) B)

Figure 4.2: A) Respiration profiles of cod homogenate samples (~10^2 cfu/g) spiked with different concentrations of E.coli. B) Resulting relationship between TT and E.coli concentration.

From these experiments, 1:20 dilutions of fish homogenates was selected as standard for further work, as it provides convenience with pipetting (standard 100 µl aliquots throughout) and no undesirable matrix effects.

4.3.4.2 Establishment of Calibration

To establish the relationships between the TVC (cfu/g) and TT (h) and generate calibrations which can be used for the analysis of samples with unknown microbial load, we analyzed panels of samples of different fish types (fresh salmon, cod, whiting, plaice and mackerel). The selection of fish was made to cover the spectrum of different types of tissue, i.e. white and red tissue, fresh and seawater fish, flat and thick body, low-fat and oily fish. Each sample homogenate underwent parallel analysis by conventional agar plating TVC method and by the respirometric assay. Accounting for potentially slower growth rates of microorganisms present in fish samples, plate monitoring time was extended to 12-16 hours.

From the ANOVA analysis (Table 4.2) it was apparent that the only significant source of variation in the calibration relation is TVC level. More specifically, the calibration relation is not significantly different across species or trial or any combination of factors. This justifies a simple regression model of Eqn 4.2, in where other factors are not included.

Table 4.2: ANOVA Table of general linear model for calibration data

Source	**D.F.**	**Sum of Squares**	**Mean Sq**	**F-statistic**	**P-value**
TVC	1	251.43	251.43	97.65	<0.0001
Species	3	11.46	3.82	1.48	0.26
Trial	16	40.95	2.56	0.99	0.51
TVC: Species	3	6.41	2.14	0.83	0.50
TVC: Trial	16	49.27	3.08	1.20	0.37
Species: Trial	19	29.82	1.57	0.61	0.84
TVC: Species: Trial	2	3.59	1.80	0.70	0.51
Error	14	36.09			

Fig. 4.3 shows the combined calibration for the four fish species (salmon, cod, whiting and mackerel), after exclusion of the top two outliers. We see that the majority

of points lie within the ± 1.39SD band, as expected. However, the R^2 value is moderate, indicating the presence of substantial variability in the data. The relationship obtained from the fitting and analytical equation for conversion of measured TT values into cfu/g is given in Fig. 4.4. It is worth noting that inclusion of the two outliers significantly changes the calibration relation (it becomes TT =– 2.40(cfu/g) + 18.69). By individually treatment of these fish types the R^2 and the parameters of equation are as follows, for salmon (TT = -2.94(cfu/g) + 21.35, R^2 = 0.72) and whiting (TT = -2.36(cfu/g) + 18.73, R^2 = 0.70) is a higher R^2 obtained and for cod (TT = -2.41(cfu/g) + 19.01, R^2 = 0.53) and mackerel (TT = -1.49(cfu/g) + 13.00, R^2 = 0.39) a lower one.

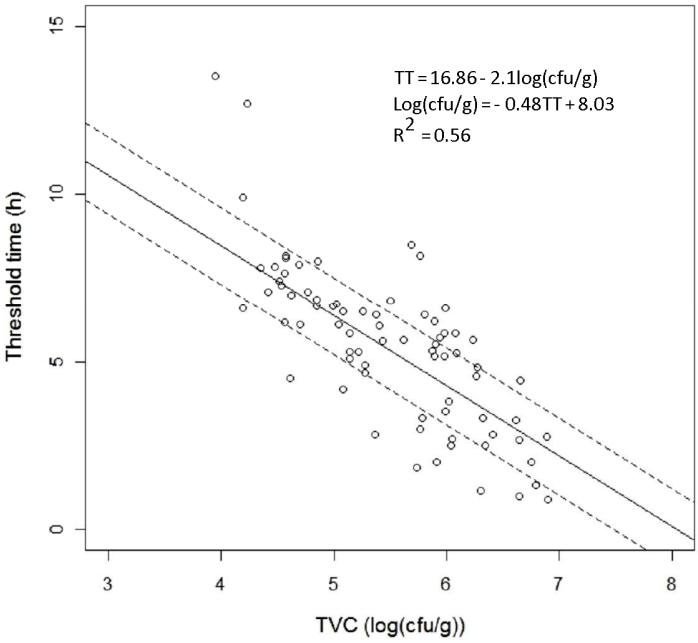

Figure 4.3: Combined calibration curve (solid line) for the fish samples (N = 75; cod: 23, Mackerel: 8, Salmon: 23, Whiting: 21), TT (hours) vs log (cfu/g). Dotted lines denote one standard deviation (SD = 1.39) band around the calibration curve.

As already mentioned fish is a quite difficult product to work with. It is less known about the chemical and physical changes what a fish is developing in his muscle tissue

post mortem and how this is influencing the respirometric method. In an earlier work performed on different types of raw meat (beef, pork, lamb and poultry) by the same method (O'Mahony *et al.*, 2009), a combined $R^2 = 0.86$ was obtained, as compared to $R^2 = 0.56$ for the fish.

At the same time, certain fish samples, particularly fresh plaice, were seen to produce high scattering of results of the respirometric assay and worse correlation with conventional TVC test (Fig. 4.4). We explain this by plaice being a flat fish with a low ratio of muscle tissue volume to skin surface, resulting in a less predictable sampling of surface bacteria than for the other fish species tested. Likewise, the scattering of results from frozen fish samples was significantly greater than for fresh fish, although the calibration equation was similar. This suggests that freezing impacts the bacteria in fish tissue and affects their normal growth during the assay. Particular reasons may include freeze damage to microorganisms by the crushing and spearing action of ice crystals as well as lethality resulting from cell dehydration effects. The rate of freezing, storage temperature and temperature fluctuations during storage influence the extent of sub lethal injury and death of microorganisms. Thawing is more injurious to microorganisms than freezing, and the effects vary according to species. Even simple thawing of a frozen microbial population without intervening storage causes slight to moderate reduction in number of live organisms (Robinson, 2000). Due to the large variance of results, plaice and frozen fish samples were excluded from further testing in the respirometric TVC assay.

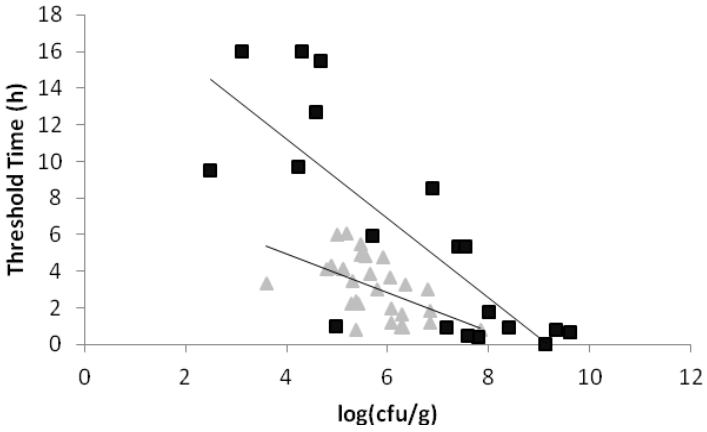

Figure 4.4: The relationship between the respirometric TT values and cfu/g in the standard TVC test for plaice (▲, y = -1.0597x + 9.1813, R^2 = 0.295) and frozen fish (■, y = -2.1725x + 19.92, R^2 = 0.639) samples.

4.3.4.3 Assessment of Assay Ruggedness

The results of assay ruggedness test with respect to pipetting volume are summarized in Table 4.3. Using this data, ruggedness was tested against two factors: 1) the level of sample contamination (high and low cfu/g), and 2) the pipetting volume (70, 100 and 120 μl). To examine the relative contributions of these factors to measurement variation, we modeled log(Response) as a function of them, yielding the analysis of variance (ANOVA) results shown in Table 4.4.

Table 4.3: Experimental data for pipetting volume ruggedness test.

Pipetting Volume error Log10 sample (**High CFU**)				Pipetting Volume error Log10 sample (**Low CFU**)				Pipetting Volume error Log10 sample (**Neg Contr**)			
Replicate	**70µl**	**100µl**	**120µl**	**Replicate**	**70µl**	**100µl**	**120µl**	**Replicate**	**70µl**	**100µl**	**120µl**
1	6.79	6.96	6.98	1	3.75	3.88	3.99	1	**<3**	**<3**	**<3**
2	6.79	6.96	6.97	2	3.66	3.77	3.93	2	**<3**	**<3**	**<3**
3	6.79	6.95	6.97	3	3.57	3.66	3.84	3	**<3**	**<3**	**<3**
4	6.79	6.94	6.96	4	3.48	3.57	3.66	4	**<3**	**<3**	**<3**
5	6.79	6.94	6.96	5	3.11	3.38	3.66	5	**<3**	**<3**	**<3**
AV	**6.79**	**6.95**	**6.97**	**AV**	**3.51**	**3.65**	**3.82**	**AV**	**-**	**-**	**-**
SD	**0.00**	**0.01**	**0.01**	**SD**	**0.25**	**0.19**	**0.15**	**SD**	**-**	**-**	**-**

Table 4.4: Two factor ANOVA for sample volume ruggedness experiment.

Factor	Degrees of freedom	Sum of Squares	Mean Squares	F-statistic	P-value
Microbial load cfu/g	1	78.83	78.83	3976	<0.001
Assay volume	2	0.29	0.147	7.4	0.002
Error	26	0.52	0.02		

As expected, Table 4.4 shows that the main source of variability is sample microbial load (*cfu/g)*, whereas variability due to pipetting volume and residual error appear to be negligible by comparison (relative means square of 0.1% and 0.02% respectively). Further analysis showed a marginally significant trend (p-value = 0.04) in measurements due to change in assay volume. We note that the significance occurs due to the very small value of residual error (due to replication).

Probe concentration ruggedness test produced similar results (Table 4.5). The main source of variability (Table 4.6) was again sample microbial load (*cfu/g)*, whereas variability due to probe concentration and residual error appear to be negligible by comparison (relative means square of 0.2% and 0.01% respectively). Further analysis showed a significant trend (p-value = 0.003) in measurements due to change in probe

concentration. We note that the significance occurs due to the very small value of residual error (due to replication).

Table 4.5: Experimental data for probe concentration ruggedness test.

Probe Concentration error Log10 sample (**High CFU**)				Probe Concentration error Log10 sample (**Low CFU**)				Probe Concentration error Log10 sample (**Neg Contr**)			
Replicate	**50%**	**100%**	**150%**	**Replicate**	**50%**	**100%**	**150%**	**Replicate**	**50%**	**100%**	**150%**
1	7.12	6.97	6.87	1	4.21	4.03	3.98	1	**<3**	**<3**	**<3**
2	7.12	6.96	6.86	2	4.21	4.00	3.98	2	**<3**	**<3**	**<3**
3	7.11	6.96	6.86	3	4.12	3.99	3.84	3	**<3**	**<3**	**<3**
4	7.10	6.96	6.85	4	4.03	3.90	3.75	4	**<3**	**<3**	**<3**
5	7.10	6.95	6.85	5	3.80	3.84	3.61	5	**<3**	**<3**	**<3**
AV	**7.11**	**6.96**	**6.86**	**AV**	**4.07**	**3.95**	**3.83**	**AV**	**-**	**-**	**-**
SD	**0.01**	**0.01**	**0.01**	**SD**	**0.17**	**0.08**	**0.16**	**SD**	**-**	**-**	**-**

Table 4.6: Two factor ANOVA for probe concentration ruggedness experiment.

Factor	Degrees of freedom	Sum of Squares	Mean Squares	F-statistic	P-value
Microbial load cfu/g	1	68.55	68.55	7336	<0.001
Probe Conc.	2	0.31	0.15	16.37	<0.001
Error	26	0.24	0.01		

4.3.4.4 Assay Validation

Fig. 4.5 shows correlation between the two methods. A diagonal line shows the ideal correlation between the two methods (predicted = observed line). Although the validation trend line produced by linear regression fit of all the data points does not match this ideal line, one can see that 93.5% of data points (158/169) lie within ± 1.96SD of the ideal line. This is close to the expected 95%. One can see that respirometric assay provides the accuracy of TVC determination in fish samples of approximately ± 1 log(cfu/g). For a simple, fast, high throughput screening test, this

analytical performance is considered to be reasonably good (though not as good as for raw meat samples).

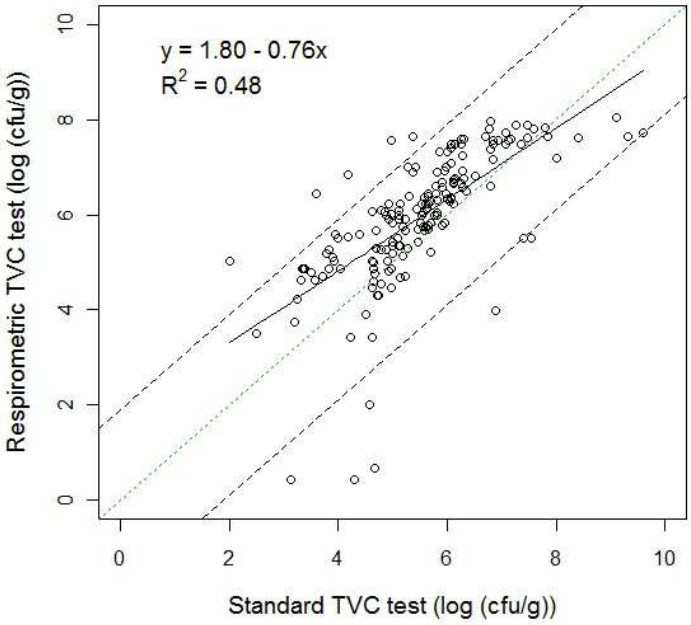

Figure 4.5: Assay validation with unknown fish samples from different retailers. Solid line was produced using linear regression fit of the respirometric and standard TVC test values. Dotted line shows the ideal case, y = x. From regression SD = 0.97 cfu/g. Dashed lines indicate sampling variability range (ideal ± 1.96SD).

In addition, storage trials were carried out to ascertain the natural spoilage rates of fish at different temperatures. It is known that bacteria grow faster at high temperatures. The Q10-rule implies that for every 10ºC increase in temperature the growth doubles, i.e. Q10 = 2 (Dworkin, 2006; Tjoelker *et al.*, 2008). Of course this can vary depending on bacteria and sample used. Representative data for salmon are shown in Fig. 4.6.

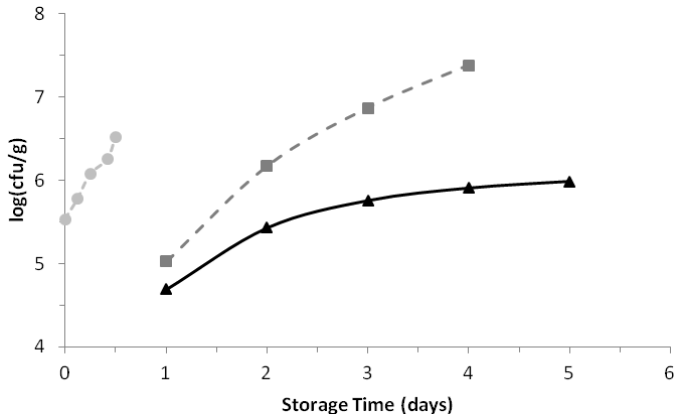

Figure 4.6: Time profiles of microbial load (log(cfu/g) for salmon filets stored at different temperatures: 24ºC (●), 14ºC (■) and 4ºC (▲).

After linearization of the three curves slopes were observed which increase from 4ºC to 24ºC with a factor of Q10 = 2.5, particularly 4ºC = 0.31, 14ºC = 0.78 and 24ºC = 1.97.

4.3.5 Conclusions

A simple, rapid and robust screening test for TVC in raw fish sample was developed which relies on fluorescence based micro-respirometry in standard 96-well plates. Assay conditions including pipetting volumes, sample dilution, matrix effects were optimized to streamline the procedure and produce reliable results. The test was applied to five different fish types: fresh cod, salmon, whiting, mackerel and plaice as well as frozen fish (all used as crude homogenates in PBW) for which individual calibrations and combined calibration were generated. The test showed good correlation with conventional TVC test (ISO:4833:2003), analytical performance and ruggedness with respect to variation of key assay parameters (probe concentration and pipetting volume). Although linear regression fit was not perfect ($R^2 = 0.56$), vast majority of data

points lay within 1.39SD. At the same time, plaice and frozen fish showed lower correlation with conventional TVC method which can be explained by generic structure of these fish samples resulting in a less predictable sampling and higher scattering of data. The respirometric test was then validated with a panel of unknown fish samples (N = 169), where it correlated well with conventional TVC test. Although correlation trend line produced by linear regression does not match the ideal line, 93.5% of points lie within ± 1.96SD, i.e. very close to the anticipated 95%.

4.4 Food Matrix: Green Produce

4.4.1 Experimental Design

The experimental design was similar to the fish study and included the assessment of matrix effects, followed by the calibration and validation. A standard sample preparation method was used, which involves preparation of crude homogenates (1:10) of salad samples in PBW on a stomacher, followed by further dilution steps: 1:2, 1:4, 1:8 and 1:16 and subsequent monitoring of their respiration profiles. Non-linear profiles would indicate some kind of matrix effect of the probe what is interfering the faultless functioning of the method. For quantitative determination of TVC in salad samples (cfu/g), calibration was established by preparing homogenates of a representative panel of samples and their parallel analysis by the GreenLight assay (at constant 1:20 dilution) and by standard agar-plating TVC method (ISO:4833:2003, 2003). Once the calibration has been established (combined for different types of salads/green produce), it was validated by analyzing another set of salad samples. Their TVC values were determined using the above calibration equation. The resulting TVC values were compared to those produced by the agar plating test conducted in a parallel blind experiment.

A total of 206 samples were assessed in this way divided into two groups of calibration and validation. All measurements for the calibration trial and the parts of the validation trial (packed at 5%, 21%, 45% and 60% O_2) were conducted at days 1, 3, 7 and 10 after packaging; the additional five salads of the validation part were assessed

only at day 3 and 7. After averaging the resulting threshold time of the triplicates for each sample the TVC was calculated and compared to the conventional agar plating values (triplicates). The number of samples measured for each type and batch of salad is stated in Table 4.7.

Blanks (homogenates without probe) and negative controls (PBW with probe) were also incorporated on the plate. To establish the calibration and validate the new assay, the same homogenates of food samples were also analyzed by conventional agar plating.

4.4.2 Selection and Preparation of Salad Samples

All salad samples, freshly manufactured, packaged and delivered in industrial environment were provided by a local fresh fruit and vegetable company based in Dublin, Ireland. They were received in conventional plastic pouches (90 g) packed under 5% O_2 or in air. Ten different salad types were chosen for the development of a new test for rapid TVC determination in various types of green produce. These samples were analyzed at different storage time to generate a combined calibration and assess the performance of the new assay. For the validation of the TVC assay determination, three salad types - Italian leaf mix salad, Caesar salad and Iceberg lettuce packaged under 5%, 21%, 45% and 60% of O_2, were selected. On day 1 some of the samples were repacked using a small scale packaging device operating with white Polystyrene-EVOH-Polyethylene trays (dimension: 203 mm x 146 mm x 60 mm (L x B x H), volume: 1000 ml) and Satina sealing film. Five further salad types packed in air were also included in the validation trial. A total of 27 batches of different salad types packaged under different conditions were prepared and analyzed. The samples were stored in a cold room set at 4˚C.

Table 4.7: Batches of salad samples used for rapid TVC assay development and validation.

	Salad type (O_2%)	N	
Calibration	Italian Mix (5%)	12	**106**
	Italian Style (5%)	12	
	Secret garden (air)	12	
	Rocket (air)	11	
	Spinach and Rocket (air)	8	
	Caesar (5%)	12	
	Spinach (air)	3	
	Iceberg (5%)	12	
	Irish Summer Leaf Salad (air)	12	
	Aromatic Herb Salad (air)	12	
Validation	Italian Mix (5%)	7	**100**
	Italian Mix (21%)	7	
	Italian Mix (45%)	6	
	Italian Mix (60%)	6	
	Caesar (5%)	7	
	Caesar (21%)	7	
	Caesar (45%)	6	
	Caesar (60%)	6	
	Iceberg (5%)	8	
	Iceberg (21%)	8	
	Iceberg (45%)	6	
	Iceberg (60%)	6	
	Aromatic Herb Salad (air)	4	
	Baby Leaf Spinach (air)	4	
	Spinach & Rocket (air)	4	
	Sweet & Crunchy Salad (air)	4	
	Wild Rocket (air)	4	

4.4.3 Results & Discussion

4.4.3.1 Development of Rapid TVC Assay for Green Produce

To assess possible interferences of the food matrix on the results of GreenLight™ TVC assay, crude homogenates of salad samples were analysed at several different dilutions (1:20, 1:40, 1:80, 1:160) in PBW by monitoring their respiration profiles and TT which reflect microbial growth. For the different dilutions of the same sample a linear relationship between the threshold time (TT) and logarithm of dilution factor was observed, as seen for the example in Fig. 4.7 for sweet & crunchy salad (in the inset the coefficient of determination is revealed for the other salads). At different dilutions these samples showed a similar shape of respiration profiles, with a robust change (increase) in the probe phosphorescent signal (intensity of lifetime) correlating with the initial number of viable bacteria (cfu/g).

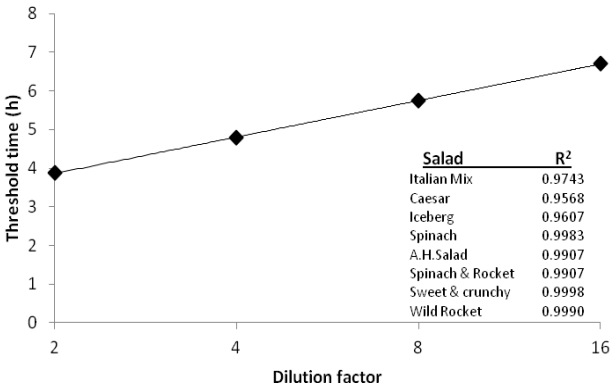

Figure 4.7: The relationship between the TT and dilution factor for the sweet & crunchy salad. The inset shows R^2 for the other salad types (linear regression fits).

Taken together, this indicates that salad matrices and their components have no significant effect on the GreenLight TVC assay, and that low working dilution of the samples (1:20) can be used. Green produce is usually rich in chlorophyll and has absorption and/or fluorescence characteristics overlapping with those of the

phosphorescence based O_2 probe GreenLight (Chen *et al.*, 2010). This can potentially cause interferences with the respirometric measuring technique used in the rapid TVC test**.** Other factors and ingredients of the sample (and other natural pigments, matrix effects) can also influence the measurements. On the other hand, the long-decay emission of GreenLight probe and time-resolved phosphorescence lifetime based detection provide high sensitivity, selectivity and signal to blank ratio, and this allows reliable monitoring of dissolved oxygen and microbial growth/respiration in complex samples such as food homogenates (O'Mahony *et al.*, 2009). Nonetheless, when developing a new TVC assay for a new group of products, these factors have to be assessed carefully.

To produce a TVC calibration curve for ready-to-eat salads, we analyzed a total of 106 salad samples, which differ in their type and freshness and cover a broad range of TVC levels and matrices. For each sample both the TT values (hours) and TVC counts (cfu/g) were generated. Fig. 4.8A illustrates the correlation of the results of the two assays for the samples measured on 4 different days. One can observe that TVC values are increasing at longer storage time. From this experiment, the following analytical relationship (equation) was determined which can be used for the determination of TVC values in salad samples based on the TT values of the respirometric assay:

$$TVC(\log(cfu/g)) = 0.544*TT(h) + 9.02. \qquad \text{Eqn. 4.5}$$

This new test is applicable to different types of ready-to-eat salads and potentially to other types of green produce. This assay shows a dynamic range of 3.5-8.3 log cfu/g, good linearity between TT and log(cfu/g) values, and correlation coefficient R^2 = 0.6231. The SD for the 106 samples was SD = 0.685 while 92% of all points lie within the 2SD band (being close to the anticipated 95%).

At the same time, not all the samples tested delivered usable data. Eleven samples showed very high bacterial load producing respiration profiles with a very early signal increase for which TT values cannot be determined. Three other samples were identified as clear outliers and also disregarded when processing the calibration data.

Correlation of the results of the newly established rapid TVC test for green produce with the ISO TVC test (48 hours) is shown in Fig. 4.8B which exhibits a good agreement between the two tests (plotted against each other with x-axis: ISO method, y-axis: respirometric method). The ideal correlation shown as dotted line should have the same TVC values on both axes. However, in the lower part of the correlation graph the points are slightly below this line indicating that the respirometric method slightly underestimates the TVC values. On the other hand, at high TVC values the results get rather close to the theoretical line crossing it at about log(cfu/g) = 7. Linear regression fit gave the following equation: Respirometric TVC(GreenLight) = 1.28(ISO TVC) – 2.08, with R^2 = 0.7749 and SD = 0.689 and 91% of all points lie within the margin of 2SD. We can therefore conclude that the new TVC assay works reliably over the TVC range 4-8 log(cfu/g), giving a linear relationship with TT and SD of less than ± 0.7 log(cfu/g).

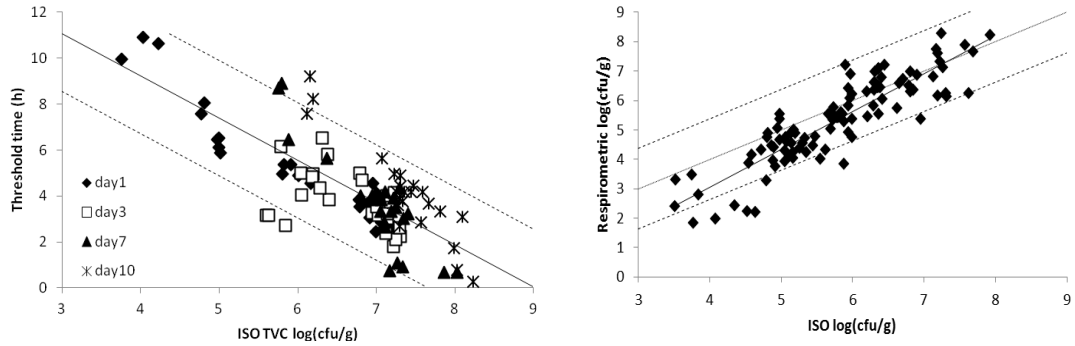

A) B)

Figure 4.8: A) Combined calibration of the respirometric TVC assay produced using for 10 different salad types, N = 106. Dashed lines denote ± 2SD (1.37) band around the calibration curve. Different symbols correspond to different storage time. B) Validation of the respirometric method using 8 different salad types, N = 100. Dashed lines indicate ± 2SD (1.38). The dotted line is the ideal line.

4.4.3.2 Quality Assessment of Packaged Salads

Profiles of microbial load over storage time for the three lettuces determined from the rapid TVC test and corresponding doubling times (DT) and R^2 values are shown in Fig. 4.9. Each salad type shows characteristic initial TVC load and pattern of microbial growth, with the same general trend - increase in cfu/g over time. So, different ready-to-eat salads exhibit characteristic bacterial counts which correlate with their type, age and packaging conditions. The highest TVC values ($\log(cfu/g) \geq 7$) were obtained for the salads packed under air, while MAP salads show reduced TVC values, i.e. better freshness and quality.

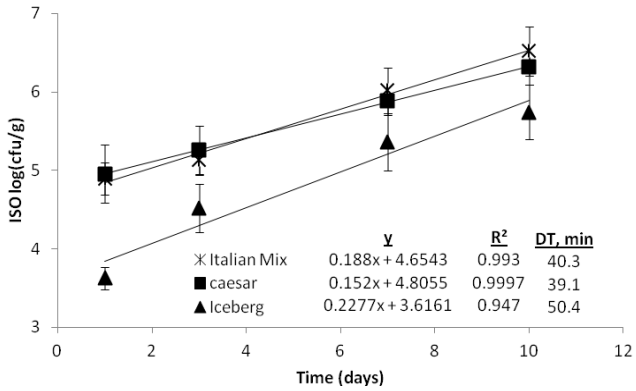

Figure 4.9: Growth rate (log(cfu) vs time) of Italian mix, Caesar and Iceberg salad (N = 12 for each sample and day) with R^2 and linear equation and doubling time.

While the O_2 was varied the CO_2 was kept on a moderate/high level of 5%. Except the O_2 concentration all the other storage parameters were kept the same for the different batches of salad. Comparing the results, Iceberg shows much lower bacteria counts than Italian mix and Caesar salad (Fig. 4.10). Iceberg starts with a log(cfu/g) = 3.55 while the others - with 4.69 (Caesar) and 4.96 (Italian mix) respectively. When focusing on the results at day 10 for all the salads, it is not obvious that higher oxygen levels inhibit or reduce the growth of microorganisms for either of the used samples. On the other hand, samples packed at 5% O_2 develop lowest TVCs. Caesar and Iceberg lettuce illustrate

close results at 21, 40 and 60% O_2 building a step to 5%, which is higher for Iceberg (~11.5%) compared to Caesar (~6%). For Italian mix 21% O_2 give highest TVC (9.5% more) whereas 45% and 60% oxygen are very close to 5% oxygen.

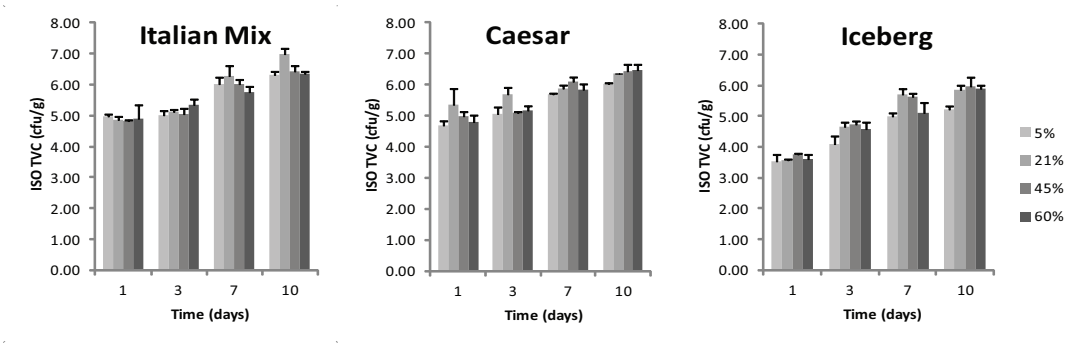

Figure 4.10: TVC results for MAP packed Italian mix, Caesar and Iceberg salad (N = 3) at different days (x-axis) and initial oxygen concentrations (5%, 21%, 45% and 60%).

Changes in headspace gas composition (CO_2 & O_2) in salad packs was monitored over a period of 10 days with the Optech (O_2) and Dansensor (CO_2) instruments. They showed a downward change in O_2 and an increase of CO_2. It is known that rapid depletion of O_2 and elevation of CO_2 can promote undesired fermentation processes, with production of ethanol and acetaldehyde leading to product deterioration and development of undesirable off-flavours and odours (Van der Steen *et al.*, 2002) and also microbial growth. The latter can be assessed by looking at the TVC data. Indeed, clusters of data points in Fig. 4.8A which correspond to salad samples of different age reveal that TVC were increasing with storage time. A clear separation is seen between days 1, 3, 7 and 10.

For the different salad packs the TVC were assessed, leading to the conclusion that MA packs exhibit lower cfu/g counts than air packed pouches, with 5% O_2 producing the lowest microbial counts (in 5% CO_2). This can be partly explained by bacteriostatic and fungistatic properties of CO_2 which air does not have. Higher O_2 content in packs is normally avoided due to its metabolic use by aerobic spoilage microorganisms and plant

tissue, but in the case of fresh fruit and vegetable products O_2 is needed for their respiration. The levels of O_2 in such packs depend on many parameters including the type of packing material, the relation between air volume and vegetable mass, illumination intensity, the type of product, proliferation rate of aerobic bacteria (as we observed for Caesar salad, Italian mix leaf salad and Iceberg lettuce). High O_2 (80-100%) was seen to reduce growth of the aerobic microbiota of fresh-cut baby spinach (Allende *et al.*, 2004), however other effects of high O_2 on fresh-cut mixed salads were also reported (Allende *et al.*, 2002).

4.4.4 Conclusions

The new analytical system GreenLight™ demonstrates good working characteristics in the assessment of MAP green produce. The simple, rapid and high throughput TVC test with GreenLight™ probe was applied to a panel of salads to generate combined calibration with a linear relationship between measured TT and log(cfu/g). This test was validated with unknown salad samples (N = 100) proving that it is widely applicable to this type of food. Each salad type showed characteristic initial TVC load and pattern of microbial growth. The lowest TVC and highest preference in visual assessment were achieved for salads packed at 5% O_2. The simple, rapid and high throughput TVC test with GreenLight™ probe exhibits good working performance with a variety of different salad types.

4.5 Comparison of Different Food Matrices

The rapid TVC test for green produce was compared to similar tests described previously for raw meat (O'Mahony *et al.*, 2009) and fish (see 4.4) samples. As can be seen in Fig. 4.11, TVC calibrations of the three food matrices, reproduced from the corresponding analytical functions, are very similar (shifted against each other by less than 1.0 log(cfu/g)). This leads to a conclusion that the respirometric TVC detection method is applicable to a wide variety of food products and matrices. At the same time,

for new products basic assessment of possible matrix effects on calibration and possible interference on the optical measurement is still necessary while the use of existing or combined TVC calibration is not recommended and this may reduce the accuracy of the assay.

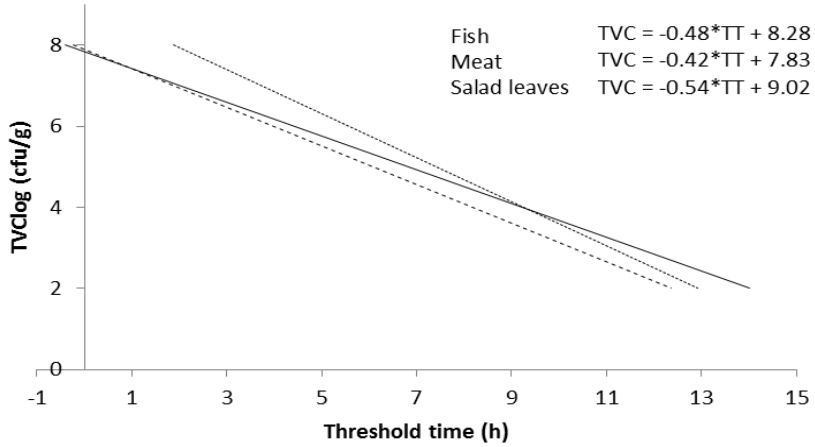

Figure 4.11: Comparison of three different food matrices, salad leaves (dotted line), fish (dashed line) and meat (solid line),using respirometric TVC method. Linear equations are shown in graph.

4.6 Overall Conclusions

The respirometric TVC test provides general simplicity (homogenization and pipetting) and miniaturization, a dynamic range (10^4-10^7 cfu/g), accuracy of ± 1.0 log(cfu/g), high speed and automation. Highly contaminated samples can be identified quickly (2-12 hours depending on the level of contamination), positive samples can be seen as the measurement progresses (real-time data output). Theoretical sensitivity of the respirometric assay is 1 cfu/well (O'Mahony and Papkovsky, 2006), however, assay volume (0.1 ml) and sample dilution during the homogenization (1:10) should be factored in for food samples. Statistical variability at low cell numbers (1-10 cells), possible matrix effects and data scattering reduce the sensitivity down to 10^3 -10^4 cfu/g (limit of detection, LOD), which is still very good and relevant to food testing and safety

assessment. Samples producing flat profiles with low phosphorescent signals are defined as negative (below the LOD). Up to 96 samples can be analyzed on a plate in one run. Its ability to assess highly perishable products such as fish and green produce in < 12 hours shows good application usage for industry in testing samples far quicker and reliably and making safety and quality assessments in large number of samples. The test offers simple set-up (conventional microplates and fluorescent reader), significant savings on labor, lab space and waste requirements, and it overcomes many drawbacks of conventional TVC testing. If required the sensitivity can be enhanced by using larger assay volumes (e.g. performing the assay in 1.5 ml and 15 ml vials) or reducing sample dilution during homogenization.

Application of this technique to quality assessment of different food products such as fresh salads or fish showed high practical utility for shelf-life stability studies, MAP process optimization and for assessing the efficiency of antimicrobial active packaging. Therefore, this system can find use in many food research, safety and QC labs, for both small and large users.

Chapter 5: The Use of Optical Sensors for Monitoring Headspace O_2 and CO_2 in Packaged Mushrooms (*Agaricus Bisporus*) during Chilled Storage

5.1 Introduction

Mushrooms (*Agaricus bisporus* L.) are very perishable horticultural products. They do not have a protective skin cover which leads to high moisture loss and a short shelf-life of 1-3 days at ambient temperature (Mahajan *et al.*, 2008). Mushrooms are very sensitive to humidity levels: high water levels favour microbial growth and discoloration; and low water levels lead to loss of weight (and thus economic value) and undesirable textural changes. Their respiration rates are high and special care should be taken to avoid anoxia which leads to rapid deterioration of tissue (Iqbal *et al.*, 2009). As a result, mushrooms are usually marketed in trays wrapped with perforated stretchable polyvinylchloride (PVC) film (Simón *et al.*, 2005) with little or no atmosphere modification being carried out. The perforations prevent anoxia and condensation inside the packages; therefore selection of optimal packaging material, density and size of micro-perforations and atmosphere within the packs is critical for maintaining mushroom quality over time.

A modified atmosphere (MA) is created inside the package and the specific atmosphere created is dependent upon a variety of factors interacting, namely; respiration rate of the mushrooms, gas permeability of the film, size and number of perforations present in the packaging materials, product to package ratio, the breathable film area and storage temperature (Mahajan *et al.*, 2007). For whole mushrooms, usually in pack O_2 concentrations are kept at 1-5 %, but not less than 1% to avoid anaerobic respiration and growth of pathogens (Tano *et al.*, 1999). In pack CO_2 concentrations should be maintain at relatively higher levels, but below 12 % to avoid physiological injuries such as browning (Parentelli *et al.*, 2007). Micro-perforated films are used for

achieving the appropriate gaseous composition in MA packs of fresh horticultural produce, especially for highly respiring products such as mushrooms (González *et al.*, 2008). Mahajan *et al.* (2009) reported that the degree of perforations affected final gas contents inside the packages, with a level of perforations between 2 to 8 holes of 0.25 mm diameter. Oliveira *et al.* (2012b) reported that 2 perforations (0.33 mm in diameter) were optimal for 110 grams of sliced mushrooms at 10°C, yielding 3.6% of O_2 and 11.5% of CO_2 at equilibrium. However, these parameters may vary for different package size, type of mushrooms, packaging and storage conditions.

Mushroom quality is determined by a combination of factors, but among the most important is consumer preference. An ideal mushroom is white, unblemished, possess a firm texture and is present in an immature state (i.e. the veil is totally closed). A loss of mushroom quality can be expressed through the measurement of several parameters, including; water loss, pH, texture, colour (L*, a*, b*), microbial counts and polyphenol oxidase (PPO) activity. Colour change is one important measurable parameter with a proposed limit of acceptance of $L^* = 80$ (Gormley, 1975). Another parameter is mottled brown discolouration caused by microorganisms, primarily *Pseudomonas tolaasii* (Simón *et al.*, 2005). PPO enzyme (Mohapatra *et al.*, 2008) produces brown melanin pigments when it makes contact with the mushrooms substrate. This reaction leads to a breakdown of mushroom fibers and causes further softening of mushroom caps. The shelf-life of mushrooms may be prolonged by slowing product respiration, thereby delaying microbial activity and preventing excessive water loss (Mahajan *et al.*, 2008). Brennan and Gormley. (1998) reported that chilled storage (4°C) of mushrooms from harvest to cooking helps to maintain quality by reducing the rate of bacterial growth and enzyme activity. Low temperature storage, together with low O_2 and high CO_2 levels, are known to reduce the respiration rate of fresh mushrooms and extend their shelf-life.

Non-invasive measurement of O_2 and CO_2 can be performed with optical sensors. Both absorbance and fluorescence based sensors for O_2 detection have been reported with a high suitability for food packaging applications. The response of absorbance based sensors is typically indicated by colour change, enabling semi-quantitative O_2 detection with no need for spectroscopic equipment (Eaton, 2002). Alternatively,

luminescence based sensors provide quantitative O_2 detection by using an external detector which allows a more precise evaluation of packaging headspace. These sensors usually consist of a phosphorescent dye incorporated in a polymer membrane which is quenched by headspace O_2. Optical CO_2 sensors consist of a CO_2 sensitive polymeric membrane based on a pH-sensitive indicator dye producing changes in colour or fluorescence which correlate with CO_2 concentration. These sensors were initially described by Mills (Mills *et al.*, 1992) in which the pH sensitive dye was incorporated in a hydrophobic polymeric membrane together with a hydrophobic phase transfer agent (PTA). By changing the PTA from tetraoctylammonium hydroxide (TOA-OH) to cetyltrimethylammonium hydroxide (CTA-OH) sensitivity to CO_2 in the range 0-40% can be achieved (Borchert *et al.*, 2012b). Current optochemical CO_2 sensors are not as developed as the phosphorescent O_2 sensors and require significant improvement of their stability, accuracy and robustness. While not quite ready for large scale industrial applications, they are suitable for food research and non-destructive headspace gas analysis in MAP packs. A handheld scanning device, similar to the one used for O_2 detection, has not been developed so far for CO_2 sensors. However; these sensors show colour change due to a pH-sensitive indicator dye, and can be used for semi-quantitative CO_2 detection. To the best of our knowledge, neither O_2 nor CO_2 optical sensors have been applied to study the headspace gas composition in packaged mushrooms.

The aim of this study was to non-destructively monitor the changes in gas composition with optochemical O_2 and CO_2 sensors and assess their impact on relevant microbiological and physicochemical quality parameters of packaged fresh white mushrooms during chilled storage at 4°C for up to 7 days.

5.2 Experimental

5.2.1 Materials

Button mushrooms (*Agaricus bisporus*) were supplied by a fresh produce supplier (Total Produce, Togher, Cork). Commercially used blue mushroom trays were purchased from Quinn Packaging (Dublin), cling film was obtained from Bunzl Irish Merchants (Dublin). Disposable O_2 sensor stickers and handheld detector Optech^{TM} were from Mocon (Minneapolis, MN) and Platinum(II)- tetrakis(pentafluorophenyl) porphyrin (PtTFPP) was obtained from Frontier Scientific (Carnforth, UK). Alpha-naphtholphthalein (NP), poly(isobutyl methacrylate) (P(IBM)), cetyltrimethylammonium hydroxide (CTA-OH), tetraoctylammonium hydroxide (TOA-OH), toluene, sodium phosphate buffer, polyvinylpyrrolidone (PVP-40) and catechol were purchased from Sigma- Aldrich. Mylar® polyester film was from Du Pont and 25 mL polystyrene screw cap tube were obtained from Sarstedt (Germany). Whatman paper (No. 1) was from Whatman Ldt (Maidstone, UK). Maximum recovery diluent, ringer solution, brilliance *E. Coli*/coliform Selective Agar, Pseudomonas agar base and CFC supplement were purchased from Oxoid (Basingstoke, UK). Total count plates were from Nissui Pharmaceutical (Co. Ltd., Japan) and stomacher bags were obtained from Seward (UK).

5.2.2 Sample Preparation and Experimental Set-up

Whole mushrooms of similar size were packed within 6 hours post-harvesting. Mushrooms were weighed (250 g ± 1%) into commercial blue tray (polypropylene/recycled high density polyethylene (PP/rHDPE), mushroom punnet 250 g, P3-57, w: 11.9 cm x l: 16 cm x h: 5.8 cm). Prior to over wrapping the mushrooms punnets with cling film (oxygen transmission rate: 6000/8000 cm^3/m^2/24hr and carbon

dioxide transmission rate: 40,000/60,000 cm^3/m^2/24hr), two O_2 sensors were fixed to the inside of the package wrapping film separated ~2 cm between them and two CO_2 sensors having different formulations were fixed to the punnet sidewall. The micro-perforation system for mushrooms is well established, to prevent excessive CO_2 accumulation and O_2 depletion in packaged mushrooms; therefore, the size and number of micro-perforation were estimated from the respiration rate and mathematical modelling principle as reported by Mahajan *et al.* (2007) and later applied for whole mushrooms (Mahajan *et al.*, 2009). Accordingly, to achieve an equilibrium modified atmosphere inside the package, it was perforated with two holes using a needle of 0.25 mm diameter. Packed mushrooms were stored in a cold room at an average temperature of 4°C ± 0.51 for the whole duration of the trial. Two trials were performed each consisting of 15 punnets. For quality determination 5 packs were opened on days 0, 2, 5 and 7.

5.2.3 Monitoring of O_2 and CO_2

The O_2 content inside the packs were measured non-invasively with disposable O_2 sensor stickers and Optech^{TM} Platinum O_2 handheld detector. An optical contact was created between the instrument and the sensor (5-10 mm distance) to produce the O_2 reading (% of O_2, compensated for temperature and pressure variation). Single measurement takes about 1 second and can be repeated as many times as necessary. In the first 2 days the O_2 levels were measured twice a day and once a day afterwards.

A) 

B) 

Figure 5.1: Standard colour score card used with the CO_2 sensors. A) Sensor formulation containing TOA-OH was used for lower CO_2 concentrations, B) Sensor formulation containing CTA-OH was used for higher CO_2 concentrations.

Headspace CO_2 concentration was determined with the colourimetric CO_2 sensors (Borchert *et al*., 2012b) by comparing them to a standard colour score card (Fig. 5.1). Low concentrations were recognized immediately by sensor formulation consisting PTA TOA-OH (0-3%, Fig. 5.1A) whereas higher concentrations were determined by the second sensor formulation consisting PTA CTA-OH (up to 40%, Fig. 5.1B). For each sensor formulations a colour code card was used covering the corresponding CO_2 region.

The performance of the optical sensor systems was verified with destructive gas analyzer Checkmate 9900 (PBI-Dansensor, Denmark).

5.2.4 Quality Parameter Measurements

For measurement of the microbiological and physico-chemical quality parameters, 5 mushroom packs, each containing 250 g of produce were opened on each measuring day. Each sample was used for one measurement only.

5.2.4.1 Physico-Chemical Analysis

Product weight loss (W_L) in each package was determined by transferring the mushrooms into a new tared tray and weighed on scales (Mettler Toledo B303, Switzerland). It was expressed as percentage of the initial weight:

$$W_L = \frac{W_i - W_t}{W_i} * 100 \qquad \text{Eqn. 5.1}$$

W_i is the initial weight of the mushrooms and W_t is the weight of the mushrooms at the sampling point.

Sensory evaluation of mushrooms throughout the storage was undertaken by a panel of 10 internally trained members (6 males/4 females, aged from 20 to 35 years) of the School of Food and Nutritional Sciences, University College Cork (conforms with ISO standard, 1998), using a 10 cm line scale with 0 at the extreme left and 10 at the extreme right and rating scores subsequently in cm from the left. Each panelist was presented with one white plate containing three randomly coded samples. The parameters evaluated by the assessors on the mushrooms during storage were: overall appearance (0 = extremely poor to 10 = excellent), degree of browning (0 = no browning to 10 = intense browning), veil development (0 = totally open to 10 = totally intact), texture (0 = extremely soft to 10 = extremely firm), sliminess (0 = not slimy to 10 = slimy), aroma (0 = non typical aroma to 10 = full typical aroma) and overall acceptability (0 = dislike extremely to 10 = like extremely).

Mushroom texture was measured using a texture analyzer TA-XT2i (Texture Technologies, USA) equipped with a 35 mm diameter cylindrical aluminium probe. 13 whole mushrooms of uniform size were selected for textural analysis (with stem removed) and compressed by 50% of the sample height by using following settings: pre-test speed: 5 mm/s, test speed: 5 mm/s, post-test speed: 10 mm/s, load cell: 5 kg. The firmness of the whole mushrooms was expressed in Newtons (N).

The colour of the mushroom cap and extract was determined based on the CIE colour parameters (L*, a* and b*) using a chroma meter (CR-400,) connected to data processor (DP-400), both from Konica Minolta, Japan. Browning index (BI) as reported by Maskan (2001) was calculated using eq. (Eqn. 5.2) and (Eqn. 5.3):

$$BI = \frac{100(x - 0.31)}{0.17} \qquad \text{Eqn. 5.2}$$

$$x = \frac{a + 1.75L}{5.645L + a - 3.012b} \qquad \text{Eqn. 5.3}$$

Whiteness index (WI) was calculated using eq. (Eqn. 5.4) (TAPPI, 2007).

$$WI = L - (3b) + (3a) \qquad \text{Eqn. 5.4}$$

Total colour difference (ΔE) and hue were also calculated as reported by (Cruz-Romero *et al*., 2007).

An average of 10 measurements per mushroom sample were taken on the surface of the mushroom cap. For the measurement of colour of the mushroom extract, the extract was prepared by mixing mushrooms without stems with Ringer solution in a ratio of 1:4 and stomaching (Seward, UK) for 2 minutes. The homogenates were centrifuged at 12,000 *x* g (Model J2-21, Beckman Co., USA) for 15 minutes at 4°C and the supernatant was transferred in a 25 ml polystyrene screw cap tube. The colour was measured on the surface of the clear solution. For each measurement day, four extracts were made and at least 10 measurements were taken for each sample.

Spectrophotometric measurement of PPO activity was introduced by Galeazzi *et al.* (1981). In order to obtain a representative sample, a number of subsamples of the outer skin of three mushrooms without stems were taken using sterile scalpels from

different parts of the mushrooms cap into a sterile stomacher bag, pooled and thoroughly mixed and 10 ± 0.02 g of the pooled mushrooms samples were weighted into a beaker and 20 ml of 0.5 M sodium phosphate buffer (pH 6.5) containing 1 g of polyvinylpyrroline were added. The samples were homogenized under ice using an ultra-turrax homogenizer (T 25, IKA –Werke GmbH & Co KG, Germany) at 8,000 rpm for 1 minute. Subsequently the homogenates were centrifuged at 12,000 *x* g for 30 minutes at 4°C in a Beckman centrifuge (Model J2-21, Beckman Co., USA). The supernatant was filtered using a Whatman filter paper and the filtrate was used as crude enzyme extract and the enzymatic activity measured immediately. PPO activity was assessed, based on oxidation of catechol. The absorbance was measured at 400 nm by UV–Vis Spectrophotometer

FT-IR analysis of the extract (as used for PPO activity) was performed on a Varian 660 FT-IR spectrometer using ATR Golden Gate (Specac). Spectra were taken using 32 scans in absorbance mode at 4 cm^{-1} resolution in a wavenumber range from 4000 to 500 cm^{-1}. To obtain IR spectrum of the sample, the spectrum of the 0.5 M sodium phosphate buffer pH 6.5 was measured and subtracted. Each sample was measured in duplicate.

The pH of mushrooms was determined by mixing 10 g of mushroom (without stem) with 90 ml of distilled water and homogenizing for 2 minutes in a stomacher and taking 5 measurements per sample on a pH meter (Mettler Toledo, Switzerland). Prior to the measurements the pH meter was calibrated with standard buffers of pH 4 and 7.

5.2.4.2 Microbiological Analysis

Microbiological analyses of mushrooms during storage at 4°C were performed in triplicate on each measurement day. In order to obtain a representative sample, six mushrooms without stems were taken aseptically using sterile forceps and scalpels from different parts of the pack, placed into a sterile stomacher bag, pooled and thoroughly mixed for 3 minutes using a stomacher (Seward, UK). 10 g of the pooled mushrooms

samples were weighted aseptically into a stomacher bag in a vertical laminar-flow cabinet and a primary 10-fold dilution was performed by the addition (90 ml) of sterile maximum recovery diluent (Oxoid, Basingstoke, UK). Following homogenization in a stomacher for 3 minutes, homogenates were serially diluted 10-fold in maximum recovery diluent, and 1 ml of each appropriate dilution was inoculated on duplicated plates in the centre of compact dry-total count plates (20 cm^2) (Nissui Pharmaceutical, Co. Ltd., Japan) for enumeration of total mesophilic aerobic bacteria following incubation at 30°C for 48 hours. Total coliforms and *E.coli* were enumerated on Brilliance *E. Coli*/coliform Selective Agar (Oxoid) following incubation at 37°C for 24 hours. Oxoid *Brilliance E. coli*/coliform Selective Agar is a chromogenic medium for the detection and enumeration of *E. coli* and other coliforms (important hygiene indicators) from food. Chromogenic agents in the medium were used to detect the ß-glucuronidase activity of *E. coli* and the ß–galactosidase activity of coliforms (including *E. coli*), allowing them to be clearly differentiated on the culture plate (coliforms – pink, *E. coli* – purple). Pseudomonas spp. was enumerated after 2 days incubation at 30°C on Pseudomonas agar base (Oxoid) to which CFC (cetrimide, fucidin, cephaloridine; Oxoid) supplement was added. Bacterial numbers were converted to $\log_{10}$ colony-forming units per gram sample (cfu/g sample) prior to statistical analyses.

5.2.5 Statistical Analysis

Statistical analysis was carried out using IBM SPSS statistics software, version 20. To determine differences between samples measured at different storage time, Duncan tests were applied and significant differences were established at $P < 0.05$. The degree of correlation of quality parameters and gases (CO_2 and O_2) was estimated using the Pearson test; at the level of significance was set at $P < 0.05$.

5.3 Results & Discussion

5.3.1 O_2 and CO_2 Headspace Concentrations

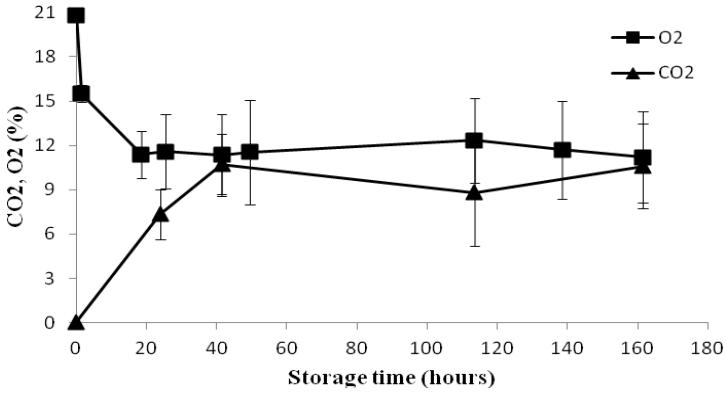

Figure 5.2: Changes in O_2 and CO_2 concentrations in the headspace of packaged mushrooms during storage at 4°C measured with optical sensors. Error bars represent standard deviations of data from duplicate trials (n = 10).

Changes in O_2 concentration in packaged mushrooms simulating commercial packaging practices are shown in Fig. 5.2. The concentration of O_2 decreased significantly ($P < 0.05$) over the first 18.5 hours reaching a concentration of 11.4%. After this a slow increase in the O_2 levels was observed but this increase was not significant. Therefore, equilibrium of O_2 levels in the packaged mushrooms was reached after 18.5 hours storage. This is lower than reported in the study by Oliveira *et al.* (2012a), in which equilibration time was determined to be around 24 hours at 5°C. The difference can be due to variations in product weight, number of ventilation holes present in package materials, storage temperature, ratio weight/packaging volume, mushrooms size and method of measurement. A two-stage respiration process, the first being rapid and the second slower, has been extensively reported in the literature (Halachmy and Mannheim, 1991; Tano *et al.*, 1999; Oliveira *et al.*, 2012a). The initial stage of fast respiration is probably due to the high concentration of O_2 in the pack and

high temperature of the mushrooms (~12°C). It becomes slower at lower temperature and availability of O_2. The plateau was attained when equilibrium was reached. At the end of the storage (161.5 hours) the concentration of O_2 reached the value of 11.2%. Fonseca *et al.* (2002) reported that during storage of mushrooms lowered O_2 concentration is normally preferred in order to slow down respiration processes and oxidative breakdown of complex substrates. However, very low O_2 leads to anaerobic condition and this condition can promote the growth of some pathogenic bacteria such as *Clostridium* spp. (Tano *et al.*, 1999). In this study, the concentration of O_2 stayed above 0% throughout the storage time (Fig. 5.2), therefore, avoiding anaerobic conditions. In order to assess the quality parameters and correlate it to gas composition; it is essential to determine continuously the gas composition of the headspace during the entire storage life.

CO_2 concentration increased ($P < 0.05$) significantly from 0.04% (air concentration) reaching equilibrium level of 10.7% after 41.5 hours and then remained practically unchanged and not exceeding 12%. Tano *et al.* (1999) reported that CO_2 concentrations of 12% and higher are known to cause loss of firmness and increase browning in mushrooms. In mushrooms, CO_2 concentration has also been reported to have an inhibitory effect on the respiration rate (Fonseca *et al.*, 2002).

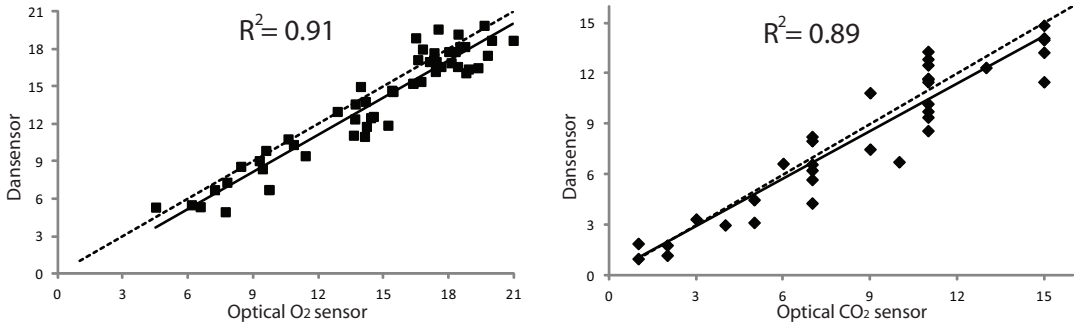

Figure 5.3: Correlation of readings from the optical O_2 (A) and CO_2 (B) sensors and commercial Dansensor^{TM} instrument. Dashed lines represent the ideal correlation and solid lines represents linear trendlines.

For comparison purposes, the O_2 gas composition in the headspace of packaged mushrooms was determined using a well-established method (Dansensor^{TM}) and non-invasive measurement using optical sensors (Optech^{TM} system). The correlation obtained between the two methods showed a coefficient of correlation of $R^2 = 0.91$ (Fig. 5.3A) with slightly higher oxygen concentration (~1% O_2) being determined when measured using the Optech^{TM} system.

The correlation obtained for the CO_2 concentration measurement between both CO_2 optical sensors and Dansensor^{TM} was $R^2 = 0.89$ (Fig. 5.3B). Despite the fact that CO_2 was determined semi-quantitatively using a visual assessment *via* a colour score card (Fig. 5.1), the prediction of CO_2 was found to be quite reliable.

Therefore, both O_2 and CO_2 in the headspace of packaged mushrooms can be measured rapidly and non-invasively using optical sensors what is of horticultural industrial interest. As these sensors were attached to the sidewall and lid of the package they did not interfere with the product headspace at any time when concentration of gases was measured during shelf-life.

5.3.2 Sensory Evaluation

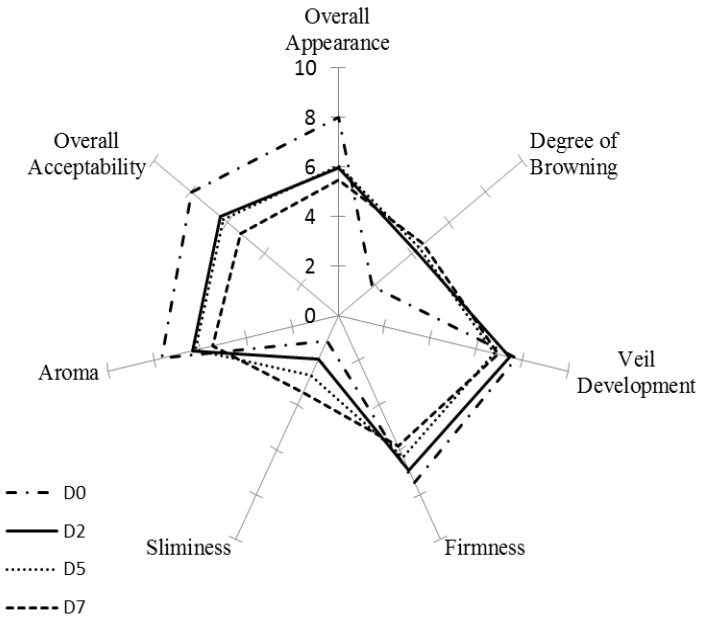

Figure 5.4: Changes in the sensory scores during storage of packaged mushrooms at 4°C. Each point is an average of 60 observations (n = 60).

The results of the quantitative descriptive analysis of packed whole mushrooms are presented in a spider plot (Fig. 5.4), where each corner contributes to an attribute and each line to the scores using 10 levels of classification. Throughout the storage time (7 days) all 7 quality parameters assessed changed in score intensity.

The sensory analysis of the packaged mushrooms showed that the overall appearance decreased ($P < 0.05$) significantly during storage. This attribute correlated well with the degree of browning of the mushroom caps ($R^2 = 0.982$) which was significantly higher ($P < 0.05$) at day 7 compared to samples at day 0. Browning is an important quality parameter responsible for quality loss in mushrooms. Major changes in both parameters, overall appearance and browning intensity, occurred within the first 2 days of storage. It has been reported that the significantly decrease in O_2 concentration causes a decrease in activity of oxidases, such as PPO and that the increase in CO_2 concentration increase the bacteriostatic effect on microorganisms and various

enzymatic reactions (Kader, 1986; Daniels et al., 1985). The aroma of the packed mushrooms changed significantly during the storage time, the intensity of full typical aroma was lower at the end of the storage. No significant changes in veil development were observed in the sensory analysis of the packaged mushrooms. The firmness of the mushrooms determined by the texture analyser decreased during storage at 4°C; the mushrooms were significantly ($P < 0.05$) softer at day 7 compared to day 0. However, the sensory analysis results of firmness did not correlate to the measured firmness determined by the texture analyser (chapter 5.3.4).

The sliminess of the mushroom caps increased significantly ($P < 0.05$) during storage; the mushroom caps were slimier at day 7 compared to day 0. It has been reported that the increase in the microbiological counts, especially *Pseudomonas* spp., produces exopolysaccharides and form a biofilm on the mushrooms surface, making the mushrooms slimier (Fett, 1995). The results showed that the intensity of the sliminess increased over time, so as the microbial load of *Pseudomonas* spp. (chapter 5.3.8). To the best of our knowledge, this parameter was not used previously in sensory analysis of mushrooms and the sensory data on the sliminess attribute correlated well with the microbiological spoilage of the mushrooms.

A general significant ($P < 0.05$) decrease in the overall acceptability was noticed throughout the storage time with a score of 5.3 obtained at day 7 which was close to the limit of acceptability (score 5) for the average consumer. The overall liking of the mushrooms decreased over time. Mohapatra *et al.* (2011) reported that the parameter of overall acceptability was an appropriate indicator by which other mushroom quality indicators such as maturity and cap hardness could be determined.

5.3.3 Measurement of Polyphenol Oxidase (PPO) Enzyme Activity

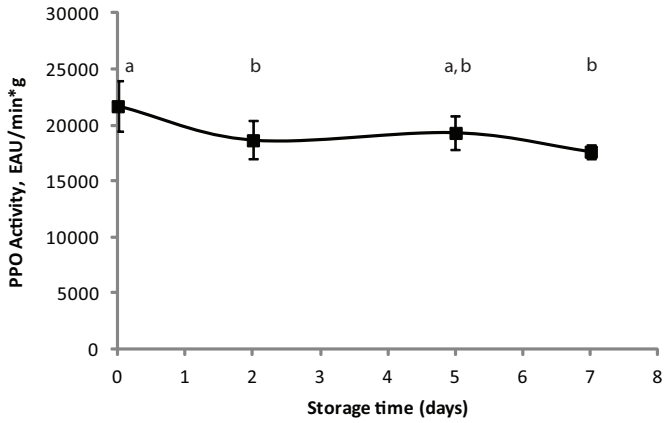

Figure 5.5: Changes in the polyphenol oxidase activity during storage of packaged mushrooms at 4°C. Letters a and b above the data points indicate significant differences ($P < 0.05$).

The pattern of the PPO enzyme activity (Fig. 5.5) showed a decrease in activity during the storage, with significant decreases ($P < 0.05$) on day 2. However, no significant changes were observed after day 2. Beaulieu *et al.* (1999) reported that PPO produced black, brown or red pigments (polyphenols) causing fruit browning. The presence of PPO in the mushrooms correlated well with sensory results. High PPO activity makes mushrooms prone to browning. The early decrease in PPO activity is unusual as it typically increases over time (Tao *et al.*, 2007), even when analysis is performed at different temperatures (Mohapatra *et al.*, 2008). The results showed that the decrease in enzymatic activity was correlated to the increase of CO_2 concentration in the first 2 days. However, after 2 days storage little changes in the enzymatic (PPO) and CO_2 concentration were noticed. Enzymatic inhibition effect due to increased CO_2 concentration has been reported by Farber (1991) and includes direct inhibition of enzymes and decrease on enzyme reactions rate.

5.3.4 Textural Analysis

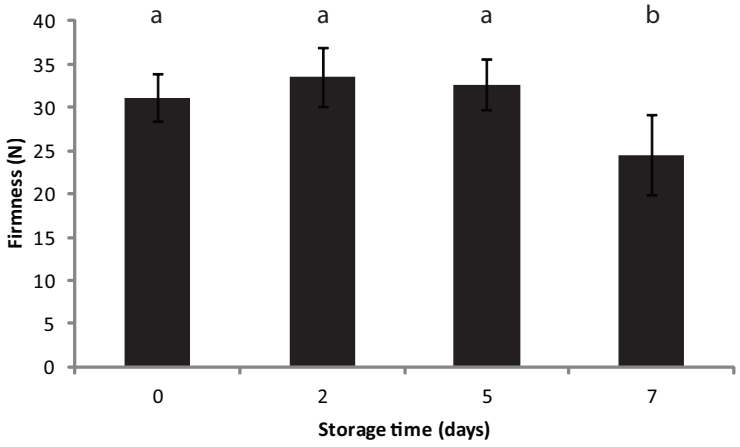

Figure 5.6: Changes in the firmness of packed mushrooms during storage at 4°C. Error bars represent standard deviation of n = 13 replicates; letters a and b above the bars indicate significant differences ($P < 0.05$).

A non-significant increase in the firmness of the mushrooms was noticed up to day 5; however, after day 5 a significant ($P < 0.05$) decrease in firmness on the mushroom caps were noticed (Fig. 5.6). These results did not correlate with the results found in sensory analysis: in which a significant ($P < 0.05$) decrease on firmness decrease was noticed on day 5 by the sensory panel. Tano *et al.* (1999) reported an initial increase in firmness, and this increase was correlated to cap expansion due to growth related chitin production in the mushroom tissue during the first 6 days of storage at 4°C. Furthermore, it has been reported that texture changes are also related to protein and polysaccharide degradation, hyphae shrinkage, central vascuole disruption and expansion of intracellular space (Zivanovic *et al.*, 2000). Mohapatra *et al.* (2011) reported that variability in the sensory evaluation of the cap hardness was affected significantly by batch variability than by sensory panel variability. Furthermore, a correlation between texture and CO_2 concentration has been proposed; this being that as CO_2 concentration increases, textural loss decreases (Briones *et al.*, 1992). In this study, the headspace gas composition correlated well with sensory data; however, significant

($P < 0.05$) decrease in the firmness measured using a texture analyser was detected after day 5.

5.3.5 Colour Measurement

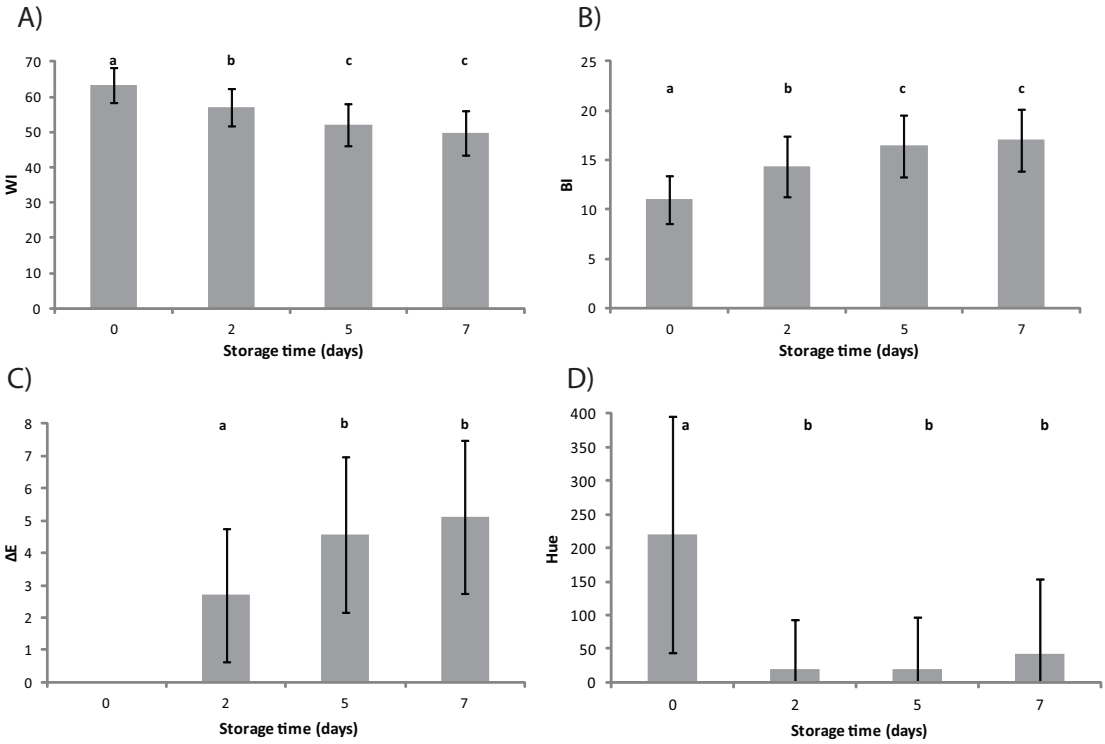

Figure 5.7: Changes in the A) whiteness index (WI), B) browning index (BI), C) total colour difference (ΔE) and D) hue of mushroom cap during storage at 4°C. Error bars represent standard deviation of n = 40; letters a, b and c above the data points indicate significant differences ($P < 0.05$).

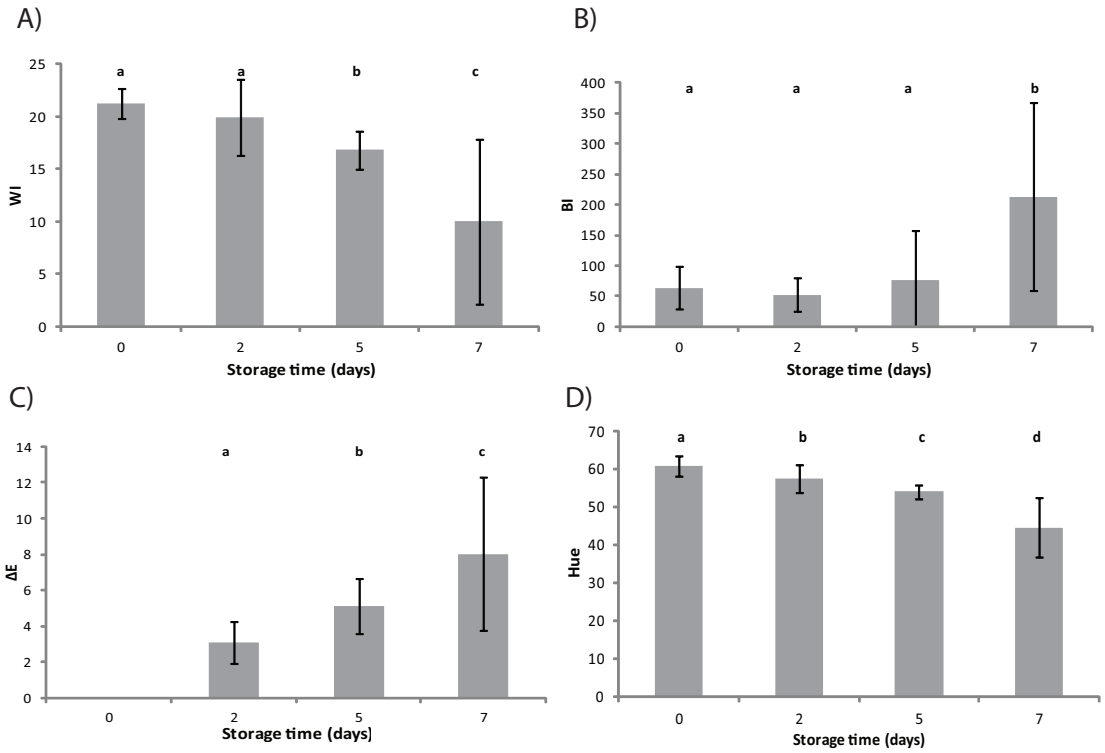

Figure 5.8: Changes in the A) whiteness index (WI), B) browning index (BI), C) total colour difference (ΔE) and D) hue of mushroom extract during storage at 4°C. Error bars represent standard deviation of n = 40; letters a, b, c and d above the data points indicate significant differences ($P < 0.05$).

Changes in the whiteness index (WI), browning index (BI), total colour difference (ΔE) and hue values are shown in Fig. 5.7 for the caps and in Fig. 5.8 for the extract. For both WI decreased significantly ($P < 0.05$) throughout the storage. For mushroom caps, the WI parameter is directly correlated to a higher L* values that represents whiter samples and reciprocal to the browning index. Over time, the whiteness of mushrooms decreased: mushroom caps were darker at day 7 compared to samples at day 0 (Fig. 5.7A). Our results are in agreement with the results reported by Sapers *et al.* (2001) and Oliveira *et al.* (2012a) where L* values decreased in whole and sliced mushrooms stored at 4 or 5°C, respectively. Sapers *et al.* (2001) reported a decrease of L* values for whole mushrooms from 93.3 to 89.6 on day 8 of storage at 4°C which are in agreement with

our results (decrease from 92.58 ± 1.31 to 89.76 ± 1.53 on day 7 of storage at 4°C). Both, WI and L* values of mushroom caps decreased significantly in the first 2 days of storage and this changes correlated to significant increase in CO_2 and decrease in O_2 concentration. Changes in WI and L* values were minimal after day 2 as a corresponding equilibrium of gas concentration in the headspace was reached.

The BI of mushroom caps (Fig. 5.7B) increased significantly ($P < 0.05$) up to day 5; however, no significant changes were noticed after day 5. The BI of the mushroom extract (Fig. 5.8B) did not increase significantly up to day 5; however, significant changes were noticed after this time point. The results of changes in the BI of mushroom caps are in agreement with those of Mohapatra *et al*. (2010), who found that the BI increased during storage from 11 at day 0 to 13 at day 7.

The ΔE values, an indicator of total colour difference, showed that there were significant differences ($P < 0.05$) in the colour of mushroom caps (Fig. 5.7C) and extracts (Fig. 5.8C) during storage. The smaller the value of ΔE, the closer samples are in colour. Values of ΔE between 0 and 0.2 indicate an imperceptible colour difference; 0.2–0.5 a very small difference, 0.5–1.5 a small difference, 1.5–3.0 a distinct difference, 3.0–6.0 for a very distinct change, 6.0–12.0 for a great change and values >12 representing a very great difference. Using this classification scale for total colour difference reported by Cruz-Romero *et al*. (2007), it can be concluded that distinct changes in colour were obtained for mushrooms stored up to 2 days. Very distinct differences in the colour of the mushrooms were observed following 2 days storage. For the extracts, the ΔE values obtained up to day 5 indicated that these were very distinct changes compared to samples at day 0, and a great difference in colour was observed following 5 days storage. The changes in the ΔE values are in agreement with the changes in ΔE values reported by Oliveira *et al*. (2012a) who found increased ΔE values during the storage of sliced mushrooms.

In general, the hue angle of the mushroom cap and extract decreased significantly ($P < 0.05$) with increasing storage time, corresponding to a decrease in the intensity of greenness and an increase in yellowness (Little, 1975). The results indicated that the changes in colour indices of the mushroom cap and extract followed the same pattern

(Fig. 5.7D and 5.8D), indicating that the measurement of these colour parameters during storage at refrigeration temperature can be measured in the mushrooms extract, giving a more representative measurement of the colour of the whole mushroom instead of specific point measurement on the individual mushroom obtained in the mushroom cap.

5.3.6 Product Weight Loss & pH Measurement

Table 5.1: Changes in pH and weight loss (WL) during a storage at 4°C of packed mushrooms*

Day	pH	WL (%)
0	6.44 ± 0.03 [a]	-
2	6.94 ± 0.11 [b]	0.86 ± 0.14 [a]
5	6.83 ± 0.19 [c]	1.45 ± 0.09 [b]
7	7.19 ± 0.06 [d]	1.75 ± 0.21 [c]

a,b,c,d: different letters in the same row indicate significant differences ($P < 0.05$).

*Values are means ± standard deviation. pH (n=4) and WL (n=10)

The pH of fresh mushrooms was 6.44, in agreement with previous reported data (Jaworska *et al*., 2010; Oliveira *et al*., 2012b). The pH increased significantly ($P < 0.05$) over storage time (Table 5.1). Conversely, Oliveira *et al.* (2012b) reported a slight pH decrease in sliced mushrooms due to the production of organic acids by microorganisms. However, the pH increase in this study might be due to the production of aldehydes and ammonia due autolytic reactions and deamination of amino acids (Eady and Large, 1971) by bacteria species such as *Pseudomonas* that possess amine dehydrogenase, which predominantly are present in mushroom samples during prolonged storage, accompanying bacterial decay.

Significant ($P < 0.05$) increases in WL were observed during the storage of packaged mushrooms and highest WL values were observed over the first two days of storage (Table 5.1). Simon *et al.* (2005) reported a higher WL after 7 days storage, 2.0 or 2.5% for non-perforated or perforated PVC films, respectively. These findings were

also dependent upon the relative humidity inside the package and the water vapour transmission rate of the packaging film used. Non-perforated films usually present some condensation due to water loss of the mushrooms, therefore, micro-perforation is recommended for packaging mushrooms. However, the number and size of micro-perforation needs be to be optimized considering both recommended gas levels and relative humidity inside the package. For sliced mushrooms, a WL of 3.8% after 6 days of storage at 5°C was obtained in packs of 110 g and 1 perforation (Oliveira *et al.*, 2012a). This increased WL was due to a greater surface to volume area which caused increased transpiration.

5.3.7 Fourier Transformed-Infrared Spectroscopy (FT-IR)

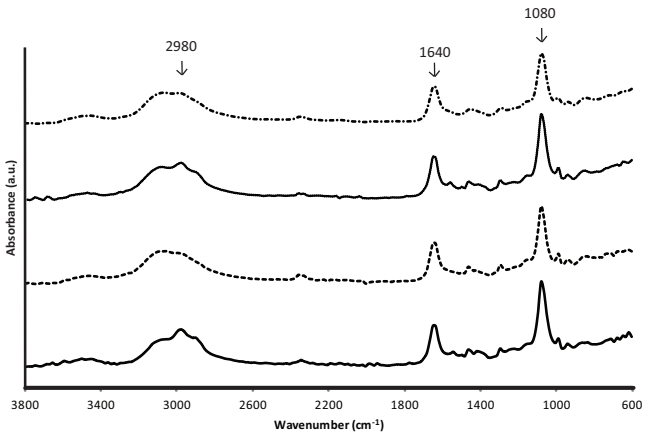

Figure 5.9: FT-IR spectra of mushroom extract at various storage times: day 0 (—), day 2 (---), day 5 (···) and day 7 (-·-).

Three major bands have been identified in the mushroom extract spectra which varied with storage time (Fig. 5.9). While the first two were sharp and narrow bands in nature at 1080 cm^{-1} (indicative of S=O or OH-groups) and at 1640 cm^{-1} (indicative of aromatics and alkenes), the third one was rather broad at 2980 cm^{-1} (indicative of aromatics and alkenes) (Silverstein and Webster, 1998) and exhibited a plateau with some minor peaks on top (day 0 and day 7). The peak heights correlated with the

polyphenol oxidase activity: day 0 > day 5 > day 2 > day 7 from highest to lowest activity. By using FT-IR some characteristic functional groups can be identified which might be produced in the presence of enzymes by degrading mushroom tissue (hydroxylation and oxidation processes) (Mayer, 2006). As this approach for the quantification of enzyme concentration is quite new, we can speculate that the higher the enzymatic activity present in mushrooms, the greater the number of functional groups that might be present in the extract. Thus, the use of FT-IR has good potential for assessing rapidly enzymatic activity of mushrooms during storage and need to be explored further.

5.3.8 Microbiological Analysis

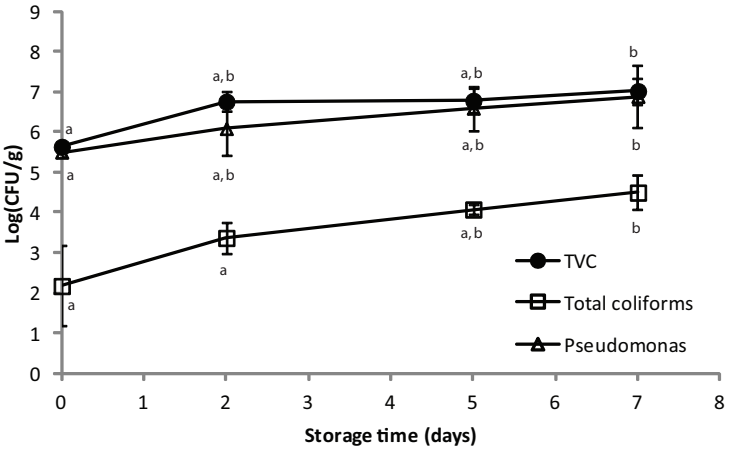

Figure 5.10: Microbiological changes occurring during the storage of packed mushrooms. Error bars represent standard deviation of n = 4 replicates; letters a and b above or below the data points indicate significant differences ($P < 0.05$).

Initial microbiological counts and changes in TVC, *Pseudomonas* spp., and total coliforms during chilled storage are shown in Fig. 5.10. On day 0 the TVC, *Pseudomonas* spp. and total coliforms were determined to be 5.6, 5.5 and 2.2 log cfu/g sample, respectively. At the end of the storage (day 7), TVC, *Pseudomonas* spp. and

total coliforms were 7.0, 6.9 and 4.5 log cfu/g sample, respectively. *Pseudomonas* spp. was the main spoilage microorganism at the end of storage (comprising 98.6% of the total microbiological flora). A high percentage of the strictly aerobic *Pseudomonas* spp. being present in mushrooms has been previously reported (Simón *et al.*, 2005, González-Fandos *et al.*, 2000). According to Dainty and Mackey (1992) environmental conditions with residual oxygen is theoretically sufficient to support the growth of these bacteria. The gas composition during storage reached a headspace equilibrium value of 11.4% and 10.7% for O_2 and CO_2 concentration, respectively. This concentration of oxygen is enough to support the growth of *Pseudomonas* spp. The bacteriostatic effect of CO_2 with increasing CO_2 concentration, thus during the first 2 days storage, correlated well with the bacterial growth rate (Fig. 5.10). This is in general noticed with an increased lag phase and generation time during growth of microorganisms (Phillips, 1996). It has been reported that aerobic bacteria, such as *Pseudomonas* are inhibited by moderate levels of CO_2 (10-20%) (Farber, 1991).

5.3.9 Correlations of Headspace Gases and Mushroom Quality Parameters

The correlation of different mushroom quality parameters and headspace gas composition is shown in Table 5.2. Pearson correlation analyses of the quality parameters and gases indicated a strong positive or negative relation between CO_2 or O_2 and the most of the assessed quality parameters (such as PPO, TVC, *Pseudomonas*, total coliforms, pH, WL; Colour indexes BI_{cap}, WI_{cap}, ΔE_{cap}, Hue_{cap} , $WI_{extract}$, $\Delta E_{extract}$ and $Hue_{extract}$, and sensory parameters (overall appearance, degree of browning, texture, veil development, sliminess, aroma and overall acceptability)) with a significance level of $P < 0.05$ (Table 5.2).

Table 2: Pearson correlations of quality parameters and colour indexes to headspace gas (CO_2 & O_2) composition of packaged mushrooms stored at 4°C.

	CO_2	O_2
PPO	-.692**	.649**
TVC	.884**	-.911**
Pseudomonas	.735**	-.712**
Total Coliforms	.704**	-.757**
pH	.841**	-.834**
WL	.886**	-.862**
Texture	-.037	.037
S: O. Appearance	-.941**	.961**
S: L. Browning	.978**	-.947**
S: Veil development	-.788**	.815**
S: Texture	-.688**	.703**
S: Sliminess	.750**	-.690**
S: Aroma	-.813**	.845**
S: O. Acceptability	-.875**	.900**
BI cap	-.882**	.909**
WI cap	.843**	-.861**
ΔE cap	-.871**	.895**
Hue cap	.652**	-.643**
BI extract	-.230	.308
WI extract	.574*	-.576*
ΔE extract	-.739**	.765**
Hue extract	.637**	-.632**

**. Correlation is significant at the 0.01 level (2-tailed).
*. Correlation is significant at the 0.05 level (2-tailed).
S- Sensory.

Due to mushroom respiration process, CO_2 concentration increased over time while O_2 concentration decreased. Therefore, a negative correlation was observed for CO_2 and overall appearance (R = -0.941, P = 0.000) and O_2 and degree of browning (R = -0.947, P = 0.000). However, a lower correlation was observed between gas composition (O_2: R = 0.649; $P < 0.01$ and CO_2: R = -0.692; $P < 0.01$) and PPO enzyme activity. It has been reported that increased concentrations of CO_2 have an enzymatic inhibitory effect (Farber, 1991) and this was observed in the first 2 days of storage (Fig. 5.2). Furthermore, there was not significant correlation between the headspace gas (CO_2 and O_2) content and instrumental texture; however, good correlations of these gases to

texture obtained by sensory means of mushrooms were observed (Table 5.2). Texture loss was related to increasing CO_2 concentration (Briones et al. 1992). The large negative correlation of CO_2 and texture indicated that the increased CO_2 concentration resulted in a texture loss. The colour indexes of the caps (except Hue) and the colour index ΔE of the extract correlated very well to the changes in the headspace gas composition (Table 5.2).

Table 3: Correlation of quality parameters of packaged mushrooms stored at 4°C.

	Pearson Correlation
S: D.Browning/PPO	.707**
S: D.Browning/TVC	.883**
S: D.Browning/*Pseudomonas*	.806**
S: D.Browning/S: O.Appearance	-.945**
S: Sliminess/TVC	.700**
S: Sliminess/*Pseudomonas*	.749**
S: Texture/texture	.634**
S: O.Appearance/S: O.Acceptability	.967**

**. Correlation is significant at the 0.01 level (2-tailed).
S- Sensory.

Correlation of quality parameters are presented in Table 5.3. A good correlation of TVC (R = 0.700, $P < 0.01$) and *Pseudomonas* (R = 0.749, $P < 0.01$) to the sensory parameter sliminess were observed. The increased values of sliminess may be due to the production of exopolysaccharides produced by *Pseudomonas spp.* (Fett, 1995). TVC, *Pseudomonas* and PPO activity correlated well to the degree of browning of the mushroom cap, indicating that possibly bacteria and enzymes were responsible for the browning. The sensory attribute overall appearance revealed a very strong positive correlation to the overall acceptability (R = 0.967, $P = 0.000$) and degree of browning (R = -0.945, $P = 0.000$). This result indicates that the degree of browning influenced overall appearance and this attribute influenced the overall acceptability of mushrooms. The instrumental firmness of the mushrooms did not correlate well to any of the other

assessed quality parameters, however, the instrumental firmness texture correlated to firmness obtained by sensory analysis ($R = 0.634$, $P < 0.01$).

5.4 Conclusions

This study showed that headspace gases in the packed mushrooms can be measured using a non-expensive, simple non-destructive, non-disturbing method through the application of optical sensors. The concentration of CO_2 and O_2 in package headspace correlated well with a well-known destructive method (Dansensor^{TM}), and this is of particular interest to the fresh produce industry. Good correlation of quality parameters to headspace gas (CO_2, O_2) composition of packaged mushrooms was observed. *Pseudomonas* spp. was the main spoilage microorganism at the end of storage comprising 98.6% of the total microbiological flora which also correlated well with sensorial determined sliminess in mushroom caps. The results in this study showed that an increase in CO_2 concentration was directly correlated to partially inhibition of enzymatic activity. Beside the traditional spectrophotometric method to assess enzymatic activity, FT-IR has a good potential for assessing rapidly enzymatic activity of mushrooms during storage and need to be explored further. Furthermore, the new method developed for colour measurement using a mushroom extract, giving a more representative measurement of the colour of the whole mushroom instead of a specific spot measurement on the individual mushroom obtained in the mushroom cap showed great potential as an alternative colour measurement method for product evaluation, as this may make the measurement of colour more representative.

Overall Discussion

Safety of food products need to be constantly improved, leading to extended shelf-life, information and consumer convenience and to protect the food against an increasing amount of hazards. In first instance that means to transform and adapt new packaging developments, such as intelligent packaging, and secondly to quick test food itself before further processing. Intelligent packaging devices are able to monitor certain conditions inside the pack in a more eloquent way than traditional systems can do by applying new sensor technology to measure the inside gas composition. This technology is based on indicators and sensors comprising dyes incorporated into polymer matrices dissolved in organic solvents. Of practical use for intelligent packaging are solid state sensors which can be easily incorporated on the inside of the package and be read through the material. Their advantages against traditional methods, such as Dansensor or gas chromatography is to provide fast, non-destructive and reliable determination of important packaging conditions. These optical sensor spots can be measured as many times as necessary without any change of the inside conditions.

O_2 and CO_2 are beside the filling agent N_2 the most important gas components in MAP. For example, a change in O_2 or CO_2 concentration can indicate the growth of microorganisms (Mattila *et al.*, 1990) or packaging damage and can be important for freshness and shelf-life studies (Fu *et al.*, 1992) by relating their changes to food quality inside the pack. Optical O_2 gas sensors are the most developed and already commercialized by PreSense, OxySense, Mocon and Luxcel Biosciences. These sensors are based on luminescent quenching of phosphorescent platinum(II)-porphyrin complexes incorporated in polystyrene matrix giving signals in the microsecond range and optimized for O_2 sensing in the range 0-21% O_2. They have already been tested in many different food matrices, including meat (Smiddy *et al.*, 2002a), fresh produce (Borchert *et al.*, 2012), cheese (Hempel *et al.*, 2012b), beer (Hempel *et al.*, 2012a). Several CO_2 sensors are described in the literature as feasible for food packaging but less of them have been technically applied. One common strategy is to use 1-

hydroxypyrene-3, 6, 8-trisulfonate (HPTS) and Ru-(dpp) in a sol-gel matrix applying the Dual Luminophore Reference (DLR) scheme (Bültzingslöwen *et al.*, 2002).

Instead of using two single sensors, one for O_2 and one for CO_2 detection, a measurement system of both gases at the same time and in the same spot would be revolutionary for food pakaging as it safes time, space and money. Such multi-parametric-systems combine the measurement of at least two parameters within one sensor system, usually by incorporating several dyes in one polymer encapsulating media. In my knowledge dual systems for O_2 and CO_2 sensing for food packaging have not been realized so far. Nevertheless, there are some sensors available with the potential for food packaging. One approach of O_2/CO_2 sensing makes use of PtTFPP in PS for O_2 detection and HPTS (ion paired with TOA-OH) in EC microparticles incorporated in a PDMS rubber as second layer (Borisov *et al.*, 2006).

As these cocktails are often quite complicated the use of only one dye would simplify the mechanism and preparation. One dual analyte O_2/pH sensor is described in Chapter 2 comprising a typical O_2 sensitive dye PtOEP or PdCP. Through the modification of the structure, a Schiff-base group (SB) has been attached at one meso-position proximal to the macrocycle, the dye became sensitive to protons by constant O_2 sensitivity. The sensor allows the detection of the two analytes with just one phosphorescent reporter dye, with internal referencing schemes and no interfering cross-sensitivity. This concept can be applied to other types of sensor materials (e.g. nanosensors (Borisov and Klimant, 2008; Peng *et al.*, 2010), magnetic particles (Mistlberger *et al.*, 2010)), analytes (temperature, CO_2, NH_3, ions, enzyme biosensors based on O_2 and pH transducers (McDonagh *et al.*, 2008)), and sensing schemes (de Silva *et al.*, 2009; McDonagh *et al.*, 2008; Wolfbeis, 2008) and integrated with optical imaging systems. In the medium and long term this approach can be of high use for the food packaging industry, although it still requires more development to improve performance and pH range. As the majority of existing optochemical CO_2 sensors are based on pH indicators this sensor system was developed to show similar sensitivity to gaseous CO_2. When water is present in the sensing system, being that by using PTA, CO_2 can be detected due to its high solubility in water. Carbonic acid is formed and gets dissociated into

hydrogen carbonate and carbonate ions (Mills and Skinner, 2011). As water becomes acidic through this reaction, the pH change is detected and is converted into CO_2 concentration using calibration. As this system lacks of sensitivity to gaseous CO_2, other sensor schemes were tested, such as intensity based systems, DLR, inner filter quenching and FRET, being the latter one as most appropriate. A CO_2 sensor based on this scheme make use of two dyes in one matrix with one being short lived and CO_2 sensitive (NP) and the other one being long lived (PtTFPP) but insensitive to CO_2. Chapter 3 describes the development of a FRET based CO_2 sensor with robust changes in phosphorescence LT of the PtTFPP dye in response to CO_2 concentration with fast response and recovery time. The use of long-decay emitting dye is advantageous compared to the absorbance or fluorescence-based CO_2 sensors since it enables stable calibration and simple readout of the optical signal in phosphorescence lifetime mode. These sensors show potential for food packaging applications on disposable basis, but further investigation is needed to extend the measurement range up to 100% CO_2 from the current 0 to 40%.

Chapter 5 describes the use of two optical sensors to detect the two headspace gas concentrations O_2 and CO_2 in continuous mode on the example of mushrooms. In here, the established optical O_2 sensor developed in earlier projects by our team and the in chapter 3 described optical CO_2 sensors has been applied to the inner atmosphere of fresh whole mushrooms. The CO_2 content was measured semi-quantitatively by applying a colour score card and O_2 by applying a handheld instrument Optech^{TM}. Good correlation with standard Dansensor method was achieved for these optical sensors, thus proving their ability to determine accurately and non-invasively the CO_2 and O_2 content in individual packs. O_2 supports growth of bacteria and activity of enzymes while CO_2 inhibits growth, at high concentration they can rapidly damage the product. Therefore, optical CO_2 and O_2 sensors are well suited for food quality assessment. Potentially, both analytes can be measured with one device but currently this is only feasible for O_2 concentration using the Optech^{TM} system.

The quality of some food products need to be determined before they can be further processed by the industry. Beside identification of specific pathogenic microorganisms,

the determination of the TVC is important for general quality estimations. TVC determination provides a general estimate of the microbial population. Microbial testing is done by many food microbiology laboratories for the purpose of revealing important information about the status of a food product, whether it can be consumed without causing food poisoning, whether it was handled correctly, and whether it is old or fresh. With this information one can distinguish between good or bad products in order of origin, age and handling. Conventional microbial tests are based on aerobic plate count methods, which are specified as the standard ISO 4833:2003 method in the food industry (ISO:4833:2003, 2003). They are time consuming and space, waste and material intensive.

Some biosensor systems for quick determination of microorganisms in food samples based on fluorescent dye technology are available. MicroFoss^{TM} by Biosys, Inc., developed by Ann Arbor, includes a computerized instrument with disposable vials based on the detection of metabolic processes of organisms. An optical sensor allows screening results in as little as 7-18 hours, depending on microbial contamination (Odumeru and Belvedere, 2002). A microtitre-plate TVC test based on monitoring of bacterial respiration using phosphorescent oxygen sensing probes and fluorescent plate reader detection was described by O'Mahony *et al.* (2006) and applied to analysis of aerobic bacteria in complex samples such as broth and food homogenates (O'Mahony and Papkovsky, 2006), and in meat samples for the enumeration of total viable counts (O'Mahony *et al.*, 2009). Compared to different meat samples we have demonstrated its ability to assess other highly perishable products such as fresh fish and green produce (chapter 4) to test such samples quickly (< 12 hours) and reliably and perform safety and quality assessments of large number of samples. The test offers simple set-up (conventional microplates and fluorescent reader), significant savings on time, labour, lab space and waste. Application of this technique to quality assessment of different food products showed high practical utility for shelf-life stability studies and MAP process optimization. Therefore, this system can find use in many food research, safety and QC labs.

Further development of optical sensor technology is expected to continue with emphasis on flexibility (multiple systems), easy handling and integration into packaging systems, improvement of performance and development of dedicated instrumentation.

Overall Conclusions

- Realization of a dual-analyte optochemical sensor for dissolved O_2 and pH with one bi-functional reporter dye, which is technically applicable for food packaging.
- The new FRET based CO_2 sensor (with TOA-OH) shows potential for food packaging applications on disposable basis in the range of 0 - 40% CO_2.
- The respirometric TVC test can be applied for quality assessment of different food products such as fresh salads or fish and showed high practical utility for shelf-life stability studies and MAP process optimization.
- The concentration of CO_2 and O_2 in package headspace correlated well with a well-known destructive method (Dansensor^{TM}). Therefore, packed mushrooms can be measured using a simple non-destructive, non-disturbing method through the application of optical sensors.

Thesis Outcomes

Peer reviewed papers:

Borchert, N., Ponomarev, G.V., Kerry, J.P., Papkovsky, D.B. (2010). O_2/pH Multisensor Based on One Phosphorescent Dye. Anal. Chem., 83:18-22. DOI: http://dx.doi.org/10.1021/ac1025754.

Hempel, A., Borchert, N., Walsh, H., Roy Choudhury, K., Kerry, J., Papkovsky, D. (2011). Analysis of Total Aerobic Viable Counts in Raw Fish by High-Throughput Optical Oxygen Respirometry. J Food Prot, 74: 776-782. DOI: http://dx.doi.org/10.4315/0362-028X.JFP-10-352.

Borchert, N., Hempel, A., Walsh, H., Kerry, J.P., Papkovsky, D.B. (2012). High throughput quality and safety assessment of packaged green produce using two optical oxygen sensor based systems. Food Control, 28: 87-93. DOI: http://dx.doi.org/10.1016/j.foodcont.2012.04.044.

Borchert, N.B., Kerry, J.P., Papkovsky, D.B. (2012). A CO_2 sensor based on Pt-porphyrin dye and FRET scheme for food packaging applications. Sensors Actuat. B: Chem., in Press. DOI: http://dx.doi.org/10.1016/j.snb.2012.09.043.

Submitted paper:

Borchert, N., Cruz-Romero, M., Mahajan, P., Ren, M., Papkovsky, D., Kerry J. (2012). The use of optical sensors for monitoring headspace O_2 and CO_2 in packaged mushrooms (*Agaricus bisporus*) during chilled storage.

Patent application:

Papkovsky D.B., Borchert N., A sensor material and uses thereof to simultaneously sense two analytes. Application filed by Luxcel Biosciences on 29. March, 2010, Cork, Ireland. EP2371925 (A1).

Conference Abstracts:

Borchert, N.B., Kerry, J.P., Papkovsky, D.B. (2010). A two-analyte O_2/pH sensor based on one phosphorescent dye. In: Book of Abstracts of the European Optical Sensor Conference, Europtrode, Prague, Czech Republic, March 28-31, P61.

Borchert, N.B., Hempel, A., Walsh, H., Kerry, J.P., Papkovsky D.B. (2011). Analysis of total aerobic viable counts in raw fish by high throughput optical oxygen respirometry. In: Book of Abstracts of the 40th Annual UCC Food Research Conference, Cork, Ireland, 31st March – 1st April, P3.

Murphy B., Hynes J., Carey C., Borchert N.B., Walsh H, Fernandes R., Papkovsky D. (2011). Same day – TVC results in raw meat and fish including preparation and incubation time. In: Book of Abstracts of the European symposium on food safety, IAFP, Ede, The Netherlands, 18-20 May.

Borchert, N.B., Hempel A., Walsh, H., Kerry, J.P., Papkovsky, D.B. (2011). Analysis of total aerobic viable counts in raw fish by high throughput optical oxygen respirometry. In: Book of Abstracts of the Society for Applied Microbiology (SfAM) Summer Conference, Dublin, Ireland, 4-7th July.

Borchert, N.B., Hempel, A., Walsh, H., Kerry, J.P., Papkovsky D.B. (2012). High throughput quality and safety assessment of packaged green produce using two optical oxygen sensor systems Optech™ and Greenlight™. In: Book of Abstracts of the 2nd international meeting on materials/bioproduct interactions (MATBIM), Dijon, France, 22nd-25th April, S1P3.

Borchert, N.B., Kerry, J.P., Papkovsky, D.B. (2012). A phosphorescence-based CO_2 sensor for smart packaging of food products. In: Book of Abstracts of the 2nd

international meeting on materials/bioproduct interactions (MATBIM), Dijon, France, 22nd-25th April, S1P2.

Bibliography

Abbas, K., Saleh, A., Mohamed, A. and Lasekan, O. (2009). The relationship between water activity and fish spoilage during cold storage: A review. J. Food Agric. Enviro. 7(3-4): 86-90.

Ali, R., Lang, T., Saleh, S. M., Meier, R. J. and Wolfbeis, O. S. (2011). Optical Sensing Scheme for Carbon Dioxide Using a Solvatochromic Probe. Anal. Chem. 83(8): 2846–2851.

Allende, A., Jacxsens, L., Devlieghere, F., Debevere, J. and Artes, F. (2002). Effect of superatmospheric oxygen packaging on sensorial quality, spoilage, and Listeria monocytogenes and Aeromonas caviae growth in fresh processed mixed salads. J. Food Prot. 174; 65(10): 1565-1573.

Allende, A., Luo, Y., McEvoy, J. L., Artés, F. and Wang, C. Y. (2004). Microbial and quality changes in minimally processed baby spinach leaves stored under super atmospheric oxygen and modified atmosphere conditions. Postharvest Biol. Technol. 33(1): 51-59.

Amanatidou, A., Smid, E. J. and Gorris, L. G. M. (1999). Effect of elevated oxygen and carbon dioxide on the surface growth of vegetable-associated micro-organisms. J. Appl. Microbiol. 86(3): 429-438.

Amao, Y. and Komori, T. (2005). Optical CO2 sensor of the combination of colorimetric change of [alpha]-naphtholphthalein in poly(isobutyl methacrylate) and fluorescent porphyrin in polystyrene. Talanta 66(4): 976-981.

Amao, Y. and Komori, T. (2005). Optical CO2 sensor of the combination of colorimetric change of [alpha]-naphtholphthalein in poly(isobutyl methacrylate) and fluorescent porphyrin in polystyrene. Talanta 66(4): 976-981.

Amao, Y. and Nakamura, N. (2004a). An optical sensor with the combination of colorimetric change of [alpha]-naphtholphthalein and internal reference luminescent dye for CO2 in water. Sensor Actuat. B-Chem. 107(2): 861-865.

Amao, Y. and Nakamura, N. (2004b). Optical CO2 sensor with the combination of colorimetric change of [alpha]-naphtholphthalein and internal reference fluorescent porphyrin dye. Sensor Actuat. B-Chem. 100(3): 347-351.

Amao, Y., Asai, K. and Okura, I. (2000). Oxygen sensing based on lifetime of photoexcited triplet state of platinum porphyrin–polystyrene film using time-resolved spectroscopy. J. Porphyr. Phthalocya. 4(3): 292-299.

Amao, Y., Komori, T. and Nishide, H. (2005). Rapid responsible optical CO2 sensor of the combination of colorimetric change of [alpha]-naphtholphthalein in poly(trimethylsiliylpropyne) layer and internal reference fluorescent porphyrin in polystyrene layer. React. Funct. Polym. 63(1): 35-41.

Bailey Jr, E. and Rollefson, G. (1953). The determination of the fluorescence lifetimes of dissolved substances by a phase shift method. J. Chem. Phys. 21: 1315.

Barat, J. M., Gil, L., García-Breijo, E., Aristoy, M. C., Toldrá, F., Martínez-Máñez, R. and Soto, J. (2008). Freshness monitoring of sea bream (Sparus aurata) with a potentiometric sensor. Food Chem. 108(2): 681-688.

Basu, B. J. (2007). Optical oxygen sensing based on luminescence quenching of platinum porphyrin dyes doped in ormosil coatings. Sensors Actuat. B: Chem. 123(1): 568-577.

Beaulieu, M., D'Apran, M. B. G. and Lacroix, M. (1999). Dose Rate Effect of γ Irradiation on Phenolic Compounds, Polyphenol Oxidase, and Browning of Mushrooms (Agaricus bisporus). J. Agri. Food Chem. 47(7): 2537-2543.

Bedoya, M., Díez, M. T., Moreno-Bondi, M. C. and Orellana, G. (2006). Humidity sensing with a luminescent Ru(II) complex and phase-sensitive detection. Sensors Actuat. B: Chem. 113(2): 573-581.

bioMerieux Tempo Tested TVC Test, Granted PTM Status - Performance Tested Methods[SM]. (2008). AOAC Research institute news, May/June.

Blackburn, C., Baylis, C. and Petitt, S. (2008). Evaluation of PetrifilmTM methods for enumeration of aerobic flora and coliforms in a wide range of foods. Let. Appl. Microbiol. 22(2): 137-140.

Bodenhammer, W. T. (2002). Method and apparatus for selective biological material detection. US Patent 6376204:

Borchert, N. B., Kerry, J. P. and Papkovsky, D. B. (2012b). A CO2 sensor based on Pt-porphyrin dye and FRET scheme for food packaging applications. Sensors Actuat. B: Chem. 176: 157-165.

Borchert, N. B., Ponomarev, G. V., Kerry, J. P. and Papkovsky, D. B. (2010). O2/pH Multisensor Based on One Phosphorescent Dye. Anal. Chem. 83(1): 18-22.

Borchert, N., Hempel, A., Walsh, H., Kerry, J. P. and Papkovsky, D. B. (2012a). High throughput quality and safety assessment of packaged green produce using two optical oxygen sensor based systems. Food Control 28(1): 87-93.

Borisov, S. M. and Klimant, I. (2008). Optical nanosensors—smart tools in bioanalytics. Analyst 133(10): 1302-1307.

Borisov, S. M., Lehner, P. and Klimant, I. (2011). Novel optical trace oxygen sensors based on platinum(II) and palladium(II) complexes with 5,10,15,20-meso-tetrakis-(2,3,4,5,6-pentafluorphenyl)-porphyrin covalently immobilized on silica-gel particles. Analytica Chim. Acta 690(1): 108-115.

Borisov, S. M., Nuss, G. and Klimant, I. (2008). Red Light-Excitable Oxygen Sensing Materials Based on Platinum(II) and Palladium(II) Benzoporphyrins. Anal. Chem. 80(24): 9435-9442.

Borisov, S. M., Waldhier, M. C., Klimant, I. and Wolfbeis, O. S. (2007). Optical Carbon Dioxide Sensors Based on Silicone-Encapsulated Room-Temperature Ionic Liquids. Chem. Mater. 19(25): 6187-6194.

Borisov, S. M., Zenkl, G. and Klimant, I. (2010). Phosphorescent platinum(II) and palladium(II) complexes with azatetrabenzoporphyrins—New red laser diode-compatible indicators for optical oxygen sensing. ACS Appl. Mater. Interfaces 2(2): 366-374.

Borisov, S., Gatterer, K. and Klimant, I. (2010a). Red light-excitable dual lifetime referenced optical pH sensors with intrinsic temperature compensation. Analyst 135: 1711-1717.

Borisov, S., Krause, C., Arain, S. and Wolfbeis, O. (2006). Composite material for simultaneous and contactless luminescent sensing and imaging of oxygen and carbon dioxide. Adv. Mater. 18(12): 1511.

Boumsellek, S. and Ferran, R. J. (2001). Trade-offs in miniature quadrupole designs. J. Am. Soc. Mass Spectrom. 12(6): 633-640.

Brennan, M. H., Gormley, T. H. (1998). Extending the shelf life of fresh sliced mushrooms, in Teagasc.

Briggs, D., Brookes, P., Stevens, R. and Boulton, C. (2004). Brewing: Science and Practice. Woodhead Publishing,

Briñas, R. P., Troxler, T., Hochstrasser, R. M. and Vinogradov, S. A. (2005). Phosphorescent Oxygen Sensor with Dendritic Protection and Two-Photon Absorbing Antenna. J. Am. Chem. Soc. 127(33): 11851-11862.

Briones, G. L., Varoquaux, P., Chambroy, Y., Bouquant, J., Bureau, G. and Pascat, B. (1992). Storage of common mushroom under controlled atmospheres. Int. J. Food Sci. Technol. 27(5): 493-505.

Broenkow, W. W. (1969). An interface sampler using spring-actuated syringes. Limnol. Oceanogr. 14(2): 288-291.

Bültzingslöwen, C. (2004). Development of optical sensors ("optodes") for carbon dioxide and their application to modified atmosphere packaging (MAP). PhD Thesis. Universität Regensburg, Regensburg, Germany.

Bültzingslöwen, C., McEvoy, A. K., McDonagh, C. and MacCraith, B. D. (2003). Lifetime-based optical sensor for high-level pCO2 detection employing fluorescence resonance energy transfer. Anal. Chim. Acta 480(2): 275-283.

Bültzingslöwen, C., McEvoy, A., McDonagh, C., MacCraith, B., Klimant, I., Krause, C. and Wolfbeis, O. (2002). Sol–gel based optical carbon dioxide sensor employing dual luminophore referencing for application in food packaging technology. Analyst 127(11): 1478-1483.

Burke, C. S., Markey, A., Nooney, R. I., Byrne, P. and McDonagh, C. (2006). Development of an optical sensor probe for the detection of dissolved carbon dioxide. Sensor Actuat. B-Chem. 119(1): 288-294.

Buydens, L., Kassovsky, V. and Diels, R. (2006). Intelligent Infrared Comfort Sensors for the Automotive Environment. Adv. Microsys. Automotive Appl. 261-280.

Cajlakovic, M., Bizzarri, A. and Ribitsch, V. (2006). Luminescence lifetime-based carbon dioxide optical sensor for clinical applications. Analyt. Chim. Acta 573-574: 57-64.

Cajlakovic, M., Bizzarri, A., Suppan, M., Konrad, C. and Ribitsch, V. (2009a). Continuous monitoring of pO2 and pCO2 by microdialysis indicates physiologic status of the critically ill patients. Sensors Actuat. B: Chem. 139(1): 181-186.

Cajlakovic, M., Bizzarri, A., Suppan, M., Konrad, C., Tscherner, M., Ribitsch, V., Beran, E. and Knez, I. (2009b). Simultaneously monitoring of tissue O2 and CO2 partial pressures by means of miniaturized implanted fiber optical sensors. IEEE Sensors 2009 Conference: 31-36.

Carvajal, M. A., de Vargas-Sansalvador, I. M. P., Palma, A. J., Fernández-Ramos, M. D. and Capitán-Vallvey, L. F. (2010). Hand-held optical instrument for CO2 in gas phase based on sensing film coating optoelectronic elements. Sensors Actuat. B: Chem. 144(1): 232-238.

Chen, M., Schliep, M., Willows, R. D., Cai, Z.-L., Neilan, B. A. and Scheer, H. (2010). A Red-Shifted Chlorophyll. Sci 329(5997): 1318-1319.

Chen, Z., Chen, H., Hu, H., Yu, M., Li, F., Zhang, Q., Zhou, Z., Yi, T. and Huang, C. (2008). Versatile synthesis strategy for carboxylic acid-functionalized upconverting nanophosphors as biological labels. J. Am. Chem. Soc. 130(10): 3023-3029.

Clark, L. C. (1956). Monitor and control of blood and tissue oxygen tensions. A. Soc. Art. Int. Org. 2(1): 41-48.

Commision Directive 2002/72/EC, C. D. (2002). relating to plastic materials and articles intended to come into contact with foodstuffs. L 220: 18-58.

Cruz-Romero, M., and and Kerry, J. P. (2008). Crop-based biodegradable packaging and its environmental implications. CAB Reviews: Perspectives in Agriculture, Veterinary Science, Nutrition and Natural Resources 3(82): 25 pp.

Cruz-Romero, M., Kelly, A. L. and Kerry, J. P. (2007). Effects of high-pressure and heat treatments on physical and biochemical characteristics of oysters (Crassostrea gigas). Innov. Food Sci. Emerg. Technol. 8(1): 30-38.

Cywinski, P. J., Moro, A. J., Stanca, S. E., Biskup, C. and Mohr, G. J. (2009). Ratiometric porphyrin-based layers and nanoparticles for measuring oxygen in biosamples. Sensors Actuat. B: Chem. 135(2): 472-477.

Dainelli, D., Gontard, N., Spyropoulos, D., Zondervan-van den Beuken, E. and Tobback, P. (2008). Active and intelligent food packaging: legal aspects and safety concerns. Trends Food Sci. Technol. 19: S103-S112.

Dainty, R. H., & Mackey, B. M. (1992). The relationship between the phenotypic properties of bacteria from chill-stored meat and spoilage processes. J. Appl. Bacteriol., (Symposium Suppl. 21), 103Se114S.

Daniels, J. A., Krishnamurthi, R., Rizvi, S. (1985). A Review of effects of carbon dioxide on microbial growth and food quality. J. Food Prot. 48: 532-537.

Davies, R., Davies, O. and Abowei, J. (2009). The Status of Fish Storage Technologies in Niger Delta Nigeria. Am. J. Sci. Res.

De Silva, A. P., Moody, T. S. and Wright, G. D. (2009). Fluorescent PET (Photoinduced Electron Transfer) sensors as potent analytical tools. Analyst 134(12): 2385-2393.

De Vargas-Sansalvador, I. M. P., Fay, C., Phelan, T., Fernández-Ramos, M. D., Capitán-Vallvey, L. F., Diamond, D. and Benito-Lopez, F. (2011). A new light emitting diode–light emitting diode portable carbon dioxide gas sensor based on an interchangeable membrane system for industrial applications. Anal. Chim. Acta 699(2): 216-222.

De Vargas-Sansalvador, P., Carvajal, M., Roldán-Muñoz, O., Banqueri, J., Fernández-Ramos, M. and Capitán-Vallvey, L. (2009). Phosphorescent sensing of carbon dioxide based on secondary inner-filter quenching. Anal. Chim. Acta 655(1-2): 66-74.

Del Nobile, M., Conte, A., Cannarsi, M. and Sinigaglia, M. (2008). Use of biodegradable films for prolonging the shelf life of minimally processed lettuce. J. Food Eng. 85(3): 317-325.

Demas, J. N., DeGraff, B. A. and Coleman, P. B. (1999). Oxygen sensors based on luminescence quenching. Anal. Chem. 71(23): 793A-800A.

Dimitri, C., Tegene, A. and Kaufman, P. R. (2003). US fresh produce markets: marketing channels, trade practices, and retail pricing behavior. United States Department of Agriculture, Agricultural Economic Report Number 825(

Dolphin, D. (1978). The porphyrins. vol. 3. part. A; physical chemistry. Academic Press.

Dworkin, M., Falkow, S., Rosenberg, E., Schleifer, K.-H., Stackebrandt, E. (2006). The Prokaryotes: Symbiotic associations, biotechnology, applied microbiology. Springer.

Dybko, A., Wroblewski, W., Maciejewski, J., Romaniuk, R. S. and Brzozka, Z. (1997). Fiber optic probe for monitoring of drinking water. Proc. SPIE 3105: 361.

Eady, R. and Large, P. (1971). Microbial oxidation of amines. Spectral and kinetic properties of the primary amine dehydrogenase of Pseudomonas AM 1. Biochem. J. 123(5): 757.

European Economic Community (EEC). (1985). Official Journal of European Communities. L373: 14 ff.

European Economic Community (EEC). (1997). Official Journal of European Communities. 40(L222): 11 ff.

Farber, J. M. (1991). Microbiological aspects of modified-atmosphere packaging technology – a review. J. Food Prot. 54: 58-70.

Ferguson, J. A., Healey, B. G., Bronk, K. S., Barnard, S. M. and Walt, D. R. (1997). Simultaneous monitoring of pH, CO2 and O2 using an optical imaging fiber. Anal. Chim. Acta 340(1–3): 123-131.

Fernandez-Sanchez, J., Cannas, R., Spichiger, S., Steiger, R. and Spichiger-Keller, U. (2007). Optical CO2-sensing layers for clinical application based on pH-sensitive indicators incorporated into nanoscopic metal-oxide supports. Sensor Actuat. B-Chem. 128(1): 145-153.

Ferrati, A. R., Tavolaro, P., Destro, M. T., Landgraf, M. and Franco, B. D. G. M. (2010). A comparison of ready-to-use systems for evaluating the microbiological quality of acidic fruit juices using non-pasteurized orange juice as an experimental model. Int. Microbiol. 8(1): 49-53.

Ferreira, J. and Girotto, E. M. (2009). Optical pH sensitive material based on bromophenol blue-doped polypyrrole. Sensors Actuat. B: Chem. 137(2): 426-431.

Fett, W.F., Wells, J.M., Cescutti, P., Wijey, C. (1995). Identification of exopolysaccharides produced by fluorescent pseudomonads associated with

commercial mushroom (Agaricus bisporus) production. Appl. Environ. Microbiol. 61(2): 513-7.

Fitzgerald, M., Papkovsky, D., Smiddy, M., Kerry, J., O'Sullivan, C., Buckley, D. and Guilbault, G. (2001). Nondestructive monitoring of oxygen profiles in packaged foods using phase fluorimetric oxygen sensor. J. Food Sci. 66(1): 105-110.

Fonseca, S. C., Oliveira, A. R., Brecht, J. K. (2002). Modelling respiration rate of fresh fruits and vegetables for modified atmosphere pachages: a review. J. Food Eng. 52: 99-119.

Food and Drug Administration. (2002). Preparation of Food Contact Notifications and Food Additive Petitions for Food Contact Substances: Chemistry Recommendations.

Fu, A. H., Molins, R. A. and Sebranek, J. G. (1992). Storage Quality Characteristics of Beef Rib Eye Steaks Packaged in Modified Atmospheres. J. Food Sci. 57(2): 283-287.

Fu, L.-M., Wen, X.-F., Ai, X.-C., Sun, Y., Wu, Y.-S., Zhang, J.-P. and Wang, Y. (2005). Efficient Two-Photon-Sensitized Luminescence of a Europium(III) Complex. Angew. Chem. 117(5): 757-760.

Galeazzi, M. A. M., Sgarbieri, V. C. and Constantinides, S. M. (1981). Isolation, Purification and Physicochemical Characterization of Polyphenoloxidases (PPO) from a Dwarf Variety of Banana (Musa cavendishii, L). J. Food Sci. 46(1): 150-155.

Gillanders, R., Arzhakova, O., Hempel, A., Dolgova, A., Kerry, J., Yarysheva, L., Bakeev, N., Volynskii, A. and Papkovsky, D. (2010). Phosphorescent Oxygen Sensors Based on Nanostructured Polyolefin Substrates. Anal. Chem 82(2): 466-468.

Gonçalves, H. M. R., Maule, C. D., Jorge, P. A. S. and Esteves da Silva, J. C. G. (2008). Fiber optic lifetime pH sensing based on ruthenium(II) complexes with dicarboxybipyridine. Anal. Chim. Acta 626(1): 62-70.

González, J., Ferrer, A., Oria, R. and Salvador, M. L. (2008). Determination of O2 and CO2 transmission rates through microperforated films for modified atmosphere packaging of fresh fruits and vegetables. J. Food Eng. 86(2): 194-201.

González-Fandos, E., Giménez, M., Olarte, C., Sanz, S. and Simón, A. (2000). Effect of packaging conditions on the growth of micro-organisms and the quality characteristics of fresh mushrooms (Agaricus bisporus) stored at inadequate temperatures. J. Appl. Microbiol. 89(4): 624-632.

Gormley, R. (1975). Chill storage of mushrooms. J. Sci. Food Agri. 26(4): 401-411.

Gouterman, M., Callis, J., Dalton, L., Khalil, G., Mébarki, Y., Cooper, K. R. and Grenier, M. (2004). Dual luminophor pressure-sensitive paint: III. Application to automotive model testing. Meas. Sci. Technol. 15(10): 1986.

Gram, L. and Dalgaard, P. (2002). Fish spoilage bacteria–problems and solutions. Curr. Opin. Biotechnol. 13(3): 262-266.

Gram, L. and Huss, H. (1996). Microbiological spoilage of fish and fish products. Int. J. Food Microbiol. 33(1): 121-137.

Halachmy, I. B. and Mannheim, C. H. (1991). Modified atmosphere packaging of fresh mushrooms. Packag. Technol. Sci. 4(5): 279-286.

Han, J. H. (2005). Innovations in food packaging. Elsevier Ltd., Academic Press,

Hartmann, P. and Trettnak, W. (1996). Effects of polymer matrices on calibration functions of luminescent oxygen sensors based on porphyrin ketone complexes. Anal. Chem. 68(15): 2615-2620.

Hattula, T., Miettinen, H., Luoma, T., Arvola, A., Kettunen, J. and Setälä, J. (2002). Effects of Different On-Board Cooling Methods on the Microbiological and Sensory Quality of Baltic Herring (Clupea harengus L.). J.Aqua. Food Prod. Technol. 11(3-4): 167-175.

Hayes, R. J. and Liu, Y. B. (2008). Genetic Variation for Shelf-life of Salad-cut Lettuce in Modified-atmosphere Environments. J. Amer. Soc. Hort. Sci. 133(2): 228-233.

Hempel, A. W., Gillanders, R. N., Papkovsky, D. B. and Kerry, J. P. (2012b). Detection of cheese packaging containment failures using reversible optical oxygen sensors. Int. J. Dairy Technol. 65(3): 456-460.

Hempel, A. W., Gillanders, R. N., Papkovsky, D. B. and Kerry, J. P. (2012b). Detection of cheese packaging containment failures using reversible optical oxygen sensors. International Journal of Dairy Technology 65(3): 456-460.

Hempel, A., Borchert, N., Walsh, H., Roy Choudhury, K., Kerry, J. and Papkovsky, D. (2011). Analysis of Total Aerobic Viable Counts in Raw Fish by High-Throughput Optical Oxygen Respirometry. J. Food Prot. 74(5): 776-782.

Hempel, A., O'Sullivan, M. G., Papkovsky, D. B. and Kerry, J. P. (2012a). Use of optical oxygen sensors to monitor residual oxygen in pre- and post-pasteurised bottled Beer and its effect on sensory attributes and product acceptability during Simulated commercial storage. LWT - Food Science and Technology: doi: 10.1016/j.lwt.2012.05.026.

Hempel, A., O'Sullivan, M. G., Papkovsky, D. B. and Kerry, J. P. (2012a). Use of optical oxygen sensors to monitor residual oxygen in pre- and post-pasteurised bottled Beer and its effect on sensory attributes and product acceptability during Simulated commercial storage. LWT - Food Sci. Technology:

Hogan, S. A. and Kerry, J. (2008). Smart Packaging of Meat and Poultry Products. In: Smart Packaging Technologies, 33-59. John Wiley & Sons Ltd., West Sussex PO19 8SQ, England.

http://luxcel.com, (accessed: 11.10.2012).

http://www.aditus.se/news/2007_bioett_device.pdf, (accessed: 05.11.2012).

http://www.aeschemunex.com/microbialtestingsolutionsforalllabs,6/35,bactiflow-als-real-time-analyzer.html, (accessed: 29.08.2012).

http://www.biocontrolsystems.com/, (accessed: 29.08.2012).

http://www.dwscientific.co.uk/rabit/, (accessed: 29.08.2012).

http://www.foodsafetymagazine.com/article.asp?id=1502&sub=sub1, (accessed: 14.09.2012).

http://www.neogen.com/FoodSafety/S_Index.html, (accessed: 29.08.2012).

http://www.nissui-pharm.co.jp/english/industry/pdf/CompactDry_TC_E.pdf, (accessed: 29.08.2012).

http://www.oxysense.com/index.html, (accessed: 11.10.2012).

http://www.perceptive.co.uk/applications/deft.htm, (accessed: 29.08.2012).

http://www.presens.de/, (accessed: 11.10.2012).

http://www.r-biopharm.com/product_site.php?language=english&product_id=332, (accessed: 29.08.2012).

http://www.roithner-laser.com, (accessed: 15.10.2009).

http://www.sylab.com/bactrac.htm, (accessed: 29.08.2012).

Huber, C., Klimant, I., Krause, C., Werner, T., Mayr, T. and Wolfbeis, O. S. (2000). Optical sensor for seawater salinity. Fresenius' J.Anal. Chem. 368(2): 196-202.

Hynes, J., Hill, R. and Papkovsky, D. B. (2006). The use of a fluorescence-based oxygen uptake assay in the analysis of cytotoxicity. Toxicol. in Vitro 20(5): 785-792.

Ibrahim, S., Nassar, A. and El-Badry, N. (2008). Effect of Modified Atmosphere Packaging and Vacuum Packaging Methods on Some Quality Aspects of Smoked Mullet (Mugil cephalus). J. Global Veterinaria 2(296-300.

Iqbal, T., Rodrigues, F. A. S., Mahajan, P. V. and Kerry, J. P. (2009). Effect of Time, Temperature, and Slicing on Respiration Rate of Mushrooms. J. Food Sci. 74(6): E298-E303.

ISO:4833:2003 (2003). Microbiology of food and animal feeding stuffs -- Horizontal method for the enumeration of microorganisms -- Colony-count technique at 30 degrees C.

Jacxsens, L., Devlieghere, F., Van der Steen, C. and Debevere, J. (2001). Effect of high oxygen modified atmosphere packaging on microbial growth and sensorial qualities of fresh-cut produce. Int. J. Food Microbiol. 71(2-3): 197-210.

Jaworska, G., Bernas, E., Biernacka, A., Maciejaszek, I. (2010). Comparison of the texture of fresh and preserved Agaricus bisporus and Boletus edulis mushrooms. Int. J. Food Sci. Technol. 45: 1659-1665.

Jeevarajan, A. S., Vani, S., Taylor, T. D. and Anderson, M. M. (2002). Continuous pH monitoring in a perfused bioreactor system using an optical pH sensor. Biotechnol. Bioeng.78(4): 467-472.

Jeremiah, L. (1996). Freezing effects on food quality. CRC press.

Jin, T., Sasaki, A., Kinjo, M. and Miyazaki, J. (2010). A quantum dot-based ratiometric pH sensor. Chem. Comm. 46(14): 2408-2410.

Jotcham, R. B. (2005). Authentication, antitamper, and track-and-trace technology options to protect foods. J.Food Prot. 68(6): 1314-1317.

Kader, A. A. (1986). Biochemical and physiological basis for effects of controlled and modified atmospheres on fruits and vegetables. Food Technol. 40: 99-104.

Kadish, K., Smith, K. and Guilard, R. (2010). Handbook of porphyrin science. World Scientific.

Kensy, F., Zang, E., Faulhammer, C., Tan, R. K. and Büchs, J. (2009). Validation of a high-throughput fermentation system based on online monitoring of biomass and fluorescence in continuously shaken microtiter plates. Microb. Cell Factories 8(1): 31.

Kerry, J. and Butler, P. (2008). Smart packaging technologies for fast moving consumer goods. John Wiley & Sons, Ltd., The Atrium, Southern Gate, Chichester, West Sussex PO19 8SQ, England,

Khalil, G. E., Daddario, P., Lau, K. S. F., Imtiaz, S., King, M., Gouterman, M., Sidelev, A., Puran, N., Ghandehari, M. and Bruckner, C. (2010). meso-Tetraarylporpholactones as high pH sensors. Analyst 135(8): 2125-2131.

Kim, H. K., An, D. S., Yam, K. L. and Lee, D. S. (2011). Package Headspace Composition Changes of Chill-Stored Perishable Foods in Relation to Microbial Spoilage. Packag. Technol. Sci. 24(343–352.

Kim, J. G., Luo, Y., Tao, Y., Saftner, R. A. and Gross, K. C. (2005). Effect of initial oxygen concentration and film oxygen transmission rate on the quality of fresh cut romaine lettuce. J. Sci. Food Agric. 85(10): 1622-1630.

Kirwan, M. J., McDowell, D. and Coles, R. (2003). Food packaging technology. CRC Press, Blackwell Publishing Ltd.,

Kodaka, H., Mizuochi, S., Teramura, H. and Nirazuka, T. (2005). Comparison of the Compact Dry TC Method with the Standard Pour Plate Method (AOAC Official Method 966.23) for Determining Aerobic Colony Counts in Food Samples: Performance-Tested MethodSM. J. AOAC Int. 88(6): 1702-1713.

Kosch, U., Klimant, I., Werner, T. and Wolfbeis, O. S. (1998). Strategies To Design pH Optodes with Luminescence Decay Times in the Microsecond Time Regime. Anal. Chem. 70(18): 3892-3897.

Kramer, R. A., Flehr, R., Lay, M., Kumke, M. U. and Bannwarth, W. (2009). Comparative Studies of Different Quinolinone Derivatives as Donors in Fluorescence-Resonance-Energy Transfer (FRET) – Systems in Combination with a (Bathophenanthroline)ruthenium(II) Complex as Acceptor. Helvetica Chim. Acta 92(10): 1933-1943.

Kuswandi, B., Wicaksono, Y., Jayus, J., Abdullah, A., Heng, L. and Ahmad, M. (2011). Smart packaging: sensors for monitoring of food quality and safety. Sensing Instr. Food Qual. Safety 5(3): 137-146.

Lakowicz, J. (2006). Principles of Fluorescence Spectroscopy. Springer, NY, USA,

Lakowicz, J. R., Szmacinski, H. and Karakelle, M. (1993). Optical sensing of pH and pCO2 using phase-modulation fluorimetry and resonance energy transfer. Anal. Chim. Acta 272(2): 179-186.

Lang, C. and Hübert, T. A Colour Ripeness Indicator for Apples. Food Biopr. Technol. 5(8): 3244-3249.

Lee, D. S., Yam, K. L. and Piergiovanni, L. (2008). Food packaging science and technology. CRC press,

Lee, J. H. (2008). Extending Shelf-Life of Leaf Lettuce Using Active Packaging. J. Food Technol. 6(14-19.

Leese, R. A. and Wehry, E. L. (1978). Corrections for inner-filter effects in fluorescence quenching measurements via right-angle and front-surface illumination. Anal. Chem. 50(8): 1193-1197.

Leiding, T., Górecki, K., Kjellman, T., Vinogradov, S. A., Hägerhäll, C. and Årsköld, S. P. (2009). Precise detection of pH inside large unilamellar vesicles using membrane-impermeable dendritic porphyrin-based nanoprobes. Anal. Biochem. 388(2): 296-305.

Li, H., Ashcraft, D. K., Freeman, B. D., Stewart, M. E., Jank, M. K. and Clark, T. R. (2008). Non-invasive headspace measurement for characterizing oxygen-scavenging in polymers. Polym. 49(21): 4541-4545.

Liebsch, G., Klimant, I., Frank, B., Holst, G. and Wolfbeis, O. S. (2000). Luminescence Lifetime Imaging of Oxygen, pH, and Carbon Dioxide Distribution Using Optical Sensors. Appl. Spectrosc. 54(4): 548-559.

Liebsch, G., Klimant, I., Krause, C. and Wolfbeis, O. S. (2001). Fluorescent Imaging of pH with Optical Sensors Using Time Domain Dual Lifetime Referencing. Anal. Chem. 73(17): 4354-4363.

Lindfors, T. and Ivaska, A. (2002). Potentiometric and UV–vis characterisation of N-substituted polyanilines. J.Electroanal.Chem.535(1–2): 65-74.

Little, A. (1975). Off on a tangent [Colorimetry in food science]. J. Food Sci. 40: 410–1.

Lübbers, D. W. and Opitz, N. (1983). Opticl fluorescence sensors for continuous measurement of chemical concentrations in biological systems. Sensors Actuat. B: Chem. 4(0): 641-654.

Mahajan, P. V., Oliveira, F. A. R. and Macedo, I. (2008). Effect of temperature and humidity on the transpiration rate of the whole mushrooms. J. Food Eng. 84(2): 281-288.

Mahajan, P. V., Oliveira, F. A. R., Montanez, J. C. and Frias, J. (2007). Development of user-friendly software for design of modified atmosphere packaging for fresh and fresh-cut produce. Innov. Food Sci. Emerg. Technol. 8(1): 84-92.

Mahajan, P.V., Rodrigues, F.A.S., Seguy, M. & Leonhard, A. (2009). Development of modified atmosphere and humidity packaging for fresh mushrooms. Italian J.Food Sci., June, 130-134.

Martin, D. S. (1932). The oxygen consumption of Escherichia coli during the lag and logarithmic phases of growth. J. Gen. Physiol. 15(6): 691.

Maskan, M. (2001). Kinetics of colour change of kiwifruits during hot air and microwave drying. J. Food Eng. 48: 169–175.

Mattila, T., Tawast, J. and Ahvenainen, R. (1990). New possibilities for quality control of aseptic packages: microbiological spoilage and seal defect detection using head-space indicators. Lebensm. Wiss. Technol. 23(3): 246-251.

Mayer, A. M. (2006). Polyphenol oxidases in plants and fungi: Going places? A review. Phytochem. 67(21): 2318-2331.

McDonagh, C., Burke, C. and MacCraith, B. (2008). Optical chemical sensors. Chem. Rev 108(2): 400-422.

McKellar, R. C., Odumeru, J., Zhou, T., Harrison, A., Mercer, D. G., Young, J. C., Lu, X., Boulter, J., Piyasena, P. and Karr, S. (2004). Influence of a commercial warm chlorinated water treatment and packaging on the shelf-life of ready-to-use lettuce. Food Res. Int. 37(4): 343-354.

McMillin, K. W. (2008). Where is MAP Going? A review and future potential of modified atmosphere packaging for meat. Meat Sci. 80(1): 43-65.

Michael, K. and McCathie, L. (2005). The pros and cons of RFID in supply chain management. Int. Conference on Mobile Business: 623-629.

Mills, A. (1997). Optical oxygen sensors. Platin. Met. Rev. 41: 115-126.

Mills, A. (2005). Oxygen indicators and intelligent inks for packaging food. Chem. Soc. Rev. 34(12): 1003-1011.

Mills, A. and Chang, Q. (1993). Fluorescence plastic thin-film sensor for carbon dioxide. Analyst 118(7): 839-843.

Mills, A. and Skinner, G. A. (2010). Water-based colourimetric optical indicators for the detection of carbon dioxide. Analyst 135(8): 1912-1917.

Mills, A. and Skinner, G. A. (2011). A novel 'fizziness' indicator. Analyst 136(5): 894-896.

Mills, A. and Thomas, M. (1997). Fluorescence-based Thin Plastic Film Ion-pair Sensors for Oxygen. Analyst 122(1): 63-68.

Mills, A., Chang, Q. and McMurray, N. (1992). Equilibrium studies on colorimetric plastic film sensors for carbon dioxide. Anal. Chem. 64(13): 1383-1389.

Mills, A., Lepre, A. and Wild, L. (1997). Breath-by-breath measurement of carbon dioxide using a plastic film optical sensor. Sensor Actuat. B-Chem. 39(1-3): 419-425.

Mills, A., Lepre, A. and Wild, L. (1998). Effect of plasticizer-polymer compatibility on the response characteristics of optical thin CO2 and O2 sensing films. Anal. Chim. Acta 362(2-3): 193-202.

Mills, A., Skinner, G. A. and Grosshans, P. (2010). Intelligent pigments and plastics for CO2 detection. J. Mater. Chem. 20(24): 5008-5010.

Mistlberger, G., Koren, K., Scheucher, E., Aigner, D., Borisov, S. M., Zankel, A., Pölt, P. and Klimant, I. (2010). Multifunctional Magnetic Optical Sensor Particles

with Tunable Sizes for Monitoring Metabolic Parameters and as a Basis for Nanotherapeutics. Adv. Funct. Mat. 20(11): 1842-1851.

Mohapatra, D., Bira, Z. M., Frias, J. M., Kerry, J. P. and Rodrigues, F. A. (2011). Probabilistic shelf life assessment of white button mushrooms through sensorial properties analysis. LWT - Food Sci. Technol. 44(6): 1443-1448.

Mohapatra, D., Bira, Z. M., Kerry, J. P., Frías, J. M. and Rodrigues, F. A. (2010). Postharvest Hardness and Color Evolution of White Button Mushrooms (Agaricus bisporus). J. Food Sci. 75(3): E146-E152.

Mohapatra, D., Frias, J. M., Oliveira, F. A. R., Bira, Z. M. and Kerry, J. (2008). Development and validation of a model to predict enzymatic activity during storage of cultivated mushrooms (Agaricus bisporus spp.). J. Food Eng. 86(1): 39-48.

Mohr, G. J. and Wolfbeis, O. S. (1994). Optical sensors for a wide pH range based on azo dyes immobilized on a novel support. Anal. Chim. Acta 292(1–2): 41-48.

Mohr, G. J., Klimant, I., Spichiger-Keller, U. E. and Wolfbeis, O. S. (2001). Fluoro Reactands and Dual Luminophore Referencing: A Technique To Optically Measure Amines. Anal. Chem. 73(5): 1053-1056.

Mu, J., Zhang, F., Zhu, X. and Dong, X. (2009). A gas chromatography method established for oxygen transfer efficiency measurement. J. Environ. Sci. 21, Supplement 1(0): S146-S148.

Nakamura, N. and Amao, Y. (2003). Optical sensor for carbon dioxide combining colorimetric change of a pH indicator and a reference luminescent dye. Anal. Bioanal. Chem. 376(5): 642-6.

Neurauter, G., Klimant, I. and Wolfbeis, O. S. (1999). Microsecond lifetime-based optical carbon dioxide sensor using luminescence resonance energy transfer. Anal. Chim. Acta 382(1-2): 67-75.

Neurauter, G., Klimant, I. and Wolfbeis, O. S. (2000). Fiber-optic microsensor for high resolution pCO2 sensing in marine environment. Fresenius J. Anal. Chem. 366(5): 481-487.

Niu, C., Gui, X., Zeng, G., Guan, A., Gao, P. and Qin, P. (2005). Fluorescence ratiometric pH sensor prepared from covalently immobilized porphyrin and benzothioxanthene. Anal. Bioanal. Chem. 383(2): 349-357.

O'Mahony, F. C., O'Riordan, T. C., Papkovskaia, N., Kerry, J. P. and Papkovsky, D. B. (2006). Non-destructive assessment of oxygen levels in industrial modified atmosphere packaged cheddar cheese. Food Control 17(4): 286-292.

O'Mahony, F., Green, R. A., Baylis, C., Fernandes, R. and Papkovsky, D. (2009). Analysis of total aerobic viable counts in samples of raw meat using fluorescence-based probe and oxygen consumption assay. Food Control 20(2): 129-135.

O'Riordan, T. C., Voraberger, H., Kerry, J. P. and Papkovsky, D. B. (2005). Study of migration of active components of phosphorescent oxygen sensors for food packaging applications. Anal. Chim. Acta 530(1): 135-141.

Odumeru, J. and Belvedere, J. (2002). Evaluation of the MicroFoss system for enumeration of total viable count, Escherichia coli and coliforms in ground beef. J. Microbiol. Meth. 50(1): 33-38.

O'Farrell, M., Sheridan, C., Lewis, E., Zhao, W. Z., Sun, T., Grattan, K. T. V., Kerry, J. and Jackman, N. (2007). Design of a slim-line integrated probe using optical fibre technology that is suitable for microwave environments and measures reflection spectroscopy and temperature. Proc. IEEE Sensors: 652-655.

Ogurtsov, V. I. and Papkovsky, D. B. (1998). Selection of modulation frequency of excitation for luminescence lifetime-based oxygen sensors. Sensors Actuat. B: Chem. 51(1–3): 377-381.

Oliveira, F., Sousa-Gallagher, M. J., Mahajan, P. V. and Teixeira, J. A. (2012a). Development of shelf-life kinetic model for modified atmosphere packaging of fresh sliced mushrooms. J. Food Eng. 111(2): 466-473.

Oliveira, F., Sousa-Gallagher, M. J., Mahajan, P. V. and Teixeira, J. A. (2012b). Evaluation of MAP engineering design parameters on quality of fresh-sliced mushrooms. J. Food Eng. 108(4): 507-514.

O'Mahony, F. and Papkovsky, D. (2006). Rapid High-Throughput Assessment of Aerobic Bacteria in Complex Samples by Fluorescence-Based Oxygen Respirometry. Appl. Environ. Microbiol. 72(2): 1279-1287.

O'Mahony, F. C., O'Riordan, T. C., Papkovskaia, N., Ogurtsov, V. I., Kerry, J. P. and Papkovsky, D. B. (2004). Assessment of oxygen levels in convenience style muscle based sous vide products through optical means and impact on shelf life stability. Packag. Technol. Sci. 17(4): 225-234.

O'Mahony, F., O'Donovan, C., Hynes, J., Moore, T., Davenport, J. and Papkovsky, D. (2005). Optical oxygen microrespirometry as a platform for environmental toxicology and animal model studies. Environ. Sci. Technol 39(13): 5010-5014.

O'Riordan, T., Zhdanov, A., Ponomarev, G. and Papkovsky, D. (2007). Analysis of intracellular oxygen and metabolic responses of mammalian cells by time-resolved fluorometry. Anal. Chem. 79(24): 9414-9419.

Oter, O., Ertekin, K. and Derinkuyu, S. (2008). Ratiometric sensing of CO2 in ionic liquid modified ethyl cellulose matrix. Talanta 76(3): 557-563.

Pacquit, A., Lau, K. T., McLaughlin, H., Frisby, J., Quilty, B. and Diamond, D. (2006). Development of a volatile amine sensor for the monitoring of fish spoilage. Talanta 69(2): 515-520.

Papkovsky (2004). Methods in optical oxygen sensing: protocols and critical analyses. Meth. Enzymol 381: 715-35.

Papkovsky, D. B. (1995). New oxygen sensors and their application to biosensing. Sensors Actuat. B: Chem. 29(1-3): 213-218.

Papkovsky, D. B. and O'Riordan, T. C. (2005). Emerging applications of phosphorescent metalloporphyrins. J. Fluoresc. 15(4): 569-584.

Papkovsky, D. B. and Ponomarev, G. V. (1995). Phosphorescent complexes of porphyrin ketones: Optical properties and application to oxygen sensing. Anal. Chem. 67(22): 4112.

Papkovsky, D. B., O'Mahony, F. C., Kerry, J. P. and Ogurtsov, V. I. (2005). Quality assessment of packaged foods by optical oxygen sensing. Proc. SPIE 5996 599604(

Papkovsky, D. B., Papkovskaia, N., Smyth, A., Kerry, J. and Ogurtsov, V. I. (2000). Phosphorescent sensor approach for non-destructive measurement of oxygen in packaged foods: optimisation of disposable oxygen sensors and their characterization over a wide temperature range. Anal. Lett. 33(9): 1755-1777.

Papkovsky, D. B., Ponomarev, G. V. and Wolfbeis, O. S. (1996). Longwave luminescent porphyrin probes. Spectrochim. Acta A 52(12): 1629-1638.

Papkovsky, D. B., Ponomarev, G. V. and Wolfbeis, O. S. (1997). Protonation of porphyrins in liquid PVC membranes: Effects of anionic additives and application to pH-sensing. J. Photochem. Photobiol. 104(1-3): 151-158.

Papkovsky, D. B., Smiddy, M. A., Papkovskaia, N. Y. and Kerry, J. P. (2002b). Nondestructive Measurement of Oxygen in Modified Atmosphere Packaged Hams Using a Phase-Fluorimetric Sensor System. J. Food Sci. 67(8): 3164-3169.

Papkovsky, Hynes, J. and Will, Y. (2006). Respirometric screening technology for ADME-Tox studies. Expert Opin. Drug Metab. Toxicol. 2(2): 313-323.

Parentelli, C., Ares, G., Corona, M., Lareo, C., Gámbaro, A., Soubes, M. and Lema, P. (2007). Sensory and microbiological quality of shiitake mushrooms in modified-atmosphere packages. J. Sci. Food Agri. 87(9): 1645-1652.

Parker, C. A. (1968). Photoluminescence of Solutions: with applications to photochemistry and analytical chemistry. Elsevier Amsterdam,

Parry, R. T. (1993). Principles and applications of modified atmosphere packaging of food. Blackie Academic & Professional, London, UK.

Pascall, M. A., Fernandez, U., Gavara, R. and Allafi, A. (2008). Mathematical modeling, non-destructive analysis and a gas chromatographic method for headspace oxygen measurement of modified atmosphere packaged soy bread. J.Food Eng. 86(4): 501-507.

Paulsen, P., Schopf, E. and Smulders, F. J. M. (2006). Enumeration of Total Aerobic Bacteria and Escherichia coli in Minced Meat and on Carcass Surface Samples with an Automated Most-Probable-Number Method Compared with Colony Count Protocols. J.Food Prot. 69(10): 2500-2503.

Peng, H.-S., Stolwijk, J. A., Sun, L.-N., Wegener, J. and Wolfbeis, O. S. (2010). A Nanogel for Ratiometric Fluorescent Sensing of Intracellular pH Values13. Angew. Chem. 122(25): 4342-4345.

Petrova, S., Kostov, Y., Jeffris, K. and Rao, G. (2007). Optical Ratiometric Sensor for Alcohol Measurements. Anal. Lett. 40(4): 715-727.

Phillips, C. A. (1996). Review: modified atmosphere packaging and its effects on the microbiological quality and safety of produce. Int. J. Food Sci. Technol. 31: 463-479.

Pocas, M. F. F., Delgado, T. F. and F.A.R., O. (2008). Smart Packaging Technologies for Fruits and Vegetables. In: Smart Packaging Technologies, 151-166. John Wiley & Sons Ltd., West Sussex PO19 8SQ, England.

Posch, H. E., Leiner, M. J. P. and Wolfbeis, O. S. (1989). Towards a gastric pH-sensor: an optrode for the pH 0–7 range. Fresenius' J. Anal. Chem. 334(2): 162-165.

Preininger, C. and Mohr, G. J. (1997). Fluorosensors for ammonia using rhodamines immobilized in plasticized poly(vinyl chloride) and in sol-gel; a comparative study. Anal. Chim. Acta 342(2–3): 207-213.

Pringsheim, E., Terpetschnig, E. and Wolfbeis, O. S. (1997). Optical sensing of pH using thin films of substituted polyanilines. Anal. Chim. Acta 357(3): 247-252.

Rahman, M. and Brazel, C. S. (2004). The plasticizer market: an assessment of traditional plasticizers and research trends to meet new challenges. Prog. Polym. Sci. 29(12): 1223-1248.

Restuccia, D., Spizzirri, U. G., Parisi, O. I., Cirillo, G., Curcio, M., Iemma, F., Puoci, F., Vinci, G. and Picci, N. (2010). New EU regulation aspects and global market of active and intelligent packaging for food industry applications. Food Control 21(11): 1425-1435.

Roberts, L., Lines, R., Reddy, S. and Hay, J. (2011). Investigation of polyviologens as oxygen indicators in food packaging. Sensors Actuat. B: Chem. 152(1): 63-67.

Robertson, G. L. (2006). Food packaging: principles and practice. CRC press, Tylor & Francis Group.

Robinson, R. K. (2000). Freezing of Foods, In: Encyclopaedia of Food Microbiology. Pp. 842-850. Academic Press.

Rojas Graü, M. A., Oms Oliu, G., Soliva Fortuny, R. and Martín Belloso, O. (2009). The use of packaging techniques to maintain freshness in fresh cut fruits and vegetables: a review. Int. J. Food Sci. Technol. 44(5): 875-889.

Salo, S., Ehavald, H., Raaska, L., Vokk, R. and Wirtanen, G. (2006). Microbial surveys in Estonian dairies. LWT - Food Sci. Technol. 39(5): 460-471.

Sandhya (2010). Modified atmosphere packaging of fresh produce: Current status and future needs. LWT - Food Sci. Technol. 43(3): 381-392.

Sapers, G. M., Miller, R. L., Pilizota, V., Kamp, F. (2001). Shelf-Life Extension of Fresh Mushrooms (Agaricus bisporus) By Application of Hydrogen Peroxide and Browning Inhibitors. J. Food Sci. 66: 362-366.

Sax, S., Fisslthaler, E., Kappaun, S., Konrad, C., Waich, K., Mayr, T., Slugovc, C., Klimant, I. and List, E. J. W. (2009). SensLED: An Electro-Optical Active Probe for Oxygen Determination. Adv. Mat. 21(34): 3483-3487.

Schröder, C. R. and Klimant, I. (2005). The influence of the lipophilic base in solid state optical pCO2 sensors. Sensors Actuat. B: Chem. 107(2): 572-579.

Schröder, C., Polerecky, L. and Klimant, I. (2007). Time-resolved pH/pO2 mapping with luminescent hybrid sensors. Anal. Chem. 79(1): 60-70.

Schroeder, C., Neurauter, G. and Klimant, I. (2007). Luminescent dual sensor for time-resolved imaging of p CO 2 and p O 2 in aquatic systems. Microchim. Acta 158(3): 205-218.

Schulz, K., Jensen, M. L., Balsley, B. B., Davis, K. and Birks, J. W. (2004). Tedlar Bag Sampling Technique for Vertical Profiling of Carbon Dioxide through the Atmospheric Boundary Layer with High Precision and Accuracy. Environ. Sci. Technol. 38(13): 3683-3688.

Seglina, D. (2009). Influence of packaging materials and technologies on the shelf-life. Chemine Technologija 52(3): 43-49.

Severinghaus, J. W. and Bradley, A. F. W. (1958). Electrodes for blood PO2 and PCO2 determination. J. Appl. Phys. 13: 515.

Shakhsher, Z., Seitz, W. R. and Legg, K. D. (1994). Single Fiber-Optic pH Sensor Based on Changes in Reflection Accompanying Polymer Swelling. Anal. Chem. 66(10): 1731-1735.

Sharrock, K. and Henzell, R. (2009). Ethylene Ripening of Pears by Unconventional Means: Use of Experimental Thimble-Sized Ethylene Capsules inside Cartons and Clamshells. Proc. Int. Symp.Postharvest Pacifica 339-346.

Silverstein, R. M. and Webster, F. X. (1998). Spectrometric Identification of Organic Compounds. John Wiley and Sons, Inc.,

Simón, A., González-Fandos, E. and Tobar, V. (2005). The sensory and microbiological quality of fresh sliced mushroom (Agaricus bisporus L.) packaged in modified atmospheres. Int. J. Food Sci. Technol. 40(9): 943-952.

Simpson, R., Acevedo, C. and Almonacid, S. (2009). Mass transfer of CO2 in MAP systems: Advances for non-respiring foods. J. Food Eng. 92(2): 233-239.

Sipior, J., Randers-Eichhorn, L., Lakowicz, J. R., Carter, G. M. and Rao, G. (1996). Phase Fluorometric Optical Carbon Dioxide Gas Sensor for Fermentation Off-Gas Monitoring. Biotechnol. Prog. 12(2): 266-271.

Sivertsvik, M., Jeksrud, W. and Rosnes, J. (2002). A review of modified atmosphere packaging of fish and fishery products–significance of microbial growth, activities and safety. Int. J. Food Sci. Technol. 37(2): 107-127.

Smiddy, M., Fitzgerald, M., Kerry, J., Papkovsky, D., O'Sullivan, C. and Guilbault, G. (2002a). Use of oxygen sensors to non-destructively measure the oxygen content in modified atmosphere and vacuum packed beef: impact of oxygen content on lipid oxidation. Meat Sci. 61(3): 285-290.

Smiddy, M., Papkovskaia, N., Papkovsky, D. and Kerry, J. (2002b). Use of oxygen sensors for the non-destructive measurement of the oxygen content in modified atmosphere and vacuum packs of cooked chicken patties; impact of oxygen content on lipid oxidation. Food Res. Int. 35(6): 577-584.

Somani, P. R., Viswanath, A. K., Aiyer, R. C. and Radhakrishnan, S. (2001). Charge transfer complex-forming dyes incorporated in solid polymer electrolyte for optical humidity sensing. Sensors Actuat. B: Chem. 80(2): 141-148.

Stich, M. I. J., Fischer, L. H. and Wolfbeis, O. S. (2010). Multiple fluorescent chemical sensing and imaging. Chem. Soc. Rev. 39(8): 3102-3114.

Tano, K., Arul, J., Doyon, G. and Castaigne, F. (1999). Atmospheric Composition and Quality of Fresh Mushrooms in Modified Atmosphere Packages As Affected by Storage Temperature Abuse. J. Food Sci. 64(6): 1073-1077.

Tao, F., Zhang, M. and Yu, H.-q. (2007). Effect of vacuum cooling on physiological changes in the antioxidant system of mushroom under different storage conditions. J. Food Eng. 79(4): 1302-1309.

Taoukis, P. S. (2008). Application of Time-Temperature Integrators for Monitoring and Management of Perishable Product Quality in the Cold Chain. In: Smart

Packaging Technologies, 61-74. John Wiley & Sons Ltd., West Sussex PO19 8SQ, England.

TAPPI Standards Department (2007). Indices for whiteness, yellowness, brightness, and luminous reflectance factor. Method T1216 sp-03.

Terry, L. A., White, S. F. and Tigwell, L. J. (2005). The Application of Biosensors to Fresh Produce and the Wider Food Industry. J. Agri. Food Chem. 53(5): 1309-1316.

Thrall, K. D., Toth, J. J. and Sharpe, S. W. (1996). Analysis of exhaled breath by laser detection. Proc. SPIE 136:

Tian, Y., Shumway, B. R., Cody Youngbull, A., Li, Y., Jen, A. K. Y., Johnson, R. H. and Meldrum, D. R. (2010). Dually fluorescent sensing of pH and dissolved oxygen using a membrane made from polymerizable sensing monomers. Sensors Actuat. B: Chem. 147(2): 714-722.

Tjoelker, M., Oleksyn, J. and Reich, P. (2008). Modelling respiration of vegetation: evidence for a general temperature-dependent Q10. Global Change Biol. 7(2): 223-230.

Townsend, D. and Naqui, A. (1998). Comparison of SimPlate Total Plate Count test with plate count agar method for detection and quantitation of bacteria in food. J. AOAC Int. 81(3): 563-569.

Trettnak, W., Gruber, W., Reininger, F. and Klimant, I. (1995). Recent progress in optical oxygen sensor instrumentation. Sensors Actuat. B: Chem. 29(1–3): 219-225.

Truppo, M. D. and Turner, N. J. (2010). Micro-scale process development of transaminase catalysed reactions. Org. Biomol. Chem. 8(6): 1280-1283.

Turel, M., Čajlaković, M., Austin, E., Dakin, J. P., Uray, G. and Lobnik, A. (2008). Direct UV-LED lifetime pH sensor based on a semi-permeable sol–gel membrane immobilized luminescent Eu3+ chelate complex. Sensors Actuat. B: Chem. 131(1): 247-253.

Vagina, A., Efremov, N. and Churkin, A. (2009). " Smart" package of materials with thermochromic effect. Scientific Works of the University of Food Technologies Plovdiv 56(2): 349-354.

Vaikousi, H., Biliaderis, C. G. and Koutsoumanis, K. P. (2009). Applicability of a microbial Time Temperature Indicator (TTI) for monitoring spoilage of modified atmosphere packed minced meat. Int. J. Food Microbiol. 133(3): 272-278.

Van der Steen, C., Jacxsens, L., Devlieghere, F. and Debevere, J. (2002). Combining high oxygen atmospheres with low oxygen modified atmosphere packaging to improve the keeping quality of strawberries and raspberries. Postharvest Biol. Technol. 26(1): 49-58.

Vanderkooi, J. M., Maniara, G., Green, T. J. and Wilson, D. F. (1987). An optical method for measurement of dioxygen concentration based upon quenching of phosphorescence. J. Biol. Chem. 262(12): 5476-5482.

Vasil'ev, V. V. and Borisov, S. M. (2002). Optical oxygen sensors based on phosphorescent water-soluble platinum metals porphyrins immobilized in perfluorinated ion-exchange membrane. Sensors Actuat. B: Chem. 82(2–3): 272-276.

Venables, W. and Ripley, B. (2002). Modern applied statistics with S. Springer.

Vollmer, T., Engemann, J., Kleesiek, K. and Dreier, J. (2011). Bacterial screening by flow cytometry offers potential for extension of platelet storage: results of 14 months of active surveillance. Transfus. Med. 21(3): 175-182.

Wang, L., Auty, M. A. E. and Kerry, J. P. (2010). Physical assessment of composite biodegradable films manufactured using whey protein isolate, gelatin and sodium alginate. J. Food Eng. 96(2): 199-207.

Wang, X.-d., Meier, R. J., Link, M. and Wolfbeis, O. S. (2010). Photographing Oxygen Distribution. Angew. Chem. 122(29): 5027-5029.

Wencel, D., Moore, J., Stevenson, N. and McDonagh, C. (2010). Ratiometric fluorescence-based dissolved carbon dioxide sensor for use in environmental monitoring applications. Anal. Bioanal. Chem. 398(5): 1899-1907.

Winkler, L. W. (1888). Die Bestimmung des im Wasser gelösten Sauerstoffes. Berichte der deutschen chemischen Gesellschaft 21(2): 2843-2854.

Wolfbeis, O. S. (2008). Fiber-Optic Chemical Sensors and Biosensors. Anal. Chem. 80(12): 4269-4283.

Wolfbeis, O., Weis, L., Leiner, M. and Ziegler, W. (1988). Fiber-optic fluorosensor for oxygen and carbon dioxide. Anal. Chem. 60(19): 2028-2030.

Wong, F. and Fradin, C. (2011). Simultaneous pH and Temperature Measurements Using Pyranine as a Molecular Probe. J. Fluoresc. 21(1): 299-312.

Wu, M.-H., Lin, J.-L., Wang, J., Cui, Z. and Cui, Z. (2009). Development of high throughput optical sensor array for on-line pH monitoring in micro-scale cell culture environment. Biomed. Microdevices 11(1): 265-273.

Wu, S., Cheng, W., Qiu, Y., Li, Z., Shuang, S. and Dong, C. (2010). Fiber optic pH sensor based on mode-filtered light detection. Sensors Actuat. B: Chem. 144(1): 255-259.

Yam, K. L., Takhistov, P. T. and Miltz, J. (2005). Intelligent Packaging: Concepts and Applications. J. Food Sci. 70(1): R1-R10.

Young, O. A., Thomson, R. D., Merhtens, V. G. and Loeffen, M. P. F. (2004). Industrial application to cattle of a method for the early determination of meat ultimate pH. Meat Sci. 67(1): 107-112.

Zar, J. (2000). Biostatistical Analysis. Prentice Hall.

Zhang, X., Lovejoy, K. S., Jasanoff, A. and Lippard, S. J. (2007). Water-soluble porphyrins as a dual-function molecular imaging platform for MRI and fluorescence zinc sensing. Proc. Nat. Acad. Sci. 104(26): 10780-10785.

Zivanovic, S., Buescher, R. W., Kim, K. S. (2000). Textural changes in mushrooms (Agaricus bisporus) associated with tissue ultrastructure and composition. J. Food Sci. 65: 1404-1408.